

2 min  
X-650-73-316

PREPRINT

NASA TM X-70519

# EARTH OBSERVATIONS FROM SPACE: OUTLOOK FOR THE GEOLOGICAL SCIENCES

(NASA-TM-X-70519) EARTH OBSERVATIONS FROM  
SPACE: OUTLOOK FOR THE GEOLOGICAL  
SCIENCES (NASA) 119 p HC CSCL 08G

N74-12157

Unclassified  
G3/13 22465

NICHOLAS M. SHORT  
PAUL D. LOWMAN, JR.

OCTOBER 1973



— GODDARD SPACE FLIGHT CENTER —  
GREENBELT, MARYLAND

Reproduced by  
NATIONAL TECHNICAL  
INFORMATION SERVICE  
U.S. Department of Commerce  
Springfield, VA 22151

PRICES SUBJECT TO CHANGE

119

X-650-73-316

EARTH OBSERVATIONS FROM SPACE: OUTLOOK FOR THE  
GEOLOGICAL SCIENCES

Nicholas M. Short  
Paul D. Lowman, Jr.

October 1973

GODDARD SPACE FLIGHT CENTER  
Greenbelt, Maryland

## CONTENTS

|  | <u>Page</u> |
|--|-------------|
| I. INTRODUCTION . . . . .                                      | 1           |
| II. EARLY DEVELOPMENTS IN SPACE . . . . .                      | 1           |
| A. Geologic Orbital Photography . . . . .                      | 1           |
| B. Nimbus Satellite Observations . . . . .                     | 3           |
| III. THE ERTS PROGRAM - RESULTS AND EVALUATION . . . . .       | 4           |
| A. General View . . . . .                                      | 4           |
| B. Value of Synoptic Coverage . . . . .                        | 5           |
| C. Specific Geologic Applications . . . . .                    | 7           |
| (1) Map Editing . . . . .                                      | 8           |
| (2) Landforms Studies . . . . .                                | 10          |
| (3) Structural Geology . . . . .                               | 10          |
| (4) Lithologic Identification . . . . .                        | 17          |
| (5) Mineral Exploration . . . . .                              | 19          |
| (6) Environmental and Engineering Geology . . . . .            | 23          |
| D. Summary . . . . .   | 25          |
| IV. SKYLAB: THE EREP PROGRAM . . . . .                         | 25          |
| A. SL 2-5-469: S. California . . . . .                         | 26          |
| B. SL 2-5-320: Milwaukee . . . . .                             | 27          |
| C. Summary . . . . .   | 28          |
| V. CRITIQUE OF CURRENT EARTH-OBSERVATIONS<br>PROGRAM . . . . . | 29          |
| A. Resolution . . . . .  | 29          |
| B. Directions of Illumination . . . . .                        | 30          |

## CONTENTS (continued)

|  | <u>Page</u> |
|--|-------------|
| C. Stereo Viewing . . . . .                                | 30          |
| D. Spectral Discrimination . . . . .                       | 30          |
| E. Radiometry . . . . .                                    | 31          |
| F. Other Spectral Regions . . . . .                        | 31          |
| G. Processing Techniques . . . . .                         | 32          |
| VI. FUTURE DEVELOPMENT IN ORBITAL REMOTE SENSING . . . . . | 32          |
| A. Synthetic Aperture Radar . . . . .                      | 32          |
| B. Thermal Imaging Systems . . . . .                       | 33          |
| C. High-resolution Visual Range Imagery . . . . .          | 35          |
| VII. SPACE SYSTEMS BEYOND ERTS AND EREP . . . . .          | 35          |
| A. EOS . . . . .   | 35          |
| (1) Thematic Mapper (TM) . . . . .                         | 36          |
| (2) High Resolution Pointable Imager (HRPI) . . . . .      | 36          |
| (3) Synthetic Aperture Radar (SAR) . . . . .               | 36          |
| B. SEOS . . . . .  | 37          |
| VIII. SUMMARY AND PROGNOSIS . . . . .                      | 37          |
| REFERENCES . . . . .                                       | 40          |

# EARTH OBSERVATIONS FROM SPACE: OUTLOOK FOR THE GEOLOGICAL SCIENCES

Nicholas M. Short  
Paul D. Lowman, Jr.

## I. INTRODUCTION

Although geology has traditionally been a hands-on science, remote sensing has found innumerable applications in the geological sciences. Geophysical techniques such as gravity measurements have contributed to the solution of many geological problems, even at a time when the instrument was carried in horse-drawn vehicles. Aerial photography, which underwent rapid advancement during World War I, was shortly after applied to geologic mapping; today, virtually no serious geologic field investigations are carried out without the use of air photos. Remote sensing techniques in general underwent rapid development during World War II for military purposes. After the war, these techniques were quickly applied to exploration geophysics; a well-known example is the use of the airborne magnetometer, originally developed for submarine hunting, which has since become invaluable for mineral prospecting.

Since about 1960, there have been rapid advances in both remote sensing techniques and space technology, which have had a marked synergistic effect. We will explore these recent developments as they are being applied in the geological sciences, and discuss possible future progress.

## II. EARLY DEVELOPMENTS IN SPACE

### A. Geologic Orbital Photography:

The first pictures of the earth from orbital altitudes were taken after World War II by small automatic cameras carried by sounding rockets to heights of about 100 to 200 miles. Although these pictures generated considerable interest in the potential uses of orbital imagery for meteorological and military reconnaissance purposes, no geologic use was made of them until 1963, when P. M. Merifield demonstrated the geologic utility of the synoptic view provided by such pictures. These developments have been reviewed by Lowman (1965) and Merifield (1962). Merifield's work, done chiefly with Viking and Aerobee rocket photography, stimulated interest in orbital photography, and a terrain photography experiment was quickly planned for the last two manned Mercury flights in 1962 and 1963. A number of excellent pictures of remote areas such as Tibet

were returned, and demonstrated the potential value of orbital photography in geologic mapping and other fields such as forestry, hydrology, and oceanography. The most important result of this early terrain photography was the interest it generated in imagery of the earth's surface as opposed to meteorological orbital photography, whose value was well-established by 1963. A glance at the proceedings of any conference on space applications before 1963 will show no mention of terrain photography; but this situation changed rapidly. A follow-on experiment was carried out on several Gemini flights. Gemini 4, flown by J. A. McDivitt and E. H. White, returned about a hundred pictures of geologically useful quality. Many of these pictures showed totally unmapped structures, dune fields, and even an entire volcanic field in northern Mexico that had never been mapped (Lowman and Tiedemann, 1971). The scope of the terrain photography was rapidly expanded to cover areas such as hydrology and oceanography, and by the end of the Gemini Program, some 1300 useful color photographs of the earth's surface had been obtained. Some hundreds more were taken during the early Apollo missions (Figure 1) (Lowman, 1972).

While the Gemini Program was still in progress, planning began for systematic earth resources photography from Apollo missions. The need for multispectral coverage was recognized, and a 4-camera experiment planned for the Apollo Applications Program missions involving use of spent rocket stages as space stations. This concept eventually became the now successful Skylab Program. Meanwhile, the delay caused by the Apollo 204 fire permitted the multispectral terrain photography experiment (S065) to be flown on Apollo 9 (Lowman, 1969) in 1969. This experiment too was successful, not only in geology (Figure 2) but in agriculture (Colwell, et al., 1971), providing a returned-film simulation of the Earth Resources Technology Satellite. An important lesson from the S065 experiment was that multispectral imagery is not only helpful but virtually mandatory on orbital missions, because of the great variety of terrain, vegetation, and weather conditions encountered in orbital photography.

The geological results from the color and multispectral photography experiments can not be discussed here, but it was found that the main applications in geology included studies of regional structure, geologic mapping, geomorphology, and sedimentation (Merifield, 1972; Lowman, 1972; Wobber, 1967). It was also suggested that earth-orbital photography be studied in preparation for interpretation of later pictures of Mars and other planets.

The NASA earth resources program began in 1963 in close cooperation with such agencies as the U.S. Geological Survey, the Department of Agriculture, and the Navy Oceanographic Office. Under this program, an extensive series of airborne remote sensing experiments were carried out using sensors that might have eventual space application. This work, carried out not only by NASA

but by other agencies, universities, and private industry, greatly stimulated the development of remote sensing in general. Further stimulus to remote sensing was provided by growing public awareness in the late 1960s of environmental problems. These various developments culminated in the decision by NASA to develop a dedicated earth resources satellite, eventually named the Earth Resources Technology Satellite, and a set of earth resources experiments for the first United States space station, now Skylab. We shall discuss the geologic applications of both programs in Sections III and IV.

#### B. Nimbus Satellite Observations:

Nimbus 1, launched in 1964, provided the first automated satellite system that yielded visual imagery useful to geologists. Because of a more elliptical orbit (with lower perigee) than planned for, many of the TV pictures from Nimbus 1 show considerably more detail (at higher resolution) than anticipated. An illustrative example is the view of the Mojave Desert - Transverse Ranges of California (Figure 3) which compares favorably with some Gemini, Apollo, and Skylab photos of the same region (see Figure 44). Subsequent Nimbus satellites, each with improved and more diverse sensor packages, did not produce images of this quantity, although many still proved suitable for interpretation of major structural features present in the large area (hundreds of miles on a side) covered in the images. Sabatini, Rabchevsky, and Sissala (1971), have prepared a summary of information from Nimbus relevant to geology; a recent specific use of Nimbus imagery for tectonic studies in Alaska is reported by Lathram (1972).

One experiment on Nimbus 5 has direct application to geology. The Surface Composition Mapping Radiometer (SCMR) measures emitted radiation in the 8.3-9.3 (8.8) and 10.2-11.2 (10.7) $\mu$ m range; a third channel operates in the 0.8-1.1 $\mu$ m interval (equivalent to the ERTS-1 MSS-4 band). Data from any of these channels can be used to produce photo-images. When used alone, either thermal channel will give information on equivalent blackbody temperatures. The reconstructed image in Figure 4 depicts the distribution of brightness temperatures of the offshore surface waters over much of the northern Gulf of Mexico. Such information is of geologic interest in relation to temperatures affecting chemical sedimentation, to sediment load densities, and to ocean current patterns which move the sediments.

The prime purpose of the SCMR is to determine the silica content of the uppermost layers of terrestrial surfaces. Emissivities of silicates vary at different wavelengths with respect to silica content. This gives rise to departures from true temperatures at certain characteristic wavelengths. Temperature decreases are maximum near 8.8 $\mu$ m for silica-rich granites and near 10.7 $\mu$ m for silica-low dunites. Temperature differences calculated from the radiances

measured by the two thermal channels are converted to "estimates" of silica content using calibration curves derived from a variety of rock types. The method, which presently gives only approximate or semi-quantitative values, works best on acidic and ultrabasic igneous or metamorphic rocks; data from andesites and basalts are masked by interference from an ozone band in the 9.5-9.9  $\mu\text{m}$  range. Quartz sand, sandstones, shales, and most soils act somewhat like crystalline rocks but the responses of sedimentary rocks are not yet accurately determined. Carbonate rocks, vegetation, water, and other features produce thermal difference signatures that are generally separable from silicate surface materials. After difference values are obtained, these can be expressed as photo-images in which silica-rich rock or soil surfaces are light-toned and silica-poor surfaces (rocks, vegetation, etc.) are variably darker. Probably the outstanding demonstration of SCMR results from Nimbus 5 (taken in the one-month operating interval before the instrument failed) is that depicted by desert and mountain regions of Saudi Arabia and Iran (Figure 5).

### III. THE ERTS PROGRAM - RESULTS AND EVALUATION

#### A. General View:

ERTS-1 is the first space platform designed specifically to observe the Earth repetitively with sensors that produce high resolution, multiband imagery and digital data.

The ERTS-1 spacecraft (Figure 6) was launched on July 23, 1972 from NASA's Western Test Facility in California. The operational parameters and orbital characteristics selected for the satellite are summarized in Tables 1A and 1B.

Both the Return Beam Vidicon (RBV) and the Multispectral Scanner (MSS) began to transmit image data on July 26, 1972. A typical example of a scene shown in the four MSS wave bands appears in Figure 7. Owing to a switching circuit failure, the RBV was shut down in August 1972, but it can be reactivated when needed to back up or take over the image acquisition functions of the MSS. As of October 1, 1973 the MSS had imaged more than 65000 scenes covering over 80% of the Earth's land surface. About 30%, on average, of these scenes are largely cloud-free and well-illuminated. Coverage of much of North America has been continuous (through September 1973) but coverage of other continents became severely limited by tape recorder difficulties since March 1973.

The reader is urged to consult the three volume Proceedings of the Symposium on Significant Results from the Earth Resources Technology Satellite-1

(March 5-9, 1973)\* for detailed treatment by the investigators, program managers, agency representatives, and invited speakers of the major findings from ERTS-1 for the various discipline groups comprising the Earth Resources Program.

Much of the material presented in this section has been drawn from investigations reported on during this symposium or subsequently described in progress reports from the 68 investigators in geology submitted periodically to NASA.

B. Value of Synoptic Coverage:

ERTS provides a remarkable sequence of uniformly illuminated, essentially planimetric, vertical views of the Earth's surface that cover very large areas (~ 12,500 sq. miles) in each image. Like the Gemini-Apollo pictures, these images are invaluable because of their synoptic aspects — that is, a single scene covering a wide variety of terrain, geology, and land use types is presented under near-optimum viewing conditions that emphasize the contextual relations of these surface features. Unlike the Gemini and Apollo pictures, and the Skylab images discussed in the next section, the ERTS images have the unique property of being readily joined together in mosaics. This greatly increases the synoptic character of this imagery and extends the assessment of contextual relationships to regional and even subcontinental proportions. Proper processing can so minimize the join or match line differences between successive scenes in a single orbital strip, between adjacent strips on successive days, and even between strips or individual scenes obtained during different orbital cycles that only careful inspection of a mosaic close-up would detect tonal or fit variations. Only very slight "stretching" of images during mounting is needed to join continuing features along the edges of the images. The resulting mosaics are surprisingly close to being orthographic, as can be readily determined by comparing both individual images and composite mosaics to such projections as Albers Equal Area or Lambert Conformal.

The inherent advantage of ERTS images over more conventional, aircraft-acquired imagery when used in mosaics for synoptic purposes can be easily demonstrated. A region in central Wyoming outlined in Figure 8a has been imaged as mosaics produced from both low and high altitude aerial photographs. The panchromatic image shown in Figure 8b represents a mosaicking of about 100 7-1/2"

---

\*Volume I, containing investigator papers, is obtainable as NASA SP-327 (\$13.65) from the U.S. Government Printing Office, Washington, D.C. 20402. Inquiries about Volume II (X-650-73-127) and III (X-650-73-155) should be addressed to Code 430, NASA, Goddard Space Flight Center, Greenbelt, Maryland 20771.

quadrangle aerial photo sheets each constructed from parts of approximately 120 individual high resolution aerial photos.\* Careful tone balance and joining leads to a high quality photomosaic for each quadrangle that retains considerable sharpness and detail. However, much of this detail is lost or obscured, and "noise" (repetitive tonal banding) is introduced, when the composite mosaic covering about 100 miles on a side is assembled.

A somewhat better synoptic image results from mosaicking 65 individual frames (each about 15 miles on a side with optimum resolution of 35-40 feet) obtained from a NASA U-2 photomission in 1971 (Figure 8c). Tonal contrasts are enhanced by use of multiband cameras; the red band is displayed here. However, like most aerial mosaics, the join areas are conspicuous because of tonal mismatches owing to photo-density variations within individual frames (lens-related) and between frames from successive flight lines (times-of-day variant). This particular mosaic was constructed as a simulation of an ERTS image.

The shortcomings of such a simulation, and the inadequacies of low altitude aerial photomosaics, are immediately evident when the above-described products are compared to a single ERTS image (Figure 8d) covering roughly the same area of central Wyoming. Although the resolution is lower (about 210 feet) in the ERTS image at equivalent scales (1:1,000,000), the uniform lighting and the resultant tonal consistency provide a vastly superior ERTS product in terms of synoptic aspect when judged against the aerial mosaics. Overall, the information content in the ERTS image appears to be much greater, except for those data sought that require better resolution.

Now, the ease with which ERTS images can be joined into mosaics covering large areas is strikingly displayed in Figure 9 — a red band composite extending over much of Wyoming and adjacent states. The individual Wind River basin frame just described is incorporated in this mosaic (the reader is challenged to search for the join lines). Color mosaics (two different renditions) of essentially the same region have now been prepared. They constitute some of the most impressive imagery of the Earth's surface taken by any space-observational system.

Beyond the esthetic and technical achievements associated with such mosaics, the scientific merits alone — particularly in geology — are a sufficient justification for their production. A glance at small-scale geologic or physiographic maps of the northern Rocky Mountains reveals at once the remarkable utility of

---

\*The producer of this mosaic, Aero Service Corp., Philadelphia, estimates that the 1973 cost of preparing a comparable product by a similar aerial survey to be at least \$200,000.

such imagery for presenting the regional or synoptic interrelationships of major structural and landforms units. Such mosaics are especially suited to lineaments analysis where uniform illumination serves to highlight trends of continuous, often deep-seated fracture zones that frequently extend for hundreds of miles.

ERTS-1 has now acquired enough cloud-free imagery in the first year since launch to allow mosaics of vast areas of Earth to be assembled. Some spectacular examples have already been exhibited. Black and white (red band) mosaics of Nevada and Oregon are reproduced here (Figures 10 and 11). Many other states are being similarly mosaicked (Figure 12). Color mosaics have been prepared for the eastern U.S. from Maine to Florida, for Mali in west Africa, and for Iran.

The Soil Conservation Service currently is producing for NASA-Goddard a 1:1,000,000 scale mosaic in two bands (MSS 5 and 7) that embraces the entire continental United States and all of Alaska. The 48 contiguous states mosaic will cover a display area of 24 feet (east-west) by 10 feet (north-south) (Figure 13). The preliminary version of Alaska is shown in Figure 14.

To sum up, there is a growing impression among geologists that ERTS mosaics add a new dimension to space imagery of immense value in tying together and unifying diverse structural elements of the Earth's crust and geomorphic units at its surface. For the first time, a uniform photobase is available for each physiographic or geologic province which can then be integrated into more expansive bases up to continental scales.

#### C. Specific Geologic Applications:

It must be kept in mind that ERTS is basically an extension of aerial photography to large area mapping. Aerial photographs in the past have been used chiefly as aids to the geologist in preparing or revising various kinds of geologic maps. The techniques and approaches of photo-interpretation developed prior to availability of multispectral imagery from space remain the major tools by which geologists extract information from ERTS data. Because of resolution differences, some types of information found in aerial photos are inherently unrecoverable from ERTS but such deficiencies are balanced by the synoptic overviews that provide hitherto unobtainable information. Thus, certain tasks will still be done better from aircraft but others may be done best — and even exclusively — from space platforms.

One measure of success of ERTS in geology is the extent to which new information has been acquired. While it is still premature to assign a dollar value or cost-effectiveness rating to the results reported to date, it is clear

that significant benefits are gradually accruing from ERTS data to the specific applications outlined in Table 2. In time, accomplishments in each of these fields will be translated into economic payoffs as new mineral deposits and oil prospects are discovered and engineering projects are undertaken because of these scientific and technological advances flowing from ERTS and other programs that couple space-acquired data with conventional ground exploration methods. The outlook is especially promising for certain parts of the world where ERTS images represent the first detailed surface coverage of regions that have never been surveyed or mapped beyond a reconnaissance level. This applies particularly to inaccessible high mountain areas, broad deserts, tundra and steppes, and polar regions, as well as sections of underdeveloped or low population countries.

Some of these applications are reviewed in the following sections:

(1) Map Editing—To some extent, ERTS data can be used to make new maps but these would not be directly equivalent to those produced from aerial photographs. In order to construct a standard geologic map, it is normally necessary to recognize stratigraphic units and sequences at the formation or even member level and, to a lesser extent, to discriminate among the major lithologies in the area. For mapping from aerial photos, this requires recognition of unit boundaries and definition of differences among units on the basis of rock color and/or surface weathering effects, topographic and/or geomorphic expression, soil associations, and characteristic vegetative cover, among other criteria. Most units depicted on large-scale maps range in thickness from a few tens of feet to a few hundred feet at most.

Because of resolution limitations, many stratigraphic units (defined from ground studies by criteria that usually require close-up or even hand specimen examination) cannot be recognized and separated in ERTS images along the same boundaries selected for mapping purposes. Several ground-distinguishable units with similar reflectance properties might group or blend into a single discernible unit in an ERTS image that may or may not have a meaningful stratigraphic and/or lithologic significance. Such a combination has been termed a "remote sensing (rock) unit" to take into account that it is an apparent single "layer" or "band" whose spectral properties (expressed as a uniform image tone) are reasonably homogeneous. This unit may also be segregated by other unifying characteristics, such as topographic expressions, land use patterns, or vegetation cover. When examined in the field (particularly in regions where strata are inclined), some remote sensing units actually correspond to single stratigraphic units but others are comprised of several stratigraphic units, often separated at top and bottom by boundaries of indefinite stratigraphic significance.

Thus, it seems unlikely that ERTS data can be used to produce geologic maps comparable in reliability to those resulting from aerial photointerpretation. However, the prospects are improved somewhat wherever adequate ground truth is available, and even more so whenever computer processing is applied to the data. As an example, Melhorn and Sinnock of Purdue University (Paper G 25, pp. 473-481, March 1973 Symposium) employed the clustering and classification techniques of the LARSYS computer program to generate a geologic map of a small area near Durango, Colorado. The cluster classes identified in the computer analysis were approximately equivalent to several different rock types whose distribution patterns correspond closely to local stratigraphic units. These units also had distinct topographic and vegetational expression. The resulting large-scale map (Figure 15), compared with a recent one made by conventional mapping, is surprisingly accurate and in some respects more detailed.

One of us (NMS) is currently attempting to produce a map of the Rattlesnake Mountains (consisting of a complete section of inclined rocks from the Precambrian through mid-Tertiary) in central Wyoming, using the same LARSYS system. So far, it has been possible to define some broad groupings of rock units owing to differences in lithology and in associated vegetation. However, the evergreen-covered Mississippian Madison Limestone and Pennsylvanian Tensleep Sandstone respond almost identically; the Permian Phosphoria and Triassic Chugwater formations appear as one unit; and the Mowry-Dakota-Cody and upper Cretaceous-lower Tertiary sequences cannot be subdivided. Further complications are introduced in the classification because of the ubiquitous presence ("overprinting") of grassy vegetation on nearly all units and the reflectance variations associated with rugged topography. In standard color composites, these same groupings can be discerned by distinctive colors: The Mississippian-Pennsylvania units are dark red; the Permian-Triassic units are a bright yellow; the Jurassic-lower Cretaceous units are a dark bluish-gray; and many younger unit groupings are a dark brownish. Once established, these color-identifiers can be used to pick out and map the same remote sensing units elsewhere in Wyoming.

A more immediate application of ERTS images lies in map editing or revision of small-scale maps. In regions of the world where rock exposures are sharply defined (mainly in deserts or other areas of low vegetation), the correspondence of ERTS-viewed surface geology patterns with those in previous maps is almost self-evident (Figure 16a and b). But, close comparison of image to map frequently shows serious discrepancies in the map version. Reality resides in the ERTS image. Presumably the map-maker has tended to smooth out or generalize unit boundaries and surface distributions on the small-scale maps. Corrections are easily made by superimposing the ERTS image on the map through use of a Bausch and Lomb Zoom Transfer Scope or similar plotting devices.

We have identified a number of cases where the ERTS images portray geologic features that have been unrecognized or misrepresented on geologic maps. A common example involves basalt flow units whose outlines are improperly shown or may even be omitted on maps. However, boundaries selected from ERTS images are not necessarily better located than before; a case in point is illustrated in Figures 17a and b. Obviously, like any use of imagery from above ground, the relationships developed from photointerpretation of ERTS images must be field-checked and then iterated into refined maps.

(2) Landforms Studies—Before synoptic imagery offered new perspectives, most geomorphic investigations depended on ground studies tied in with topographic mapping and supplemented by surface or aerial photography. While type examples of individual landforms or local physiographic units can be illustrated effectively, it becomes increasingly difficult to represent the complex nature of a continuous surface, on which are present a variety of interlocking and sometimes superimposed geomorphic features, on small-scale maps. Among the best efforts so far are those made by Tricart (1952) and others of the French School of Geomorphology (Figures 18a and b). Most geologists think of the classic quasi-relief maps of Lobeck, Raisz, and Fenneman, sketched as impressions of the appearance of the principal mountain and valley systems, etc. as they might appear to an artist sitting out in deep space.

Apollo and Gemini photography opened up new vistas to geomorphologists. Regions extending into several physiographic provinces could be inspected in a single view. ERTS has enlarged this capability to examine large areas coherently to include coverage of the entire world. It is now plausible to consider setting up classifications of landforms tailored to regional representation as evident in small-scale imagery. Once established, and with selection of suitable symbols, maps showing the distribution of all major, and many smaller, landform types can be generated for political units (states or countries), entire continents, or the whole world if desired (Short, Salomonson, and MacLeod, 1972). Such maps inevitably will provide new insights into regional geomorphology and into the many processes that actively shape and alter the land surface and hence give rise to the great variety of scenery found over the world.

Many outstanding examples of landforms as seen by ERTS have been identified. Some of these are being assembled at Goddard in a collection of the best images from ERTS that eventually will be published in "picture book" format. Figures 19a through d on the following pages are selected from this collection to show the varieties of landforms and related surface features visible from ERTS.

(3) Structural Geology—Experience with earlier space imagery had demonstrated the exceptional value of synoptic imagery for displaying extended

structural elements such as closed anticlines, domes, and intrusive bodies, folded mountain belts, fault zones, regional joint patterns, and other fracture systems. In arid regions, especially, the surface expression of structurally disturbed parts of the crust was often better revealed in the images than in maps of the same areas. The interplay between underlying structure, topography, vegetational distributions, and solar illumination commonly enhanced the appearance of structural elements, so that subtle relationships were disclosed that were not apparent in the maps. New lineaments of considerable magnitude and extent were picked out in the images because their breadth and continuity were commonly overlooked on the ground where only small, localized effects of a segment exposed discontinuously from one outcrop or topographic expression to the next were insufficient to manifest the "whole from its parts." In some areas of the world (e.g., Gulf of Oman; the Afar; Afghanistan) space imagery has brought about a fundamental resynthesis of the tectonic framework of a region.

ERTS has broadened these observations to sections of the globe never before imaged in detail from space. Some extraordinary views of complexly folded and faulted parts of the crust have been visually documented (Figures 20a-d). Many of these are destined to become classic illustrations in future textbooks.

As expected, the principal output so far from examination of ERTS images for new structural information is the recognition of numerous linear features, ranging from 1-2 miles up to several hundred miles in length. These linears vary in those diagnostic characteristics which enable them to be seen. A linear is singled out during photointerpretation by such indicators as:

- a. Lines of variable length, straightness, and continuity, set apart by tonal contrast (usually dark against a lighter background; especially where water concentrates along a line and is viewed in an infrared band image).
- b. Tonal discontinuities, established usually as boundaries between opposing light and dark areas in a scene.
- c. Bands of variable width, set in contrast to their borders and/or adjacent areas.
- d. Alignments of topographic forms, often emphasized by shadowing.
- e. Alignments of drainage patterns.

- f. Association of vegetation along linear trends.
- g. Co-alignment of cultural features, e.g., farms, road patterns, etc. with underlying structural and/or surrounding topographic control.

Almost every ERTS image having notable geologic content is marked also by occasional to numerous linears. In the first rush to report significant results, investigators usually equated these linears with structural features such as faults, joints, or inclined strata. Many of these interpretations have stood the test of field-checking. But, others have been abandoned when individual linears were found to be lighting artifacts, spurious alignments of diverse ground features, or man-made objects; the degree to which a region is vegetated, or conversely, shows extensive rock exposures, represents another factor that influences the apparent occurrence of linears. As experience with ERTS imagery was built up, a conservative reaction set in among investigators in which the terms "faults" and "lineations" — connoting geologic structures — were replaced by the more general, non-genetic "linear". The latter term is preferred until other checks — mainly of existing maps, aerial photos, and ground studies — permit an accurate identification of any individual linear.

The geologic studies of the state of New York by Y. W. Isachsen provide a graphic case in point. By the March 1973 Symposium (Paper G-1; pp. 223-230), Isachsen had assembled a working mosaic of the state and had analyzed his imagery for structural data. His efforts were concentrated on the Adirondacks and Catskill Mountains (Figure 21a), where large crustal fractures were well-known and mapped, in part because of their control on regional topography. He has since presented an updated ERTS-based map (Figure 21b) of linears of all kinds observed in the eastern half of New York. An earlier appraisal of these linears had indicated (1) many of those already recorded from geologic studies were recognizable, (2) while other known ones which should be visible did not show up in the imagery, and (3) still others prominent in ERTS images were completely new features not defined on any maps. Showing commendable restraint, he refrained from any specific statement on (genetic) identification of individuals in this third group until he could complete a check of a representative fraction of these. The results of this check break down as follows:

| A. | <u>Category</u>                                     | <u>Number</u> | <u>Combined Length (km)</u> |
|----|---|---------------|-----------------------------|
| 1. | Previously mapped faults and topographic lineaments | 232           | 1890                        |
| 2. | Linear anomalies remaining after preliminary checks | 364           | 3130                        |

|   |     |      |
|---|-----|------|
| 3. Total seen on ERTS   | 596 | 5020 |
| 4. Mapped faults and lineaments<br>not discerned in ERTS<br>imagery | 297 | 1750 |

The second category was further subdivided, after extensive studies in the field and on photos and maps.

| B.                                       | <u>Category</u> | <u>Number</u> |
|--|-----------------|---------------|
| 1. Cultural Features                     |                 | 20            |
| 2. Linears parallel to lithologic trends |                 | 51            |
| 3. Straight segments of stream courses   |                 | 96            |
| 4. Straight stream valleys               |                 | 27            |
| 5. Winding streams                       |                 | 7             |
| 6. Elongate lakes                        |                 | 7             |
| 7. Ridge crests                          |                 | 3             |
| 8. Edges of topographic highs            |                 | 5             |
| 9. Alignment of vegetation               |                 | 30            |
| 10. Combinations of the above            |                 | 57            |
| 11. Unexplained                          |                 | <u>125</u>    |
|  |                 | 435*          |

\*The discrepancy between 435 and 363 (A.2) is not explained in Isachsen's report.

The important points drawn from these numbers are that less than 1/3 of the new linears are likely to be strictly structural in nature and that many known structural features cannot be found in the imagery. Most of these new linears in the "unexplained" category are probably structural because their trends are consistent with orientations of the principal fracture systems previously determined for the Adirondacks and Catskills. According to Isachsen, the undiscerned faults and lineaments fail to be expressed in ERTS images because of unfavorable illumination and/or (processed) image quality.

A complementary analysis of proportions of linears of diverse character has been reported by R. Weidman of the University of Montana. He has produced a mosaic of the entire state (Figure 22a) from which he has extracted extensive information on linears in the western section (Figure 22b). Approximately 40% of these linears correspond to faults, fold axes, contacts, or other geologic features depicted on published maps; 32% are not shown on maps but are consistent with known structural trends; 28% are contradictory with respect to geologic data and many may be non-geological in nature.

These, and other, reports make clear the importance of conducting suitable field studies before expressing any claims or drawing significant conclusions. Various investigators have called attention to the role of sun angle and direction in highlighting linear features that strike NE-SW. Linears thus oriented tend to be roughly perpendicular to the sun's rays at the mid-morning times of the ERTS passes. A shadowing effect related primarily to topography enhances linears with these trends; conversely, many NW-SE linears, being more or less parallel to the direction of illumination, are rendered almost "invisible" in ERTS imagery. This bias toward NE-trending linear features at the expense of those of different orientations must be taken into account in any statistical analysis of distribution of linears as determined from photointerpretation of ERTS and other image sources.

Seasonal effects are also factors in bringing out certain linears undetected in some ERTS images. The work reported by F. Wobber of Earth Satelline Corp. on snow enhancement (see Paper G-12, pp. 345-352, March 1973 ERTS Symposium) is convincing. He has found that the combination of a thin snow cover, low sun angle, and leaf-free trees — all the consequence of winter coverage — cause many linear trends to stand out in the rugged hills of New England that are otherwise hard to see in coverage from other seasons. Still another effect that depends on repetitive coverage is the subtle enhancement of some linears by either collection of moisture along cracks after rainy spells or preferential growth of vegetation along zones of suitable drainage that correspond to faults and joints.

Well over half of the ERTS investigations deal directly with extraction of structural information. Five studies are reviewed here as examples of the kinds of results fostered by ERTS-type data.

1. In many inaccessible regions, ERTS provides a quick and reasonably efficient way to put together a reconnaissance map of the structural grain or fabric exposed at the surface. This is certainly true for many parts of the Canadian Shield where previous mapping of large areas required extensive aerial photography supported by some ground studies in the "bush". Muskeg and forest cover often obscures much of the surface. ERTS images of the

Shield (Figure 23) are remarkable in capturing the structural "flavor" of the region. Where fractures control the distribution of surface water (sometimes assisted by glacial scouring), lakes and streams tend to outline the major lineations — evidenced in ERTS to a degree rarely appreciated from ground surveys.

2. The Wind River Mountains of Wyoming provide another dramatic example of the rapidity with which a mapping effort can be accomplished using ERTS imagery. Dr. R. Parker of the University of Wyoming has been mapping in the high country of this range for five years — a task carried out on pack mule and "shanks-mare" in the grand tradition. His labors led to the map reproduced in Figure 24 left. After receipt of ERTS imagery covering this range, he completed the map shown in Figure 24 right in just 3 hours. Although this map should still be rated as "preliminary" because most of the lineaments have not been verified, some confidence in the correctness of identification is afforded by field checks at several localities, where evidence of fracturing was then obtained.

Similar maps for the Bighorns (R. Hoppin; University of Iowa), and the Medicine Bow Range and Laramie Mountains (University of Wyoming) have now been completed using ERTS images supplemented by U-2 air photos. For the first time, the regional patterns of the major lineaments in the crystalline basement of Wyoming have been revealed — assuming that the uplifts are representative samples. It should now be possible to test the often-cited hypothesis of basement structural control of overlying sedimentary petroliferous anticlines and of localization of mineral belts along fractures.

3. Joints can be picked up in ERTS images where properly expressed in the terrain. Most joints tend to be too small for recognition but large, regional fractures are often visible in flat-lying sandstone-capped mesas and benchs of the Colorado Plateau. Goetz, et al., (Paper G 19, pp. 403-411, March 1973 ERTS Symposium) have developed visual and computer techniques for bringing out short linears in ERTS imagery. They have applied this approach to the Verde Valley region southwest of Flagstaff (Figure 25). Subsequent field checks suggest most of the linears are indeed joints although some are evidently faults. A map containing this wealth of detail on fractures is even now proving invaluable as a guide to prospecting for ground water. In other parts of the world (e.g., India, Australia; southern Africa), regional jointing in sandstones and limestones can readily be defined from ERTS imagery.

4. ERTS has shown a special facility for calling attention to circular as well as linear features. Most of these are volcanic or intrusive in nature and many are newly recognized. The first new structure of this type identified from

ERTS was a 25 mile diameter ring of hills just northwest of Reno, Nevada that encroaches on the east front of the Sierra Nevadas. This feature has not been fully explained but it likely is a ring complex of volcanic origin that has subsequently been disturbed by faulting. Another example (Figure 26) is an even larger elliptical feature northeast of Crater Lake, Oregon. Preliminary field studies indicate a concentration of small volcanic structures (cones and vents) along the forested rim. A ring dike system would explain this alignment.

Often, structures such as the above are subtly expressed in existing maps but these have failed to be specifically delineated as distinct surface patterns. Consider the portion of the geologic map of Arizona shown in Figure 27a. There is an elliptical outcrop pattern present, which is evident when pointed out but has not been generally recognized by geologists. But, the ERTS view of this area (Figure 27b) immediately defines a prominent drainage and topography pattern that then aids the mind's eye in pulling out the corresponding patterns on the map.

5. A few circular features have more exotic origins. Planetary-oriented geologists have learned to "think impact" whenever a structure with a near-perfect circular outline is seen in small-scale imagery. On Earth more than 70 structures ranging from a few hundred feet to over 60 miles in diameter have now been identified as recent or ancient meteorite craters. Many of these were first spotted on aerial photos.

ERTS is expected to be a powerful instrument for detecting new, large impact craters. Indeed, many of the known structures show up clearly in ERTS imagery. But, to date no proven new craters have been noted. However, one structure in Brazil some 400 miles WSW of Brasilia was just this year identified as an old crater because it contains shocked rock materials that could be caused only by impact. This feature, called the Araguainha Dome, had been listed as having a diameter of about 13 miles. As seen from ERTS (Figure 28), this old crater is found to be nearly twice as wide (~ 25 miles diameter), with two distinct dark "rings" consisting of rock units that support thicker stands of trees in the semi-jungle.

In closing this section, we shall refer to one other obvious utilization of ERTS that, again, takes advantage of the mosaics made from the imagery. ERTS mosaics are ideal for getting a perspective on the tectonic framework of large regions of the crust. Thus, through-going lineaments that continue for hundreds of miles can be integrated into a unified network which reflects the influence of fractures in an ancient basement or results from stress systems developed from more recent plate tectonic movements. Seen in a broad context, where diversities of topography and surface geology tend to be filtered out, a new synthesis of structural data can emerge. Various investigators are even

now building structural models for their home states. Several regional studies, embracing several states or countries, are underway. Some first results from one such effort are summarized in Figure 29, although no follow-up verification of the existence of the new lineaments has been reported.

(4) Lithologic Identification—Identification of rock types from aerial or space platforms has long been a goal that consistently remains elusive. The high hopes that at least the major rock groups could be recognized with sensor data have met with varied success. Depending on the experience of the interpreter and his knowledge of rock types present in the scene, the photogeologist has frequently been able to correctly identify basalts, granitic rocks, some metamorphic types, limestones, shales, and sandstones, provided resolution is sufficiently good to single out individual lithologic units. In effect, the interpreter often reacts subconsciously to "clues" found in characteristic image tones, topographic expression, structural relationships, outcrop patterns, contextual associations, and the like in deciding on the identities of distinct units. Automation of this process has not been as effective as the subjective judgement of the interpreter.

Rocks are normally identified and classified on the basis of their mineral assemblages, textural aspects, and field relationships. A preliminary general term classification (e.g., "dirty" sandstone) can usually be applied in the field but petrographic and chemical data are frequently needed to provide a more precise classification (e.g., chloritic subgraywacke). Correct assessment of lithologic types, like that of stratigraphic units, thus commonly demands painstaking, detailed examination both in the field and the laboratory.

A moment's reflection on this problem should expose the intrinsic difficulties facing remote sensing as a tool for rock identification. Unlike x-ray diffraction, for example, in which unique solutions to mineral identity result from the fundamentally different combinations of atomic structure, there is little that most remote sensing devices can measure that is exclusive to any given rock type. In the spectral range scanned by the ERTS MSS, the only rock properties directly measured are color and brightness; indirectly, derivative properties such as relative weathering (expressed topographically), surface stains, soil associations, vegetation preferences, structural response, etc., are taken into account in making identifications. However, it is not possible to set up a reliable working classification of rocks based primarily on typical colors and relative brightness. Thus, granite and schists, sandstones and limestones, shales and slates, and other lithologically dissimilar rock pairings may have roughly the same colors and brightnesses. Conversely, one given rock type may have many color variants as, for example, green, red, buff, gray, and black shales, or white, dark-gray, buff, and red limestones.

Careful appraisal of spectral response curves should likewise lead to this conclusion. Published curves by J. Salisbury and his group at the Air Force Cambridge Research Laboratory and R. Lyon of Stanford show that broad, often diagnostic differences do occur in rocks. But the characteristic curves just do not display the "fine structure" of x-ray diffraction patterns or other "fingerprint" methods that rely on specificities of atomic structure. This is further confirmed in Figure 30 — a series of spectral response curves for Wyoming rocks obtained at Goddard on a Cary 90 Reflectance Spectrometer. While differences are evident, they are not systematic or unique. Although not shown in the figure, several individual rocks displayed greater variation between spectra from fresh and weathered surfaces an inch apart than between quite different rock types. The problem of distinguishing rock types is further compounded when multi-channeled radiometer (as is the MSS of ERTS-1) are used to measure rock reflectances instead of spectrometers. Each channel averages out the energy under the spectral curve to a single value — further masking the limited "fine structure" that is sometimes diagnostic.

For radiometric data, the best recourse is to compare relative reflectances within different wave band regions either by visual inspection of "histogram" plots (energy or power versus wave band) or by selective ratioing of one band to another. A claim implied by R. K. Vincent (Paper G 16, pp. 379-386, March 1973 ERTS Symposium) suggests that rock type discrimination is considerably improved when ratios of MSS Bands 7 to 5 reflectances are compared. Our interpretation of his Figure 4 (reproduced here as Figure 31) disputes the value of this approach as a means by which useful rock discrimination can be accomplished. The spectral ratios of many unrelated rock types cluster around 1 on Vincent's plot; while the means may be slightly different, the spread of ratio values appears large enough to overlap these various rock types to a degree that precludes significant differences in a statistical sense.

We conclude therefore that rock types cannot be reliably identified solely from ERTS radiometric data simply because real discrimination criteria based on wavelength-dependent energy outputs do not exist in the spectral range considered. Granted, a few rock types (e.g., basalts) often — but not always — show some definitive characteristics. Where some a priori information relating a rock unit (often, but not necessarily, coincident with a stratigraphic unit) to certain spectral characteristics (e.g., a specific color in a color composite) is available from maps or ground truth, similar information observed elsewhere in the same ERTS scene or in different, separated scenes may properly identify the same rock type. Still, the reliability of this extrapolation remains to be appropriately tested.

(5) Mineral Exploration—Most reviews or promotional presentations of benefits to geology from remote sensing place heavy emphasis on finding ore deposits, oil, or other mineral products as the "big payoff" application. These statements seldom are accompanied by an explanation of how this worthy goal will be carried out. An aura of the "magic black box" hangs over the whole approach. Exploration geologists who have struggled for years to find just one new deposit or oil strike, aided by sophisticated geophysical techniques, meticulous mapping, and sometimes abundant drilling, have topped the list of skeptics who scoff at the value of remote sensing for such purposes. They can point to a very low success rate in finding new mineral deposits from spaceborne sensors in support of their contention.

Again, brief reflection should pinpoint two potentially useful ways in which ERTS data could help to locate conditions favorable to the concentration of metals.

First, the recognition of new crustal fractures and, especially, intersections in lineaments systems, improves the probability of finding ore if one believes in the commonly held view that such fractures control localization of mineralizing solutions. Each new fracture or intersection provides new targets for exploration. Point intersections, particularly, represent a significant narrowing in on promising zones of concentration so that exploration of vast areas can be greatly compressed.

Second, many shallow mineral deposits give rise to distinctive surface stains (gossans and blooms) caused by alteration or secondary enrichment. If broad enough, some of these stains should be detectable as color-brightness anomalies — subject to the caveats raised in the previous section on lithologic identification. A simple test of this capability could be to look at ERTS imagery for any evident visual (tonal) differences around known mineral deposits that single them out from their surroundings. Caution must be maintained in examining active mining areas to avoid confusion between surface conditions at man-made workings (excavations; mine dumps; dried-up lakes, etc.) and natural stains present before exploitation.

As of September 1, 1973, there has been little hard-core substantiation from the ERTS program of the expectations for finding mineral deposits. The proof must inevitably come from discovery of new deposits. No reports of an ore body discovered exclusively from ERTS are in hand. Some allusions to new prospects have come to our attention. The best example was presented by M. Viljoen (Paper G 26, pp. 483-492, March 1973 ERTS Symposium). He described a cluster of gabbroic intrusions, some known earlier to be nickel- and copper-bearing, in South West Africa. The exact extent and outline of these intrusives were poorly mapped. The ERTS based map provides a major

improvement in setting forth the regional geology. We have also heard — but cannot verify — of possible ERTS-related discoveries of uraniferous igneous complexes in Brazil, uranium- and copper-rich structures in Australia, and nickel-bearing intrusives in Canada.

Three relevant mineral investigations, all involving ERTS to some extent, warrant some critical appraisal here:

1. During the March 1973 ERTS Symposium, R. K. Vincent (op. cit.) offered evidence of "probable" success in recognizing iron oxides by use of MSS Bands 7 to 5 ratios (see page 18). As indicated in Figure 32, he found limonite and hematite to have ratio ranges that differ from most other common mineral and rock types (but are close to that of serpentine, a sharply dissimilar rock). Vincent then analyzed ERTS data for the Wind River Mountains of west central Wyoming to determine whether the large iron deposits in metamorphic rocks at the Atlantic City mine could be distinguished from their surroundings. Employing a computer-based recognition technique, Vincent has prepared a map (Figure 32) which seems to indicate that the reflectance ratio at the Atlantic City mine is a singular and diagnostic value relative to the terrain in its vicinity. A computer-enhanced enlargement of a ratio rendition of the ERTS image shows a tonal anomaly around the mine. Color composites (MSS 4 blue; 5 green; 7 red) invariably represent the area as a deep blue.

We cannot dispute these conclusions by citing any counter-evidence based on rigorous data processing. One of us (NMS) is familiar, however, with the Atlantic City region and is compelled to put forth these observations.

- a. The ratio image shows several other areas with similar dark tones; these areas are not loci of iron enrichments although the reddish-colored (iron-caused) Chugwater formation does have comparable tones.
- b. The Atlantic City mine is now largely an open, cleared area in which most trees have been felled and much of the weathered rock-soil surface veneer is removed. The underlying greenish-gray bedrock schists are generally dark. Lack of reflective vegetation and the low reflectivity of the metamorphic rocks could account for the low 7:5 ratio (dark image tone) and would mean that a color composite will show the area as bluish because the green band (blue filter) should have the highest reflectivity and the IR band (red filter) the lowest (the ferric oxide-colored Chugwater formation invariably appears yellowish in such a color composite).

- c. During field work in Wyoming in September, 1973, one of us (NMS) visited the Atlantic City mine to take readings with a radiometer that measures radiances in the same four channels as the ERTS MSS. Owing to an instrument calibration problem (the MSS-1 or green equivalent channel reads low) and other factors, the data have not been reduced or corrected for "look" angle and irradiance variations. The raw data are, nevertheless, instructive:

| Rock Type                                  | MSS Equivalent Channels* |      |      |       |
|--|--------------------------|------|------|-------|
|  | 1                        | 2    | 3    | 4     |
| Taconite Band                              | 2.47                     | 3.25 | 3.09 | 3.45  |
| Interbedded Greenstone                     | 2.13                     | 2.67 | 2.53 | 2.88  |
| Road Outcrop: Green Schists                | 2.25                     | 2.97 | 2.87 | 3.40  |
| Limonite Stained surface at road outcrop   | 3.69                     | 5.73 | 5.88 | 6.75  |
| Chugwater Formation near Lander (red beds) | 1.35                     | 3.52 | 4.17 | 5.22  |
| Nugget Sandstone near Lander               | 2.56                     | 5.18 | 6.26 | 8.00  |
| Aspen trees                                | 1.80                     | 2.50 | 7.90 | 12.40 |
| Douglas Fir stand                          | 1.00                     | 1.80 | 3.30 | 5.05  |
| Ilsmanite**                                | 1.80                     | 1.79 | 1.68 | 1.83  |

\*In units of watts/m<sup>2</sup> - ster.

\*\*A dark blue uranium molybdate mineral measured at the Lucky Mc. Mine (uranium pits) near Ervay, Wyoming

Even without the appropriate corrections, the above data (whose channel values are internally consistent for any one set of readings) indicate several interesting conclusions:

- For the same large specimen of taconite bands within green-stone, the readings for the two phases (made under identical lighting and viewing angle conditions) show these phases to be

very similar in relative reflectances, even though the taconite contains at least 20% by weight more  $\text{Fe}_2\text{O}_3$ .

- Regardless of iron content (the uranium mineral contains very low amounts), all dark rocks measured show a slight decrease in reflectance in MSS Channel 3 (0.7–0.8  $\mu\text{m}$ ) relative to MSS-2 and MSS-4 values.
- However, in usually lighter-colored rocks, the MSS-3 value increases with respect to MSS-2 (but is less than MSS-4). This holds for the Nugget sandstone (limonite-colored), the somewhat darker Chugwater shales (generally hematite red in color owing to presence of iron oxide), and for Madison limestone (grayish-tan), Tensleep sandstone (light buff), and Dakota sandstone (brownish) measured during field work in Wyoming. This relationship seems, therefore, to be largely independent of iron content.
- Ratios of bands 7 to 5 (MSS-4 to MSS-2 on the radiometer) for these field specimens show little difference among the taconite bands, greenstone, and ilsmannite — three phases which show a wide spread of iron oxide contents. Granted that this observation might change when reduced data are used, still it is not obvious from the unprocessed data that iron is a major variable in controlling the reflectances of these rocks.

2. A related approach to recognition of iron-oxides recently reported by A. F. H. Goetz (JPL) and L. C. Rowan (U.S.G.S.) seems to be more convincing. From field and laboratory reflectance spectrometer measurements, these two investigators also conclude that limonite has a spectral response quite different from most other common minerals. This response can be made more sensitive when several ratios of different ERTS MSS band pairs are calculated. This concept is applied to an ERTS scene by computing ratios for different band combinations (e.g., 5 to 7, 4 to 6, 7 to 6, etc.) on a pixel to pixel level. Each ratio represents a variable signal which, like individual MSS band analog signals, can be used to construct photo images. In this manner, Goetz and Rowan produce color composites by passing computer-generated ratio signals through an optical processor equipped with color filters. From trials with various filter combinations, they have found a color rendition in which three narrow ranges of reflectance ratios are presented in a yellowish-brown color much like that of iron stain (limonite or rust). Different rock types, vegetation, etc., also take on distinctive color hues. They have tried out their method on an ERTS scene of central Nevada that includes the Goldfield mining district. Prominent yellow-brown color patterns are observed around Goldfield and other areas where

surface iron stains were known before. The composite has now been field checked from the air and ground during which many of these color anomalies were verified. Insofar as gossans are indicators of potential mineralization, this enhancement technique for revealing the distribution of hydrous iron oxides in ERTS images, if it bears up under further testing, now stands as a major breakthrough in mineral prospecting.

3. Many ERTS investigations are indirectly providing valuable information, previously described, relevant to the search for oil. Almost none, however, are being conducted by petroleum geologists specifically to prove the worth of ERTS as a new exploration technique. The several in this category have yet to respond in reports with well-documented evidence that ERTS is truly helpful. Conclusions are confined to brief "show and tell" statements like "we can see the anticlines already mapped" or "the salt domes have recognizable surface expression" or "there are some fracture trends that appear to pass through the oil fields and probably exercise some control."

The main reason why ERTS will undoubtedly prove to have real merit in finding oil have already been discussed in earlier sections. These include: the regional or synoptic viewing aspect; the map editing capability; the source of new data in poorly mapped regions of the world; the definition of structural relations in a broader context. In its simplest essence, an ERTS image is a large area counterpart to an aerial photo and will be used by petroleum geologists in much the same way.

One example here will illustrate most of these points. Many parts of Iran offer promise of becoming oil producers and new petroleum concessions are being granted. The Earth Satellite Corp. is currently engaged in a survey of the entire country from ERTS supported by field studies. Earth Sat geologists have now mapped the region around Tabas (some 300 miles southeast of Tehran) from ERTS images and the ground in greater detail than before (Figure 33). New fracture systems have been found which could have considerable significance in future oil and mineral prospecting.

(6) Environmental and Engineering Geology—Many geologically-related applications from ERTS have been delegated to other disciplines in the ERTS investigations program. Several will be reviewed here.

1. Coastal processes and sedimentation studies are usually assigned to the marine resources and ocean-surveys discipline category. ERTS has produced some incredible images showing sedimentation patterns in the open oceans or restricted embayments where rivers are carrying their loads into marine waters (Figure 34a and b). Sedimentologists are afforded an opportunity to observe

modern-day offshore transportation and deposition processes at a viewing scale never before available. Seasonal and long-term changes can now be monitored over much of the continental shelf environments on a worldwide basis. Development of new sedimentation models will have obvious practical applications to harbor and shoreline maintenance, ocean waste disposal, marine pollution, and fisheries.

2. Studies of active glaciers monitored continuously from space should give new impetus to current hypotheses on the growth and recession of ice and on the likelihood of renewed continental glaciation. Surging glaciers have already been observed from ERTS (Figures 35 and 36). Vast regions subjected to extensive permafrost can be inspected for evidence of effect which will influence engineering activities (Figure 37). Other areas influenced by piedmont or mountain glaciers reveal new relations between the present ice bodies and the out-wash and depositional plains beyond (Figure 38). ERTS views of parts of the northern hemisphere where previous advances of continental glaciers have greatly modified the surface terrain are disclosing new patterns of morainal deposits, buried topography, and drainage shifts of significance to ground water hydrologists, construction (foundation) engineers, builders seeking gravel, clays, and other raw materials, land use planners, recreationalists, and farmers. The year-round surveillance of sea ice in the two polar regions (Figure 39) provides a continual record of the status of these frozen wastes to meteorologists concerned with weather-making conditions and shippers seeking new routes through the Arctic.

3. Internal changes and shifts of individual or grouped sand deposits, including extensive sand seas, can be looked at continuously to learn about the dynamics of aeolian processes and to predict encroachments on developed land. A typical example of sand features in an arid region appears in Figure 40.

4. Environmentalists have repeatedly expressed concern with the adverse influence of strip mining on the face of the land. As surface extraction of coal, clays, limestone, uranium, copper and other mineral products accelerates in response to demand, the transient and permanent damaging effects on vegetation, animal life, recreational activities, land development, and stream loads balance become ever more critical to be inventoried and assessed. ERTS offers a new means to monitor these effects over wide areas. The detection of strip-mined areas in ERTS imagery is straightforward. Maps made from ERTS (Figure 41) showing their extent and distribution are generally more current than those heretofore available to control commissions. Because strip mining advances rather rapidly, the repetitive coverage from ERTS allows updating on an annual schedule. Recovery of the land by replanting can also be monitored effectively from ERTS data. Land use maps made from ERTS prior to extraction serve as an essential data base for planning purposes; such a base has been prepared for

the Powder River basin in Wyoming as an aid to its future development by the coal industry. Finally, ERTS data on lineaments can play a vital role in problems of underground mine safety. The detection of surface fracture patterns in Ohio, noted in aircraft and then ERTS images, assists operators in spotting potential dangers and in deciding where new workings should be placed. Such data would also aid civil engineers in locating tunnels, roadways, and dams where failure along zones of weakness is a major hazard.

#### D. Summary:

Inspection of the first year's investigator products from ERTS leads us to conclude that this satellite can do most of the same prime tasks in geological applications that have been done in the past four decades with aerial photography. Only in the production of detailed (large-scale) stratigraphic and structural geology maps is there still a clear superiority inherent to the use of aircraft, largely because of the high resolutions obtainable from film cameras operating at the much lower altitudes. Where regional or synoptic coverage of large areas is required, the ERTS multispectral scanner proves to be a vastly better system. Such coverage offers new, hitherto unobtainable insights into the distribution of major structural elements of the crust and into certain types of dynamic processes that must be studied over wide areas simultaneously and in different seasons. The year-round, cyclic operational mode of ERTS also make effective use of such image enhancement factors as low sun angles, contrast-improving snow cover, bare tree conditions, vegetation associations, and moisture concentration effects.

### IV. SKYLAB: THE EREP PROGRAM

The first American space station, Skylab, had as its objectives the study of the Earth, the sun, man's response to prolonged space flight, and space technology. The Earth Resources Experiment Package (EREP), then, is but one of several operations to be carried out by the crew.

The EREP consists of five main instruments, as shown in Table 3. This payload is by far the most earth-oriented complex remote sensing package ever flown on a civilian space mission, and covers a wide-range of the electromagnetic spectrum (there are no force-field sensors). The fields of view vary from one instrument to another. The Skylab orbit has an inclination of 50°, which does not permit global coverage, but all of the conterminous United States is covered as well as much of western Europe.

Although the various instruments have numerical designations like formal space experiments (e.g., S190), they are not experiments in the sense that one

investigator is in charge of each and has temporarily exclusive use of the data. The instruments are instead considered facilities, and a large group of investigators receives the data, as with ERTS-1. Many investigators in fact have similar experiments for both ERTS and EREP.

The data load from Skylabs I and II was immense, and its distribution to the investigators, to say nothing of data analysis, will take considerable time. Accordingly, we can report no results at this point. (Two examples from the S190A and S190B cameras are shown in Figures 42 and 43.) However, a few pictures taken at crew option with hand-held 70 mm cameras will give some idea of the apparent success of the Earth Resources Experiment Package, although these pictures were not part of a formal experiment.

The Skylab astronauts were of course extensively trained to carry out the EREP experiments. However, they were also briefed, at their own request, on subjects that might be photographed on a time-available basis with hand-held cameras. These subjects included terrain, environmental, meteorological, and dim-light phenomena. This photography actually provides an excellent demonstration of the value of man in the acquisition of earth-resources and environmental data, since it required judgement, initiative, and manual skill. Skylab I returned several hundred hand-held 70 and 35 mm color photographs. Two have been annotated and described, as follows.

A. SL 2-5-469: S. California:

This low oblique view (Figure 44) covers the Mojave Desert and surrounding areas, with the view to the southwest. This region was designated a terrain/environmental photography site; features of interest included structure of the San Andreas fault and related faults, snow cover, and smog buildup in the Los Angeles basin.

The area shown includes essentially all the Mojave Desert. Albedo and color differences are chiefly due to rock and soil characteristics, with valleys being predominantly light-colored and mountains, in which bare rock is generally exposed, being dark. Some conspicuously dark areas are recent cinder cones and lava flows. The dark tone of the Sierra Nevada, San Bernadino Mountains, and Coast Ranges however is due to heavier vegetation. The northern part of the Sierra Nevada is snow-covered. Although there was heavy cloud cover over the western Los Angeles basin, smog distribution over the eastern part shows up clearly. It appears to be confined to the Los Angeles basin, with little spill-over into the Perris basin, and apparently none in the Imperial Valley or the Mojave Desert. There is some suggestion of a concentration in the vicinity of San Bernadino; if real, this would suggest that local sources were significant at this time.

Major physiographic and geologic features are well-displayed, although with relatively low resolution because of the obliquity of the picture. The importance of faulting in physiographic development is evident; although only a few of the main faults have been shown on the index map, most of the valleys are fault-controlled.

Two structures are especially well-displayed here (Figure 45). The first, at bottom, is the Las Vegas shear zone, which is expressed not only as the valley northwest of Las Vegas but also as the pronounced deflection of strata along the zone, showing obvious right-lateral displacement of strata north of Las Vegas (here overthrust). The Las Vegas shear zone has been investigated with the use of ERTS-1 pictures by Bechtold, Liggett, and Childs (1973). These investigators tentatively interpret it as an intra-continental transform fault joining spreading centers that are expressed as belts of Tertiary vulcanism. The Skylab photograph throws no obvious light on this possibility. However, there appears to be a definite suggestion of continuity in folded and thrust-faulted sedimentary rock trends across the northwest end of the shear zone. If verified by field checking, it would tend to confirm that the shear zone dies out here, at least as a strike-slip fault.

The obliquity of the Skylab photograph produces an interesting and possibly significant effect at lower left. The Providence — New York Mountains and the McCullough Range, as seen from this angle, appear to form a structural unit at a high angle to the Las Vegas shear zone, the Garlock fault, and several other faults in the Mojave Desert as shown by Hewett (1955). The valleys north of this chain have been shown as a possible fault zone, here provisionally named the Providence Mountains fault zone. Published maps show no single fault in this location, although the Cedar Canyon fault (Hewett, 1955) crosses it at about a  $35^{\circ}$  angle. This apparent lineament may of course be an artifact, since viewing along such a feature may produce a false impression of continuity. Further investigation at any rate seems called for.

#### B. SL 2-5-320: Milwaukee:

This near-vertical view (Figure 46) covers southern Wisconsin and northern Illinois, as well as part of Lake Michigan. The entire Great Lakes region was a designated photography site, primarily for environmental subjects. Among those shown here are contrails (upper left) and sediment plumes along the shore of Lake Michigan. The direction of sediment transport appears obvious.

The most striking feature is geologic: the radiating pattern at the center, with an apparent origin in Lake Winnebago. Study of published literature (Longwell, Flint, and Sanders, 1969) reveals that this area was covered by a

lobe of the last (Wisconsin) glaciation. The radiating pattern is the expression of aligned drumlins, which are tear-drop-shaped hills produced by deposition and later shaping by continental ice-sheets. Identification was made with the help of published information, since only a few of the largest drumlins are resolved on the 70 mm transparency and might not be identifiable as such without ground truth. Other features making up the radiating pattern are bedrock striations and boulder trains, both apparently below resolution limit of the Skylab picture.

The concentric light-toned feature, marked "terminal moraine" on the map (Figure 47), marks the limit of this lobe of the ice sheet, and is a composite of at least two individual moraines (deposits at the end of a glacier). Soil and vegetation differences are presumably responsible for the tone signature; in the 70 mm transparency, the moraine is a lighter green than the terrain to the south. Only one margin has been drawn on the index map, but the two moraines shown by Longwell, et al. (Figures 12-25) are visible in many areas. Concentric lakes and streams south of the moraine are evidently periglacial features.

The foregoing discussion is a very general one. There are many terrain features not identified here that could be mapped by a specialist familiar with the area, and it seems likely that some improvement in existing maps of glacial deposits could be made with this picture.

#### C. Summary:

Firm conclusions from the Skylab EREP experience would obviously be premature at this time. However, we can suggest the following preliminary lessons. First, it is now well-demonstrated that useful earth-resources surveys can be done effectively from large manned spacecraft or space stations. Obvious as this conclusion may seem, previous problems with attitude control, fuel requirements, and contamination of the local environment with spacecraft outgassing products made it by no means certain before the Skylab mission. Second, the availability of human versatility and judgement is a real advantage in earth resources surveys despite the great success of the automated ERTS-1 mission. Justification for this suggestion is based on the probability that an unmanned earth survey satellite as complex as the Skylab EREP would probably have had equipment malfunctions comparable to those corrected by the Skylab I and II crews. Third, the problem of conflicting time and pointing requirements is indeed a severe one; on several occasions, EREP passes were canceled to permit other experiments to be performed. This experience tends to reinforce the need for free-flying remote-sensing modules, such as could be supported by the space shuttle.

Generally, it seems safe to say that there is a real place for manned earth-resources missions, despite the demonstration by ERTS-1 that a wide variety of observations, especially requiring repetitive coverage, can be done by relatively small, unmanned satellites.

## V. CRITIQUE OF CURRENT EARTH-OBSERVATIONS PROGRAMS

As were their predecessors Gemini and Apollo, both ERTS and Skylab were conceived and carried out primarily as test and research programs. The degree to which operational earth-observing systems in space are implemented routinely in the future will depend largely on the evaluation of effectiveness in the present programs. Any assessment of results in geology, as in other disciplinary fields, must also consider limiting deficiencies and practical improvements in such system components as sensors, data recording and compression, initial data processing, and specialized enhancement techniques.

On the last of the March 1973 ERTS Symposium, a working group of geologists with remote sensing expertise convened to evaluate the investigations reported on during the meeting and to identify some of the evident shortcomings in the earth resources program as applied to geology. The reader interested in an in-depth review of their findings should consult the Summary on pp. 30-42 of Volume III of the Symposium Proceedings. We have extracted some of the more salient conclusions concerning deficiencies and proposed improvements from the summary for consideration in this section, to which we have added viewpoints of our own. Results from Skylab are still too preliminary to be given much weight in our thinking.

### A. Resolution:

A satisfying surprise from ERTS has been the amount and quality of geological information present in the imagery and digital data even though the resolution is 10 to 100 times lower than normal for conventional aerial photography. The tradeoff of reduced resolution for increased area of synoptic coverage has not cost as much as some critics had predicted. Many regional problems can be attacked at the ERTS level without need of the levels of detail obtainable now only from aircraft-mounted sensors, from manned space stations, or from short-lived military satellites.

Nevertheless, resolutions from satellite platforms must improve by estimated factors of 2 to 10 if certain applications in geology are to become feasible. Such increases in resolution would bring about significant improvements in identifying and mapping lithologic and stratigraphic units, in recognizing lower orders of faulting and jointing, in picking out the smaller (and more numerous)

patches of surface mineral alteration, in following many dynamic processes now modifying the land surface or the coastal shelves, and in monitoring extraction effects in the mineral industries. It seems safe to predict that synoptic imagery from satellites will compete with or supplant aerial photography for most applications when resolutions of 10-30 feet are achieved.

B. Directions of Illumination:

Angles of solar illumination lower than those reached during the 09:30-10:00 local times of ERTS passes will favor most geologic applications. Landforms of moderate to high relief, folded beds sculpted by differential erosion, and lineaments should be better highlighted at sun angles of 10°-20°. Sun-synchronous orbits with early morning or late afternoon passes would be optimum for viewing these features. However, color and brightness differences among rocks decrease at lower angles, so that lithologic and mineral stain identification is facilitated by operation at crossing times close to noon. In order to reduce the bias in orientation of linears introduced by direction of illumination, it appears necessary to view any surface at several times of day ranging between sunrise and sunset. This can be accomplished either by a succession of sun-synchronous satellites operating at different pass times or by high resolution pointable geosynchronous satellites that observe the same area as it undergoes daily and seasonal lighting changes.

C. Stereo Viewing:

More than any other discipline, geology would benefit extensively from full stereo coverage from satellites. Topographic information is invaluable in landforms analysis, measurement of dip in structural units, and some aspects of geologic mapping. Until stereo-viewing is standard in satellite imagery, aerial photos will retain a singular advantage for applications involving structural geology. Such viewing is best achieved by decreasing the frequency or repetitive coverage to increase the extent of sidelap or by operating two scanners or TV camera simultaneously in a spacecraft with slightly different lines of sight or a time delay in the imaging sequence.

D. Spectral Discrimination:

It is not clear whether broadening the range of spectral coverage and/or decreasing the band widths and/or increasing the number of channels or bands will aid materially in identifying rock types or composition. A precise color determination usually is insufficient to fix the rock type. Brightness, furthermore, is too sensitive to surface alteration effects and vegetation cover to be a diagnostic property. But, coupled with other information, both color and

brightness can suffice to identify many rocks especially if adequate training set exposures are examined.

Using a photometric colorimeter, it is possible to specify any measured color accurately on a chromaticity diagram. Two color values,  $x$  and  $y$ , are required; these are determined with narrow bandpass color filters.

Both the MSS and RBV multichannel sensors serve as crude colorimeters but the bandpasses are too wide and too few to provide good  $x$  and  $y$  values. Surface feature colors reconstructed in ERTS color composites deviate from those observed by eye or film. Addition of a blue band to the ERTS sensor systems would shift these colors closer to a natural or true state (limited however by atmospheric interference). Subdivision of the spectral range into narrower bands (more channels) should improve the discrimination of particular colors within the visible. However, classifications of rocks based on various combinations of "artificial" or "false" colors — probably as valid as natural color classifications — can also be established from measurements in two or more spectral intervals that together do not extend through the visible region. For rocks, probably only one "index" value for brightness is needed; the energy collected in the  $0.7\text{--}0.8 \mu\text{m}$  spectral interval (MSS band 6) appears to be a sensitive indicator of reflectivity.

#### E. Radiometry:

As a corollary to the color-brightness approach, more effective use of the radiometric capability of an MSS would further assist in rock type identification. A data bank of spectral signatures of the major rock types can be built up from ERTS observations of known lithologic units. This should be supplemented with ground measurements in the field and laboratory with radiometers having ERTS-matching spectral response curves or with suitable spectrometers.

#### F. Other Spectral Regions:

Acquisition of data in other regions of the electromagnetic spectrum may ultimately be essential to solving certain geologic problems. Variations in thermal inertia or in brightness temperatures may prove to be sensitive parameters by which rock types can be identified, especially where these data are used in conjunction with color and brightness measurements in the visible-near IR. Ratios of emitted (thermal) radiation in the  $9\text{--}12 \mu\text{m}$  region vary according to the silica content of observed rocks and thus form the basis of a semi-quantitative geochemical technique for determining the composition of silicates using space-borne sensors. Radar, already proven as a remote sensing tool of great value to structural geologists, can in principle be flown on satellites as well as on airplanes.

#### G. Processing Techniques:

Perhaps the most significant new advances in geologic applications from space observations will come from new image and digital data processing techniques not yet developed or proven. So far, very little of positive value to geologic studies has emerged from the use of color additive viewers or electronic enhancement devices such as those which convert grey levels or density steps in a black and white image to a color-coded rendition on a TV screen. However, these instruments have worked mainly on "raw" or unprocessed images. Controlled changes in the density or gamma curve can lead to photographs with tonal contrasts more suited to analysis in these instruments. Scenes produced through computer reprocessing often reveal previously hidden information when graphically displayed and manipulated on an image console. Fourier analysis, either with optical filters or by computer, promises to be a powerful technique for systematically measuring directional trends and extents of linear features and other non-randomly distributed spatial elements on the ground.

### VI. FUTURE DEVELOPMENTS IN ORBITAL REMOTE SENSING

Future developments of importance for geology, in addition to continuation of orbital techniques already demonstrated by ERTS and Skylab, can conveniently be discussed under three headings: (1) synthetic aperture radar, (2) thermal imaging systems, and (3) high-resolution visual range imaging systems. We shall discuss future satellite projects in general separately.

#### A. Synthetic Aperture Radar:

The geologic value of side-looking airborne radar (SLAR) is well-proven by the fact that at least two companies now carry out SLAR surveys on a commercial basis, largely for oil and mining companies. Two examples of the high quality products, containing exceptional amounts of geologic information, appear in Figures 48 and 49. Such surveys can be carried out rapidly, because of the all-weather capability of microwave frequencies and the wide swath of SLAR, and for this and economic reasons there has been no strong demand for orbital imaging radar systems (e.g., see "Useful Applications of Earth-oriented Satellites," V.2, National Academy of Sciences Summer Study, 1969). To merit development for space use, imaging radar must be competitive with orbital photography and airborne radar; the following considerations indicate that this may in fact be true.

Under the best viewing conditions (particularly low sun angles) ERTS and EREP can produce image mosaics comparable in information content to mosaicked radar images (Figures 50 and 51). However, the superiority of orbital radar

to orbital photography lies first in its all-weather, day-night capability. Geological features of course do not change rapidly (i. e., in a few days) as a rule, and it might seem that for geological coverage one could simply wait for favorable conditions. However, there are many parts of the world, such as the Isthmus of Panama, that are essentially permanently cloud-covered, for which weather penetration would be helpful. A second area of superiority is control of illumination azimuth; in principle, one can obtain almost any azimuth with a self-illuminating system, unlike those dependent on sunlight. Third, lower frequencies, on the order of 400 to 600 MHz (L-band) can provide some penetration of dry alluvium and light vegetation (Dellwig, 1969). This is not possible in the visual and near-visual wavelengths. In general, orbital radar offers the user complete control of the incident illumination, whereas with orbital photography he must take what the sun provides.

Comparing orbital radar with airborne radar, we see the following advantages. First, and most important, orbital system can provide global repetitive coverage at regular intervals, a fundamental advantage of earth-satellites in general. This would be useful — in fact essential — for monitoring ice conditions in oceans, lakes, and rivers, for which aircraft systems would be hopelessly expensive on a global basis. Other possible applications include worldwide monitoring of sea state, oil spills, vegetation, snow-pack, and glacial advance/retreat rates. These are mostly non-geological applications. However, a world tectonic map would be of great value, and could probably be produced rather rapidly with orbital radar. A second advantage of orbital radar compared with airborne radar is the greater stability provided by spacecraft, since there are no aerodynamic forces to disturb the transmitter. This assumes that the spacecraft attitude control system is designed to provide proper conditions for the radar survey. It should be noted here that an orbital radar system was flown with great success on the Apollo 17 mission; although not intended for terrain rendition, it nevertheless produced usable imagery (W. Brown, personal communication).

It appears that there is real value in orbital radar systems for geology and other fields, and the possible development of such systems is therefore being studied by NASA for the Earth Observatory Satellite. It is not possible to specify in detail just what sort of instruments are needed. Present thinking favors X-band, cross-polarized radar. Synthetic aperture is of course a necessity for orbital systems if high resolution is desired, because the antenna size would be prohibitive for a real-aperture space system.

#### B. Thermal Imaging Systems:

As mentioned previously, the part of the thermal region in the electromagnetic spectrum for (3-5 and 8-13  $\mu$ m) which there are atmospheric "windows" is

of potential interest for geology. However, the practicability and value of orbital thermal surveys using high spatial resolution imaging systems remains to be demonstrated. One problem that can be easily foreseen is incompatibility between mission requirements for visual range and thermal range sensors. For rendition of terrain detail, as for example to reveal geologic structure, early morning or evening photography is best. But to bring out differences in thermal properties of rocks and soils, such times are precisely the worst because the various warming curves tend to converge then. Another problem is separating slight internally-caused temperature differences from those caused by solar radiation and other external causes, since the latter may swamp the former.

If problems such as these can be resolved, geologic applications for orbital thermal surveys can be foreseen. One such is the repetitive monitoring of active volcanoes and volcanic zones, perhaps in conjunction with DCPs, to aid in prediction of eruptions and throw light on the relation of geologic structure to eruptions. The feasibility of doing this with airborne sensors was demonstrated by Fischer, et al. (1964) with infrared surveys of volcanoes on the island of Hawaii by means of scanning radiometers. Orbital instruments would lose in spatial resolution, but if this loss could be tolerated, comparable surveys could be carried out in areas of high hazard, such as the andesitic volcanoes surrounding the Pacific Ocean.

A similar objective, but one of considerably more difficulty, would be the detection and mapping of undiscovered geothermal anomalies of possible value for power generation. External temperature variations mask detection of very slight temperature variations, and such surveys are not feasible from orbit at this time. Better sensors and accumulation of many cycles of data may eventually make this possible, however.

Another geological application of thermal surveys from orbit is the detection of previously unknown fresh-water discharge into the ocean. This has been demonstrated by Fischer, et al. (1966), with the same surveys cited earlier over volcanic areas of Hawaii. Imagery taken over the coast revealed many unknown springs because they were cooler than the sea water.

A final possible geologic application of thermal imagery is the delineation and mapping of lithology on the basis of differential thermal response to diurnal temperature changes. Discrimination between limestone and dolomite has been demonstrated by Watson, et al. (1971) in Oklahoma (Figure 52). When combined with other techniques, thermal surveys might thus aid in world geologic mapping in areas such as North Africa and Central Asia that are well-exposed but poorly-mapped.

### C. High-resolution Visual Range Imagery:

There is no inherent reason that imagery from orbital altitudes with resolutions of a few meters cannot be obtained. Katz (1963), for example, showed over ten years ago that ground resolution of better than one meter could be produced from 150 miles altitude with a ten-foot focal length (assuming 100 lines/mm resolution for the camera-film system). This performance is comparable to standard aerial photography, and if actually achieved from orbit, would permit orbital photography to replace aerial photography in many applications. In geology, there is no downward limit to the resolution that can be used, since major structures in, for example, batholiths, may be expressed by individual crystals and microscopic textures. More practically, resolution on the order of ten feet is probably necessary for serious geologic use of orbital photography in heavily vegetated areas with dense networks of roads, fences, and power lines, all of which obscure and confuse geologic detail. ERTS-1 pictures, for example, have been far less useful in the eastern United States than in the far west; increased resolution would probably change this situation.

## VII. SPACE SYSTEMS BEYOND ERTS AND EREP

The user community — state and federal agencies, the universities, industry, resources managers — together with the Congress and the informed public have given strong positive response to the products and projected applications stemming both from the ERTS and the Skylab resources experiments. As practical uses accumulate, increasing support from these groups for continuation and gradual expansion of the earth resources program can be safely predicted, especially in view of the awakened concern in this nation and the world for the growing problems in energy, resources and environment. New generations of earth-observing platforms are now being planned and await only approval to move off the drawing boards and into the skies. Both advanced experimental and operational satellite systems are under consideration. Some salient facts about two such programs for the future will be considered briefly here.

### A. EOS:

Flights of several Earth Observatory Satellites (EOS) have been proposed for the late 1970s, following a second ERTS launch (with an added thermal channel on the MSS) and the end of the Nimbus series. By carrying wider complements of sensors, these satellites will combine the functions of the meteorological and land resources satellites and will also be equipped to make a variety of ocean surface measurements. Mission parameters are similar to ERTS — near-polar, circular orbit at an altitude between 550 and 580 miles on a 17 day

repeat cycle with equator-crossing around 0930 local sun times. Comments about three candidate sensors, of particular interest to geology, are in order:

(1) Thematic Mapper (TM)—This instrument is an extension of the MSS on ERTS. The principal improvement is in resolution: better than 130 feet is now being sought. Spectral channels in the 1.55-1.75 and the 2.08-2.35  $\mu\text{m}$  range are added; these are of particular interest in plant and soil discrimination but offer little new information about rocks *per se*. The thermal channel (10.4-12.6  $\mu\text{m}$ ), like that of ERTS, is also of limited use for geologic purposes because of the unfavorable local solar time at which data are gathered. A pre-dawn (0500) and post-noon (1300) pass, and perhaps a third after midnight (0100) would provide near-optimum viewing times for rock identification using the thermal inertia principle. However, two or more EOS's flying concurrently at different pass times would be required to meet this objective.

(2) High Resolution Pointable Imager (HRPI)—This "pushbroom" scanning instrument is steerable, that is, it can be shifted and then aimed on command to cover selected targets falling with 26 mile wide swaths that are offset by increments normal to the ground track line. Thus, it would be possible to follow the meanderings of a wide stream and its valley or a shoreline by taking a series of images as the HRPI's optical system assumed new positions. Although the width of the flight strip or swath is reduced relative to the TM, so that some of the advantages of synoptic coverage are lost, the improvement in resolution to approximately 50 feet facilitates solution of some geologic problems that ERTS cannot handle, as for example:

- a. Delineation and mapping of smaller stratigraphic units.
- b. Monitoring of variable geologic features, such as migrating dunes, glaciers, or coastal features, with much better temporal resolution.
- c. Mapping of small landslides and lava flows.
- d. Detailed joint or vein/dike maps over large areas.

(3) Synthetic Aperture Radar (SAR)—As now conceived, this imaging instrument would have an instantaneous field of view of  $\sim$  65 feet and would examine a swath 40 nautical miles wide at a depression angle of  $50^\circ$ . Under these conditions, the same area would be revisited every 44 days. In time, world-wide data on geologic structures could lead to a global tectonic map as well as a series of radar mosaics showing major landforms. Because there are some regions on Earth that are almost always hidden by clouds, the mosaics would give the complete coverage not attainable from TM or HRPI.

## B. SEOS:

The Synchronous Earth Observatory Satellite would be a geostationary platform placed in orbit approximately 22,500 miles from Earth. Equipped with a large telescope (9.1 meters focal length; 1.7° FOV), its scanner system can observe a region of the earth's surface within an ellipse whose long axis extends over about 110° of latitude. Thus, if positioned above the 100°W longitude line, SEOS could acquire off-nadir images of the entire U.S., southern Canada, Central America, South America to the Amazon, and much of the Atlantic Ocean and the eastern Pacific. Several SEOS's in appropriate locations would cover most of the continental land mass of our planet.

The advantage of a SEOS system is that it can be pre-programmed or commanded to look at any target within its observational area at any given time (including immediately after a disaster) as long as the scene is not cloud-obscured. Two modes of operation are being considered:

- a. Field of View 200 x 1000 km at a 200 m ground resolution; spectral bands of 0.5-0.7 and 0.8-1.2  $\mu$ m.
- b. Field of View 750 x 750 km at ground resolutions ranging from 0.5 km for the 0.8-1.2  $\mu$ m spectral range through 1.5 km for the 0.4-0.8, 3.4-4.1, and 10.5-12.5  $\mu$ m bands, to 5 km for the 6.3-6.7  $\mu$ m band.

Under these viewing conditions, many transient phenomena, e.g., severe storms, floods, drifting ice, snow cover distribution, coastal sedimentation, forest fires, and oil spills can be monitored effectively as they are reported or detected. Some dynamic geologic phenomena, such as volcanic eruptions, certain aspects of earthquake damage, and storm-caused shoreline erosion, can also be monitored but many other phenomena cannot be assessed at the resolutions cited.

## VIII. SUMMARY AND PROGNOSIS

Remote sensing from space platforms is neither a panacea nor an all-purpose black-box system that will revolutionize the geological sciences. It is merely another tool available to geologists to study — and sometimes solve — certain problems. In perspective, ERTS, EREP — and their predecessor and follow-on spacecraft — are essentially only sophisticated extensions of aerial remote sensing systems. By way of an analogy, space observation platforms serve much the same function as a low-powered objective lens on a petrographic microscope: one can use the lens to look at large parts of a thin section to study overall textures and mineral distribution but other objectives of higher magnifications are brought into play to secure detailed data from selected small areas

where individual grain measurements can be made. The space platforms, then, comprise a new, extremely useful, and perhaps vital component in a multi-level system for observing the Earth over a range of "magnifications". Like aerial photography, space imagery has its own sets of limitations and special advantages coupled to the particular problems addressed. Unlike most conventional aerial photography, however, space imagery is particularly amenable to such specialized processing as optical enhancement techniques, signatures determination, computerized feature recognition and classification, and interactive computer-graphics displays — largely because of the well-designed and precision-built multispectral sensors that are being flown in space. As these new approaches are proved out, an inevitable feedback should influence operational aerial photo systems to utilize more of the remote sensing methodology that even now is moving out of the experimental stage. The ultimate criterion for success in remote sensing from any platform level will be measured by the degree to which problems are solved and tasks are accomplished better, quicker, and cheaper than by the standard aerial survey methods of the past. Presently, "the jury is still out" on evaluation of this success criterion.

A potentially large payoff looms for geology. Some kinds of scientific or applications efforts will clearly benefit from data acquired through space observations systems — other won't. The danger has been, and still is, one of overselling or misrepresentation. Certain claims made by early proponents of remote sensing have not been substantiated, either because of technical insufficiencies or because fundamental scientific principles are misapplied or violated. Any promotion of the remote sensing approach to geologists should be based solidly first on demonstrated accomplishments (reasonably supported by scientific analysis) and then on prospects for further achievements (reasonably supported by sensible extrapolations of established principles).

We now know enough from the Gemini-Apollo-Nimbus-ERTS-EREP experiences to list the major accomplishments in geology and perhaps even rank them on a value scale. Those of a primarily scientific nature (in order of decreasing importance or utility) in our opinion are:

- 1) Analysis of regional structural-tectonic relationships and their significance.
- 2) Classification of geomorphic (landforms) units within a regional context.
- 3) Editing of small-scale maps to modify contacts, re-define fractures systems, and recognize new units.

- 4) Surveillance of some dynamic geologic processes (sediment transport; glacial movements; aeolian activities) that can be monitored through repetitive coverage in a suitable time frame.
- 5) Specification of lithologic types and variants on a compositional basis.

Those accomplishments that are principally applied in nature include:

- 1) Observations of geologic phenomena that have engineering or environmental interactions, as, for example, land erosion and sand dune migration, coastal sediment shifts, glacial moraine distribution, mineral extraction effects, fracture systems in mining districts (mine hazards), newly discovered faults in zones of high seismicity).
- 2) Recognition of surface features indicative of conditions favorable to mineral concentration; mainly, lineaments and other structural patterns and, to a lesser extent, weathering or staining tied to mineral decomposition.
- 3) Detection of thermal "hotspots" as sources of geothermal power and as indications of possibly hazardous volcanic activity.
- 4) Use of orbital imagery as an adjunct to aerial imagery to assist photo-geologists in map preparation for exploration purposes.

We feel, in closing, that a broad challenge still remains for geologists to more fully exploit and extend these accomplishments. Greater advantage should be taken of the "arsenal" of remote sensing instrumentation now developed and more reliance placed on electro-optical and computer-based processing and interpretive systems. New methodologies must be sought and new applications considered. At the same time, though, geologists should avoid becoming too dependent on automated data gathering and processing and should remember that their resulting interpretations need to be continually tested in the field. Above all, geologists utilizing remote sensing must realize that, especially from space altitudes where resolution drops and many surface features "blur" into composite patterns, they have to learn to treat surfaces as surfaces. All components — organic and inorganic; natural and man-made — contribute to the information presented. For this reason, geologists who wish to use aerial and space observational systems are well-advised to team up with users and specialists in other fields. The multidisciplinist approach to remote sensing needs a geologist on the team — just as the geologist will need to rely on the experience and counsel of colleagues with different specialties if he is to continue to apply his own remote sensing skills to the study and exploration of the Earth.

## REFERENCES

- Colwell, R. H., and others, Monitoring earth resources from aircraft and spacecraft, SP-275, National Aeronautics and Space Administration, Washington, D.C. 170 p., 1971.
- Dellwig, L. F., An evaluation of multifrequency radar imagery of the Pisgah crater area, California, Modern Geology, 1, 65-73, 1969.
- Fischer, W. A., R. M. Moxham, F. Polcyn, and G. H. Landis, Infrared surveys of Hasaiian volcanoes, Science, 146, 3645, 733-742, 1964.
- Fischer, W. A., D. A. Davis, and T. M. Sousa, Fresh-water springs of Hasaii from infrared images, Hydrologic Investigations Atlas HA-218, U.S. Geological Survey, Washington, D.C., 1966.
- Katz, A. H., Observation satellites, p. 217-245 in New Space Handbook, R. W. Buchheim, editor, Random House, New York, 351 p., 1963.
- Lathram, E. H., Nimbus IV view of the major structural features of Alaska, Science, 175, 1423-1427, 1972.
- Lowman, P. D., Jr., Space photography - a review, Photogrammetric Engineering, XXXI, 1, 76-86, 1965.
- Lowman, P. D., Jr., Apollo 9 multispectral photography; geologic analysis, X-644-69-423, Goddard Space Flight Center, Greenbelt, Md., 53 p., 1969.
- Lowman, P. D., Jr., The Third Planet, Weltflugbild, Zurich, 172 p., 1972.
- Lowman, P. D., Jr., and H. A. Tiedemann, Terrain photography from Gemini spacecraft: final geologic report, X-644-71-15, Goddard Space Flight Center, Greenbelt, Md., 75 p., 1971.
- Merifield, P. M., and others, Satellite imagery of the earth, Photogrammetric Engineering, XXXV, 7, 654-668, 1969.
- Merifield, P. M., Some aspects of hyperaltitude photography, Report No. 1, Contract No. NAS 5-3390, Lockheed-California Company, Burbank, California, 1964.
- Sabatini, R. R., G. A. Rabchevsky, and J. E. Sissala, Nimbus Earth Resources Observations, Technical Report No. 2, Contract NAS 5-21617, Allied Research Associates, Concord, Mass., 256 p., Nov. 1971.

REFERENCES (continued)

- Watson, K., L. C. Rowan, and T. W. Offield, Application of thermal modeling in the geologic interpretation of IR images, Proceedings of the Seventh International Symposium on Remote Sensing of Environment, p. 2017-2041, U. of Michigan, Ann Arbor, Michigan, May 1971.
- Wobber, F. J., Space photography as a sedimentological research tool, pre-print, paper presented at the Semiannual Meeting of the American Society of Photogrammetry, San Antonio, Texas, Oct. 1, 1968.

Table 1A

## **PRIMARY GOALS: ERTS - A & B**

- TO OBTAIN MULTISPECTRAL IMAGES OF THE EARTH'S SURFACE.
- TO OBTAIN SPECIFIC MEASUREMENTS FROM REMOTE, AUTOMATIC SENSOR STATIONS AT FIXED LOCATIONS.
- TO OBTAIN MULTISPECTRAL RADIOMETRIC SCANNER DATA THAT CAN BE USED IN AUTOMATIC SIGNATURE RECOGNITION TECHNIQUES.
- TO DEVELOP THE DATA PROCESSING TECHNIQUES REQUIRED TO MAKE THE SENSOR DATA A USEFUL PRODUCT.

## **BASIC MISSION REQUIREMENTS**

- REPETITIVE OBSERVATIONS AT THE SAME LOCAL TIME.
- CAPABILITY OF NEAR GLOBAL COVERAGE.
- MULTISPECTRAL PHOTOGRAPHIC OR IMAGING DATA OF A LARGE SCENE WITH RESOLUTION SUFFICIENT FOR MAP UPDATING.
- MINIMAL IMAGE DISTORTION.
- IMAGE OVERLAP IN DIRECTION OF FLIGHT.
- IMAGE SIDELAP FROM ADJACENT ORBITS.
- COVERAGE REPEATED IN LESS THAN THREE WEEKS.
- OPERATING LIFE OF ONE YEAR OR LONGER.

Table 1B

**ORBIT**

|                      |   |
|----------------------|---|
| ● BASIC REQUIREMENT  | SUN SYNCHRONOUS (99° RETROGRADE)  |
| ● SUN ANGLE          | 35° ABOVE HORIZON AT 50° NORTH LATITUDE AT VERNAL EQUINOX   |
| ● ALTITUDE           | 496 NAUTICAL MILES  |
| ● ECCENTRICITY       | LESS THAN 0.006   |
| ● SUBSATELLITE TRACK | THE IMAGE 100 n.m. SWATH FOR A PARTICULAR ORBIT ON A GIVEN DAY ADJACENT TO THE SWATH FOR THE SAME NUMBERED ORBIT ON THE PREVIOUS DAY WITH A SIDELAP OF 10%. |
| ● PERIOD             | 103 MIN. (APPROX.)  |

**LAUNCH VEHICLE AND SITE**

|                            |   |
|----------------------------|---|
| ● LAUNCH VEHICLE           | DELTA N (NASA DESIGNATION)  |
| ● CAPACITY                 | 1200 POUNDS   |
| ● EXPECTED FUTURE CAPACITY | 1600 POUNDS   |
| ● LAUNCH SITE              | WESTERN TEST RANGE<br>VANDENBURG AIR FORCE BASE<br>LOMPOC, CALIFORNIA |

Table 2  
Applications of ERTS to Geology

Map Editing:

Boundary and Contact Location  
Stratigraphic and/or "Remote Sensing" Unit Discrimination  
Scale-change Corrections  
Computer-processed "Materials" Units Maps

Landforms Analysis:

Regional or Synoptic Classification and Mapping  
Thematic Geomorphology (e.g., Desert, Glacial, Volcanic Terrains)

Structural Geology:

Synoptic Overviews of Tectonic Elements  
Appraisal of Structural Styles  
Lineaments (and "Linears") Detection and Mapping  
Metamorphic and Intrusion Patterns  
Recognition of Circular Features

Lithologic Identification:

Color-Brightness (Spectral Reflectance) Classification  
Ratio Techniques  
Photogeologic Approach

Mineral-Exploration:

Reconnaissance Geologic Mapping  
Lineaments Trends (especially Intersections)  
Surface Coloration ("Blooms" and "Gossans")  
Band Ratio Color Renditions

Engineering and Environmental Geology:

Dynamic Geologic Processes (Sedimentation and Coastal Processes; Sea Ice; Active Glaciers; Permafrost Effects; Landslides and Mass Wasting; Shifting Sand Seas; Land Erosion)  
Strip Mining; Surface Fractures - Mine Safety  
Construction Materials

Table 3

## Earth Resources Experiment Package

| Experiment No. | Name  | Purpose  |
|----------------|---|--|
| S190A          | Multispectral Photographic Cameras (6)            | Obtain precision multispectral photography in visual and near visual range, using returned film.   |
| S190B          | Earth Terrain Camera (1)                          | Obtain high-resolution color photography in the field of view of the S190A cameras.  |
| S191           | Infrared Spectrometer                             | Provide spectral data on earth's surface in 0.4-2.4 and 6.2-15.5 micrometer region.  |
| S192           | Multispectral Scanner                             | Obtain line-scan images in 13 bands, from 0.4-12.5 micrometers, with a 74 km swath width.  |
| S193           | Microwave Radiometer/ Scatterometer and Altimeter | Provide simultaneous measurement of microwave reflectivity and emissivity of land and ocean areas; obtain altimetry data over ocean areas for sea state studies. |
| S194           | L-Band Radiometer                                 | Measure and map brightness temperature of earth's surface at 1.43 GHz frequency.   |

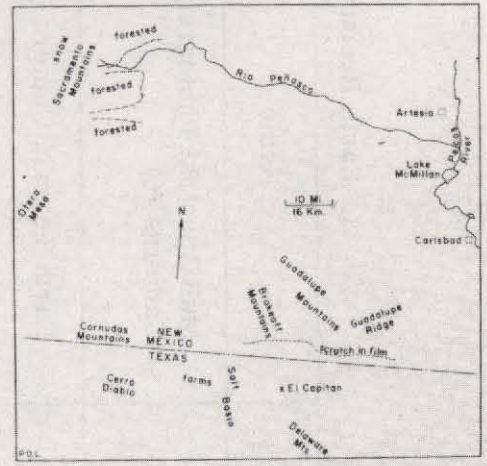
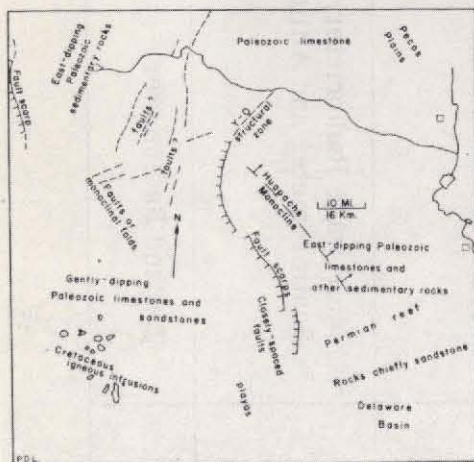
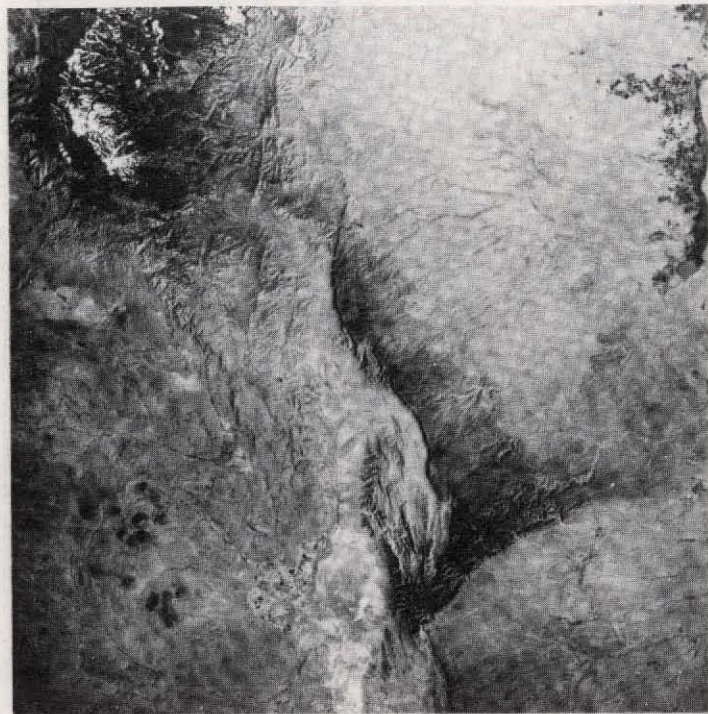
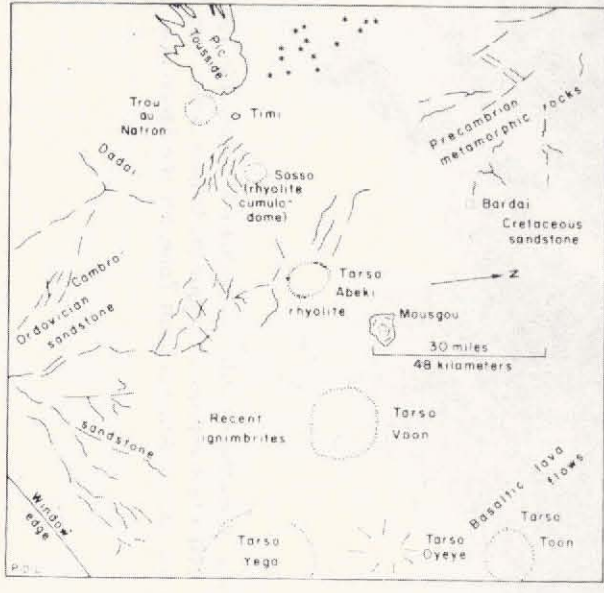


Figure 1. Apollo 6 photo (original in color) of the El Capitan region of west Texas and New Mexico.  
(Interpretation by P. D. Lowman, Jr.)



INDEX MAP  
APOLLO 9 PHOTOGRAPHS 9-20-3107  
Lithology after Vincent (1970)

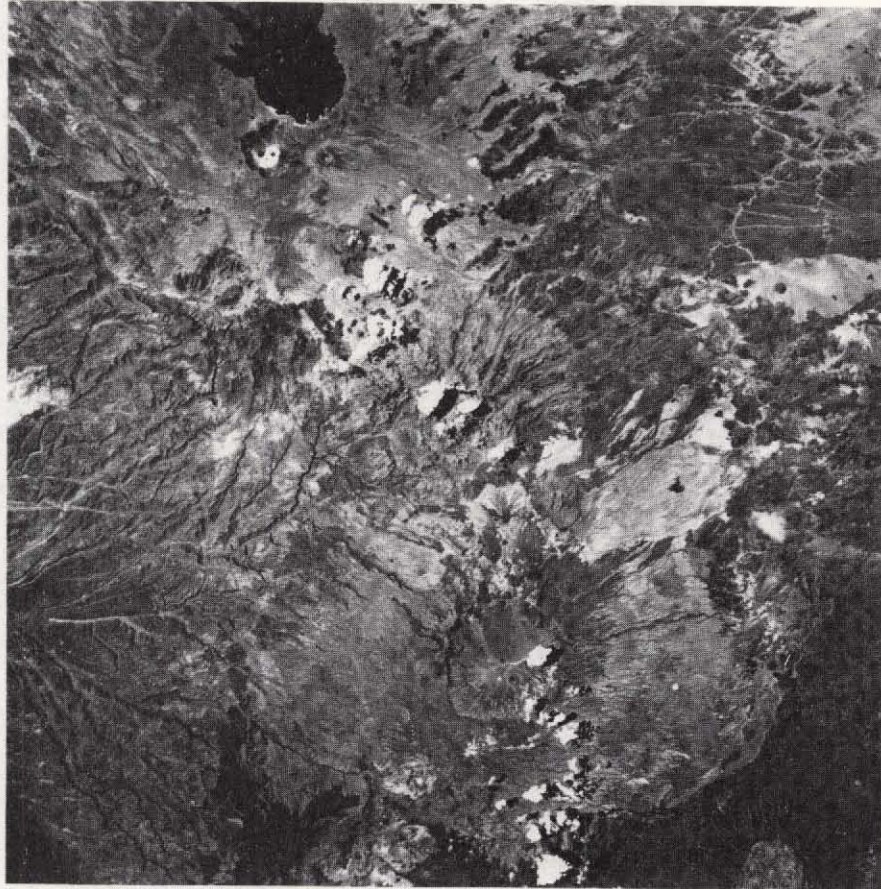


Figure 2. Apollo 9 photo showing volcanic features, rock types, and structural units in the Tibesti Mountains of Libya (north) and Chad (south).  
(Interpretation by P. D. Lowman, Jr.)

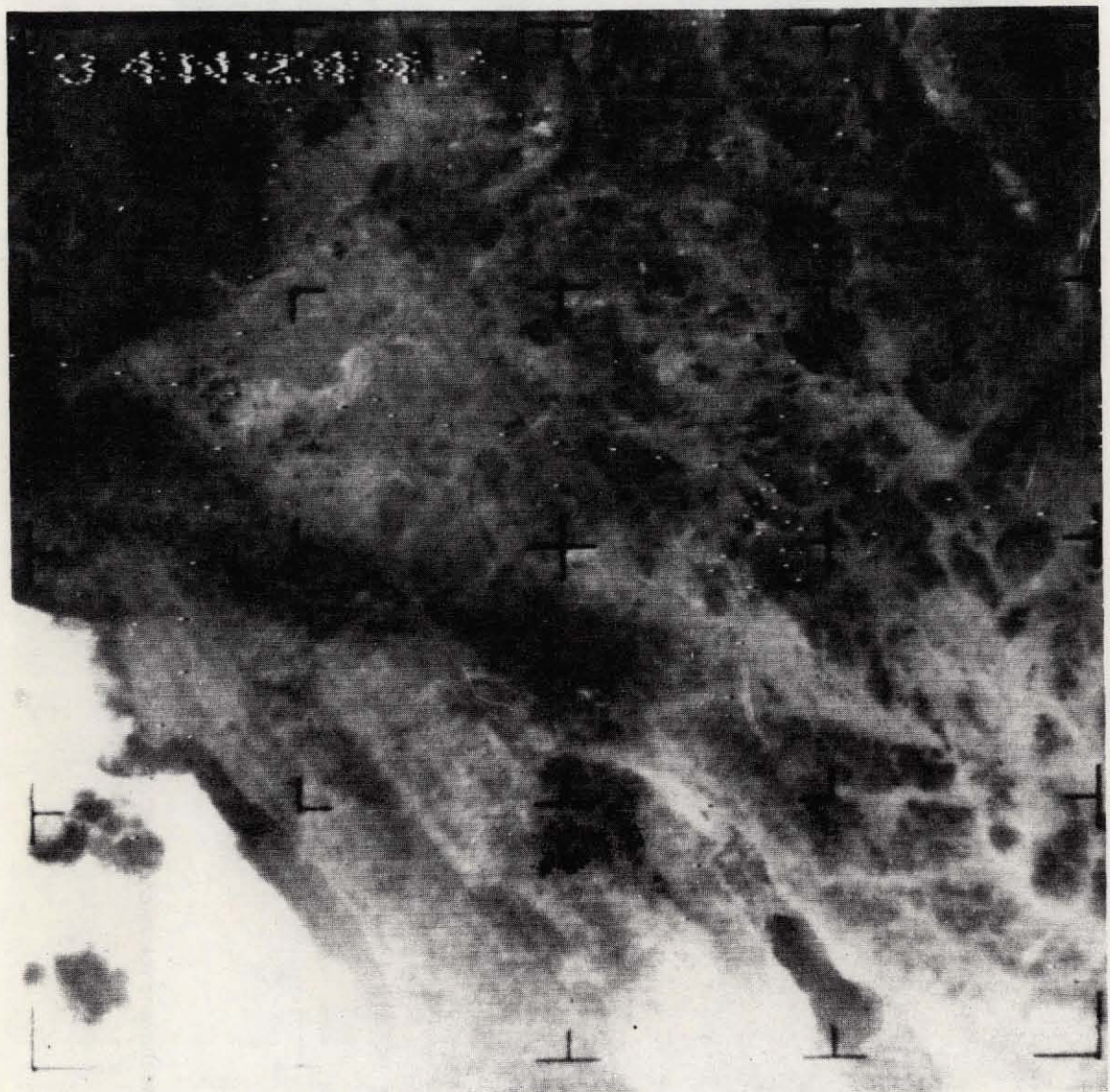


Figure 3. Video image of a portion of southern California made from Nimbus I in 1964. Area covered is about 300 miles on a side. Major features shown include the Mojave Desert, Los Angeles Basin, Transverse Ranges, San Andreas Fault Zone, and the Salton Sea.

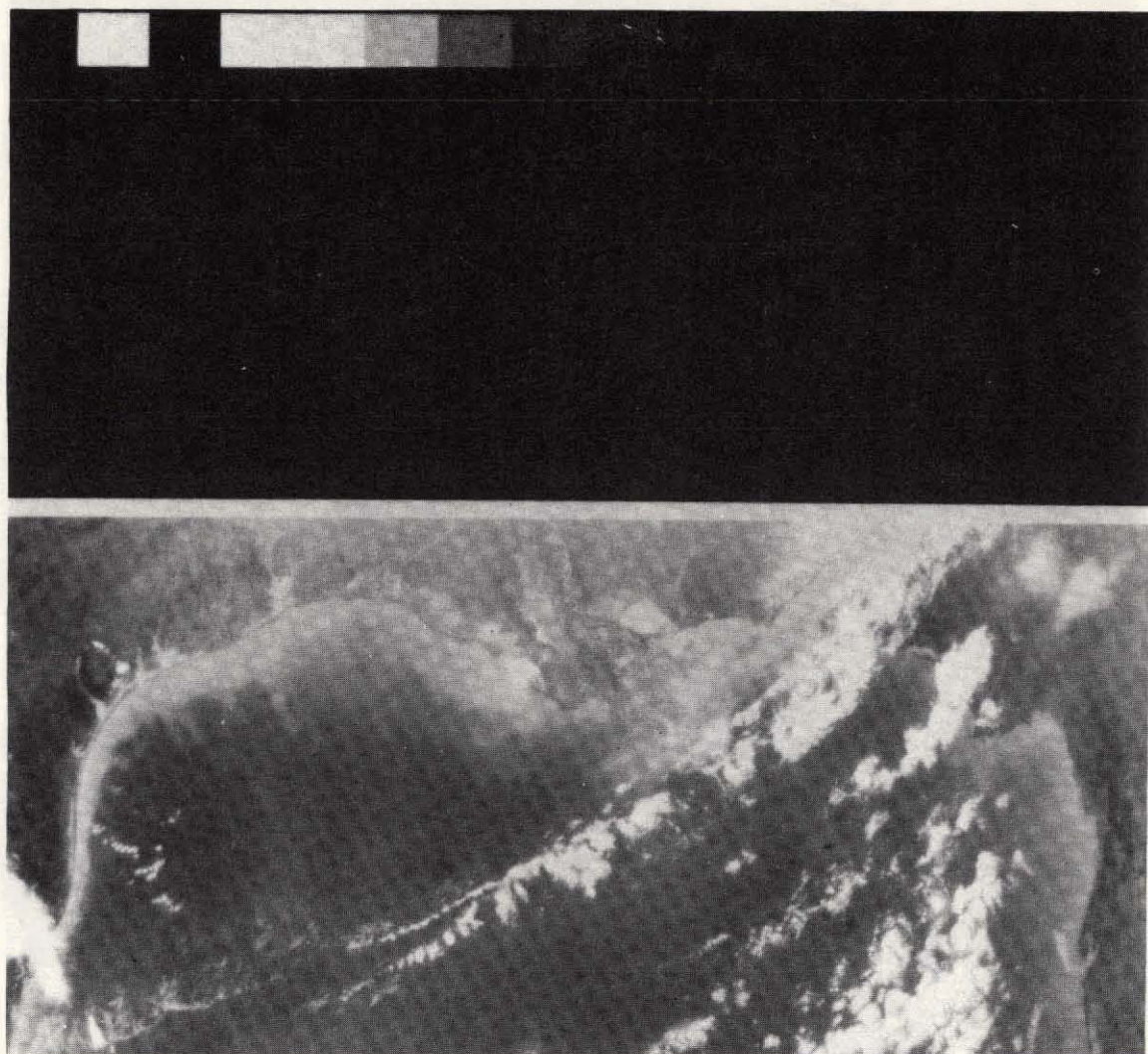


Figure 4. Image produced from  $10.7 \mu\text{m}$  thermal channel signals of the SCMR on Nimbus 5 showing water temperatures (lighter tones are cooler) in the Gulf of Mexico offshore from the coast between southern Texas and western Florida. (Courtesy W. Hovis, NASA Goddard.)

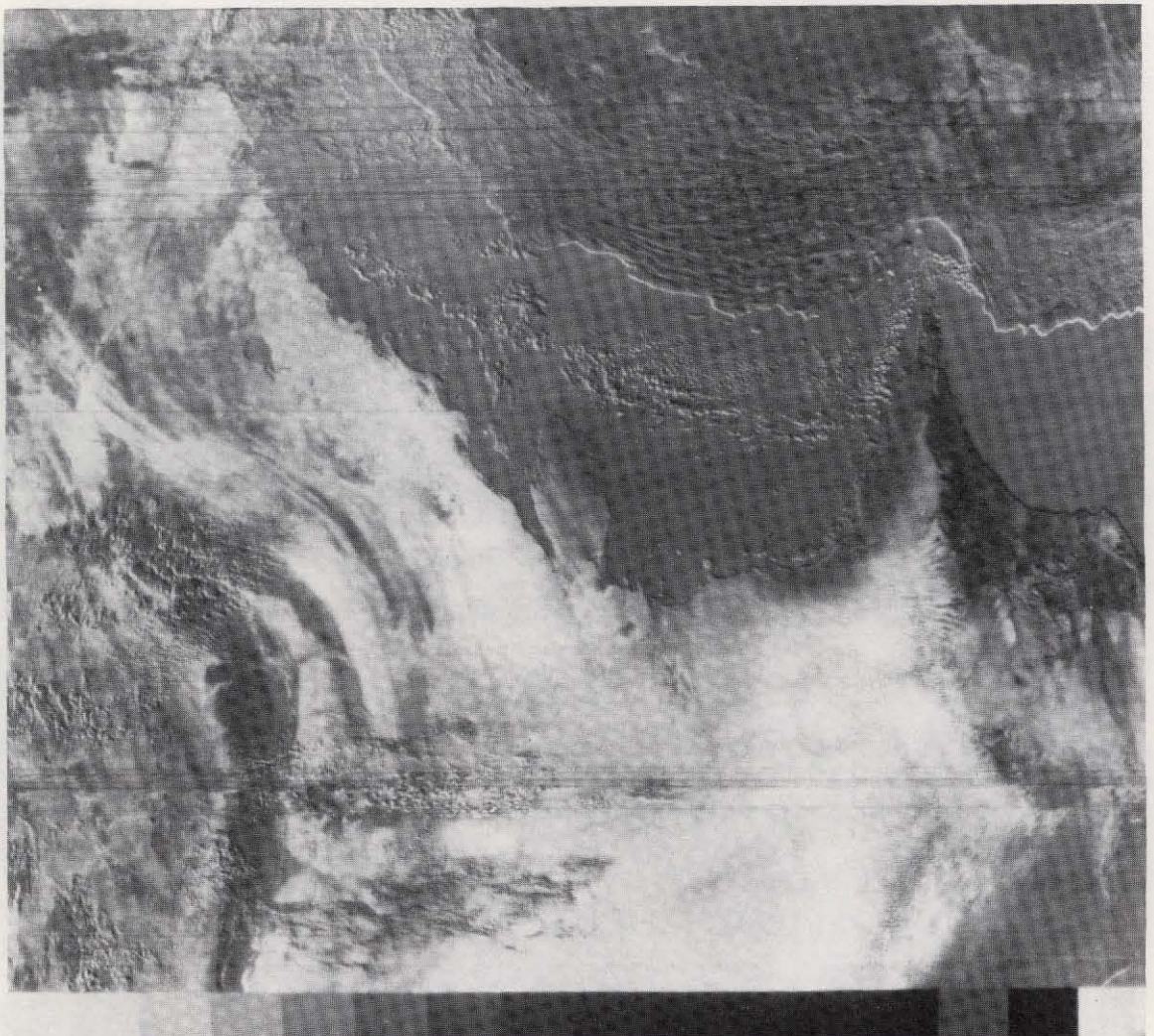


Figure 5. Image produced by subtracting the temperature values obtained from the  $8.8 \mu\text{m}$  thermal channel on the Nimbus 5 SCMR from those of the  $10.7 \mu\text{m}$ . Region depicted includes the Rub al Khali desert of Arabia, Oman peninsula, Persian Gulf, and the Zagros Mountains of Pakistan. Silica-rich areas, such as the quartz desert sands, are bright (light-toned); areas of lower silica content (including vegetation) are darker. (Courtesy W. Hovis, NASA Goddard.)

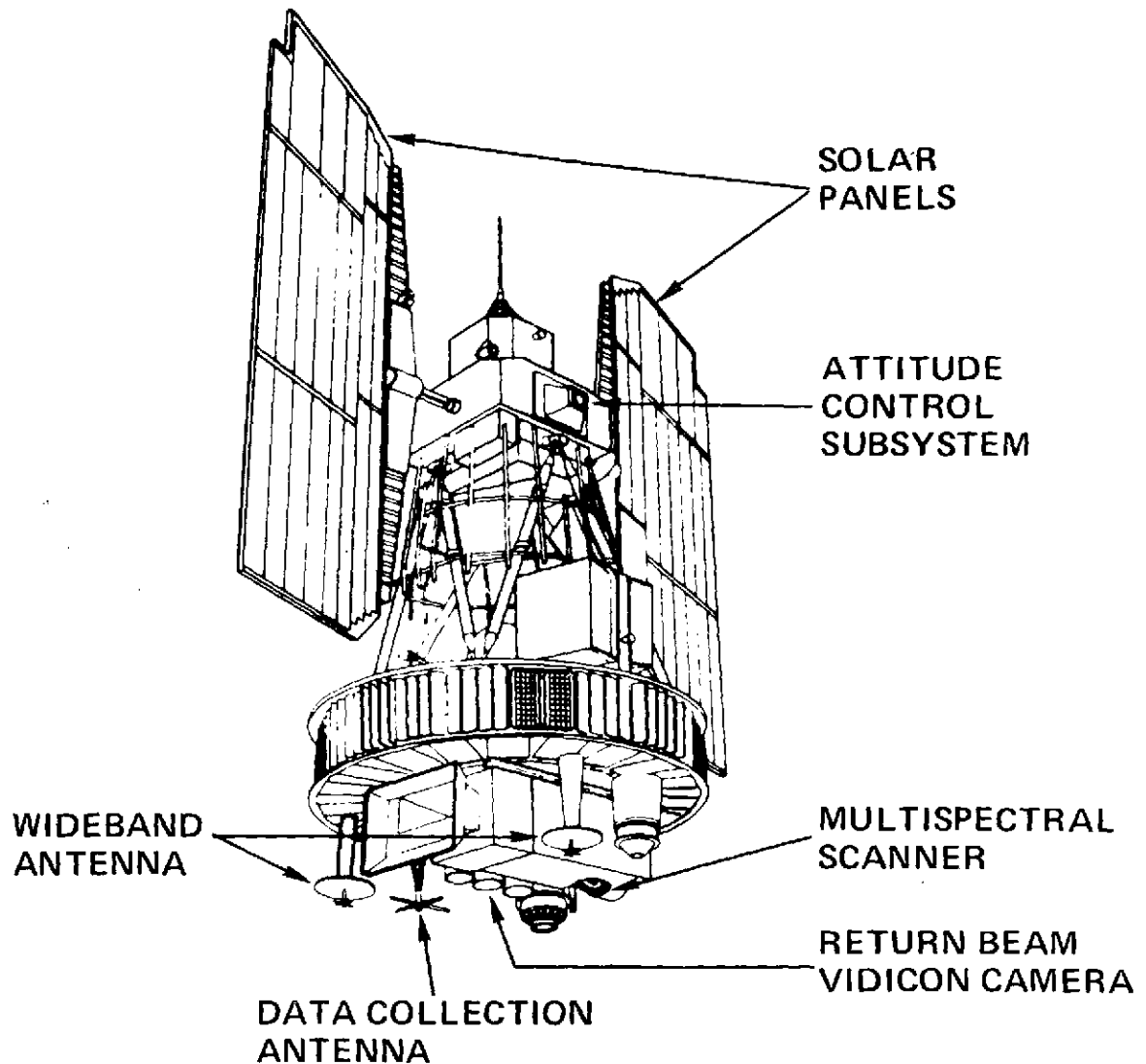


Figure 6. Schematic drawing of the ERTS-1 spacecraft indicating location of the sensor systems.

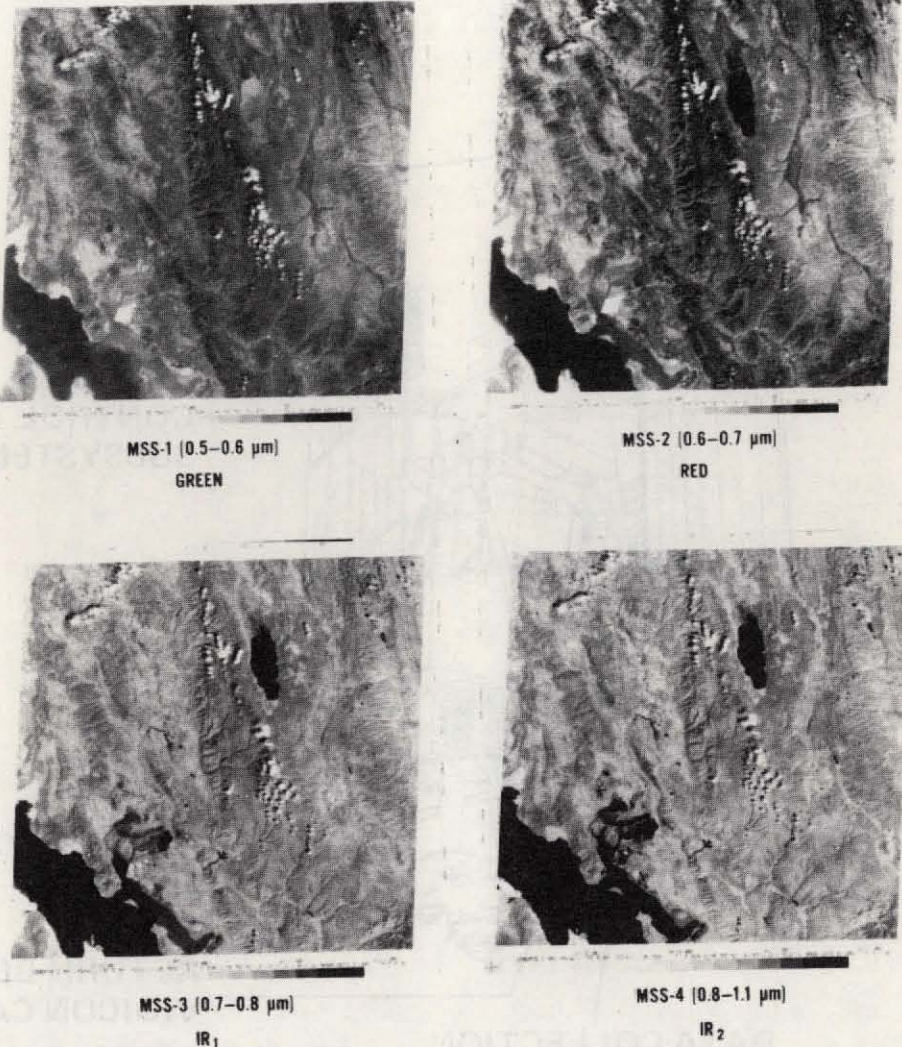


Figure 7. Illustrative photo-images produced from Bands 4 (upper left), 5 (upper right), 6 (lower left), and 7 (lower right) of the ERTS Multispectral Scanner (MSS). Area shown includes the Great Salt Lake, Bear Lake, the Wasatch Range, and other features in Utah.

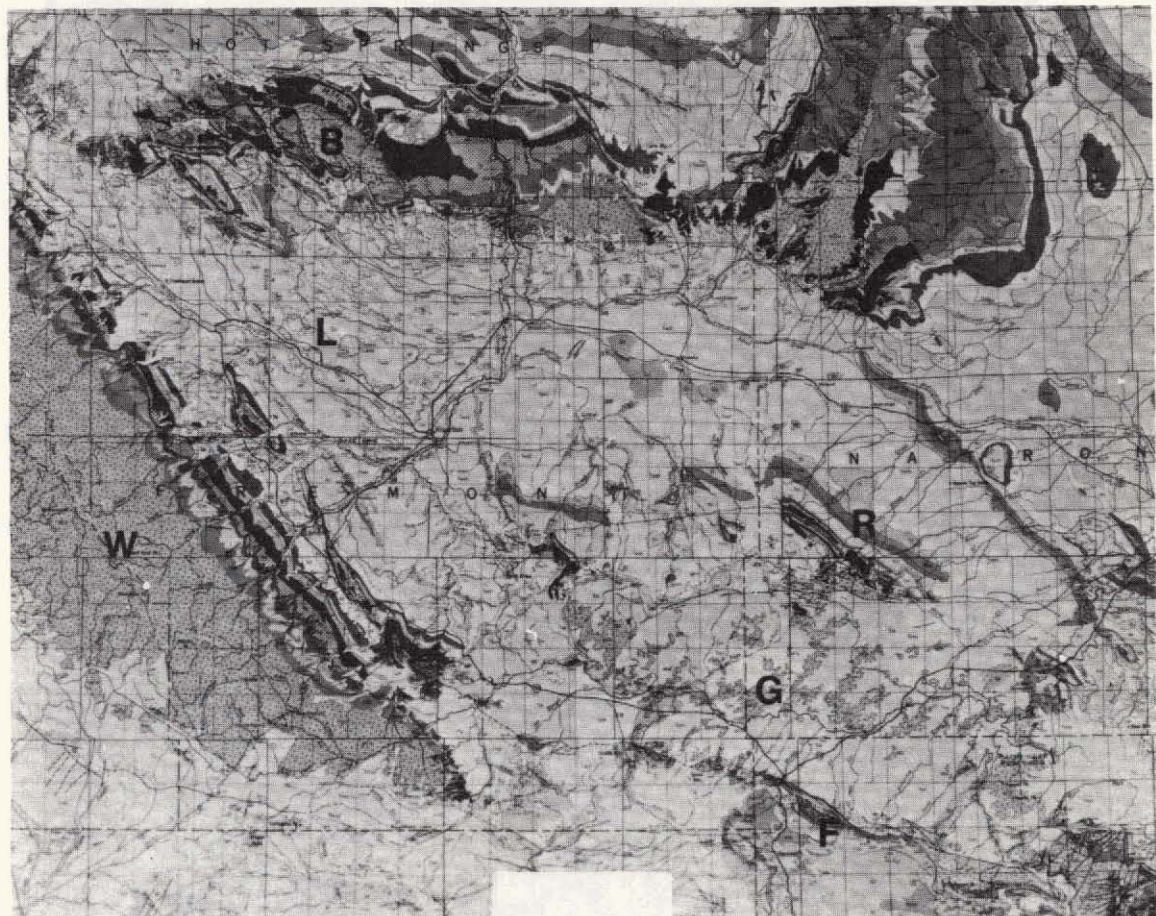


Figure 8a. Geologic Map of part of Wyoming centering on the Wind River Basin. Specific landmarks include Wind River Mountains (W), Owl Creek-Bridger Mountains (B & O), Granite Mountains (G), Ferris Mountains (F), Rattlesnake Hills (R), and Ocean Lake (L).

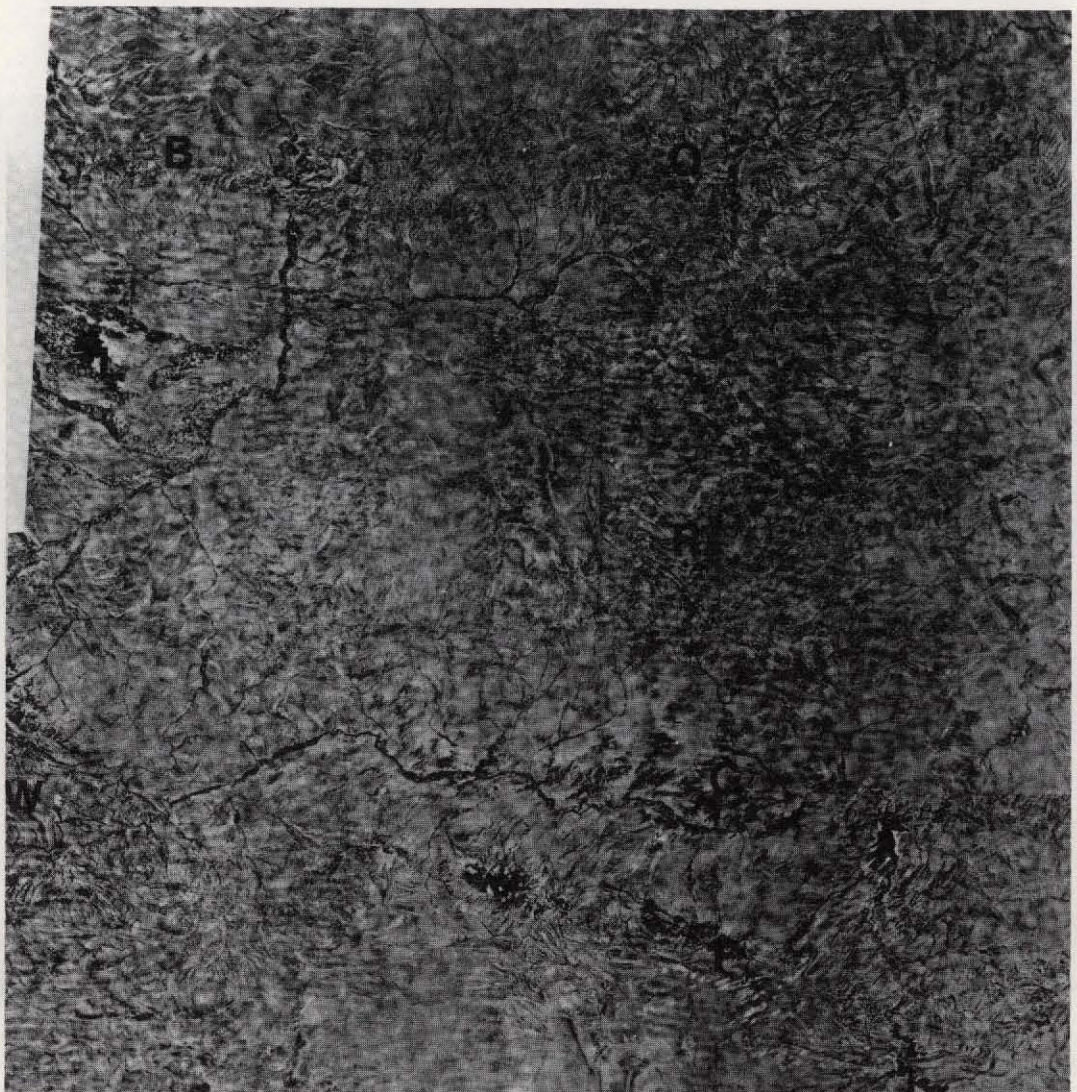


Figure 8b. Aerial photomosaic (roughly 100 miles on a side) of approximately same area outlined in 8a (letters refer to identified landmarks) made from parts of more than 10,000 individual aerial photos obtained from a series of low-altitude flights. Resolution of the product at original scale estimated to be about 10-15 feet.

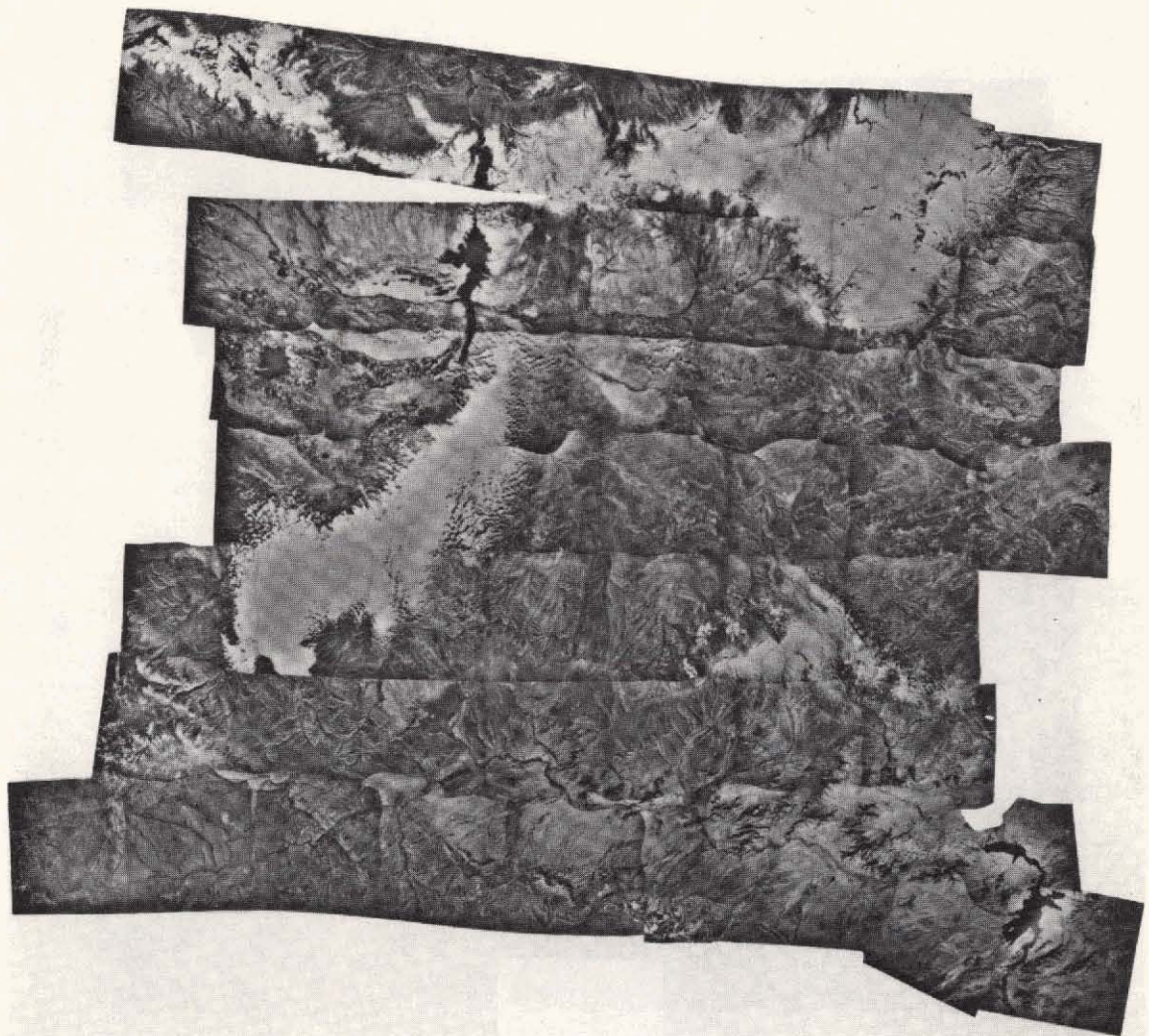


Figure 8c. Mosaic constructed from 65 high altitude aerial photos (red band equivalent to RBV 2) obtained during a NASA U-2 flight over central Wyoming. Area covered is roughly equivalent to that shown in 8b. Resolution about 45 feet.

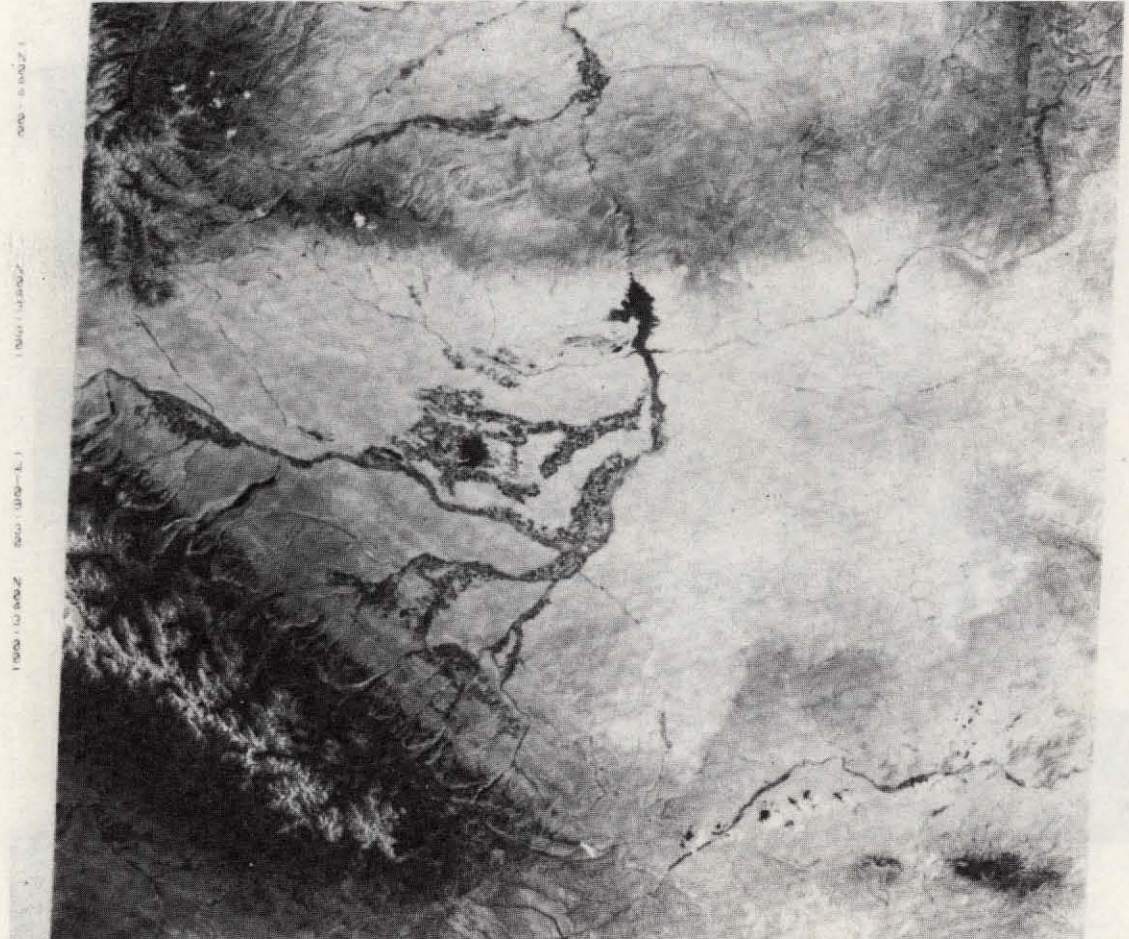


Figure 8d. MSS-5 (red band) image from ERTS-1 taken during the August 5, 1972 pass over the Wind River Basin of Wyoming. Compare with Figures 8a-c.

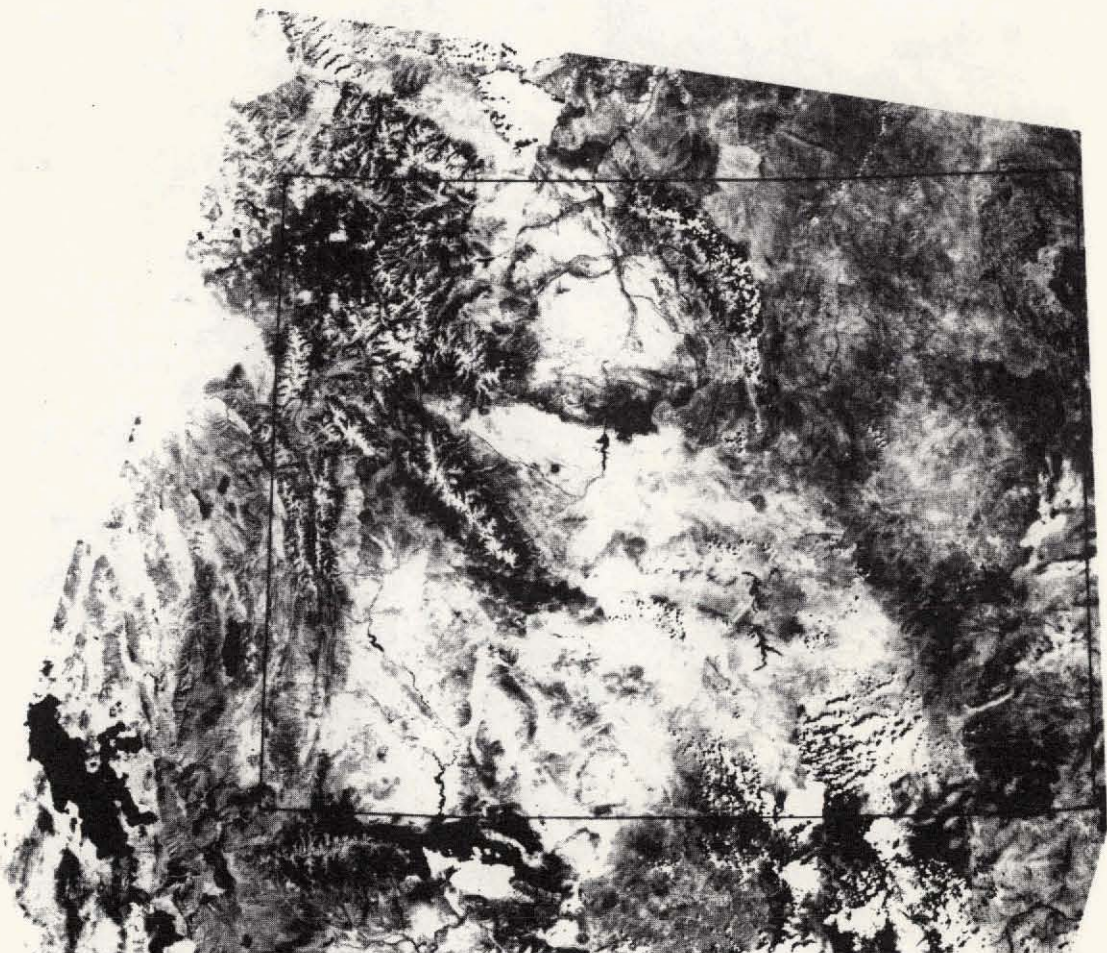


Figure 9. Black and white version of a color composite mosaic made from 25 ERTS frames covering all of Wyoming and parts of adjacent Montana, Idaho, Utah, and Colorado. Original scale 1:1,000,000. Prominent landmarks include the Great Salt Lake, Yellowstone Park, the western Black Hills.



Figure 10. Red band mosaic of the state of Nevada using ERTS data acquired in late summer of 1972. Courtesy Aerial Photographers of Nevada.



Figure 11. ERTS-1 Mosaic (red band imagery) of the state of Oregon.



Figure 12. The island of Hawaii in the Hawaiian island group shown in a two-frame mosaic. Volcanic flows emanating from Mauna Loa are prominent; Mauna Kea lies to the north and Kilauea volcano appears near the southeast coast.



Figure 13. A portion of the ERTS red band mosaic of the continental U.S. covering the west coast states eastward through Central Colorado and West Texas. This mosaic is being prepared for NASA Goddard by the Soil Conservation Service of the Department of Agriculture.

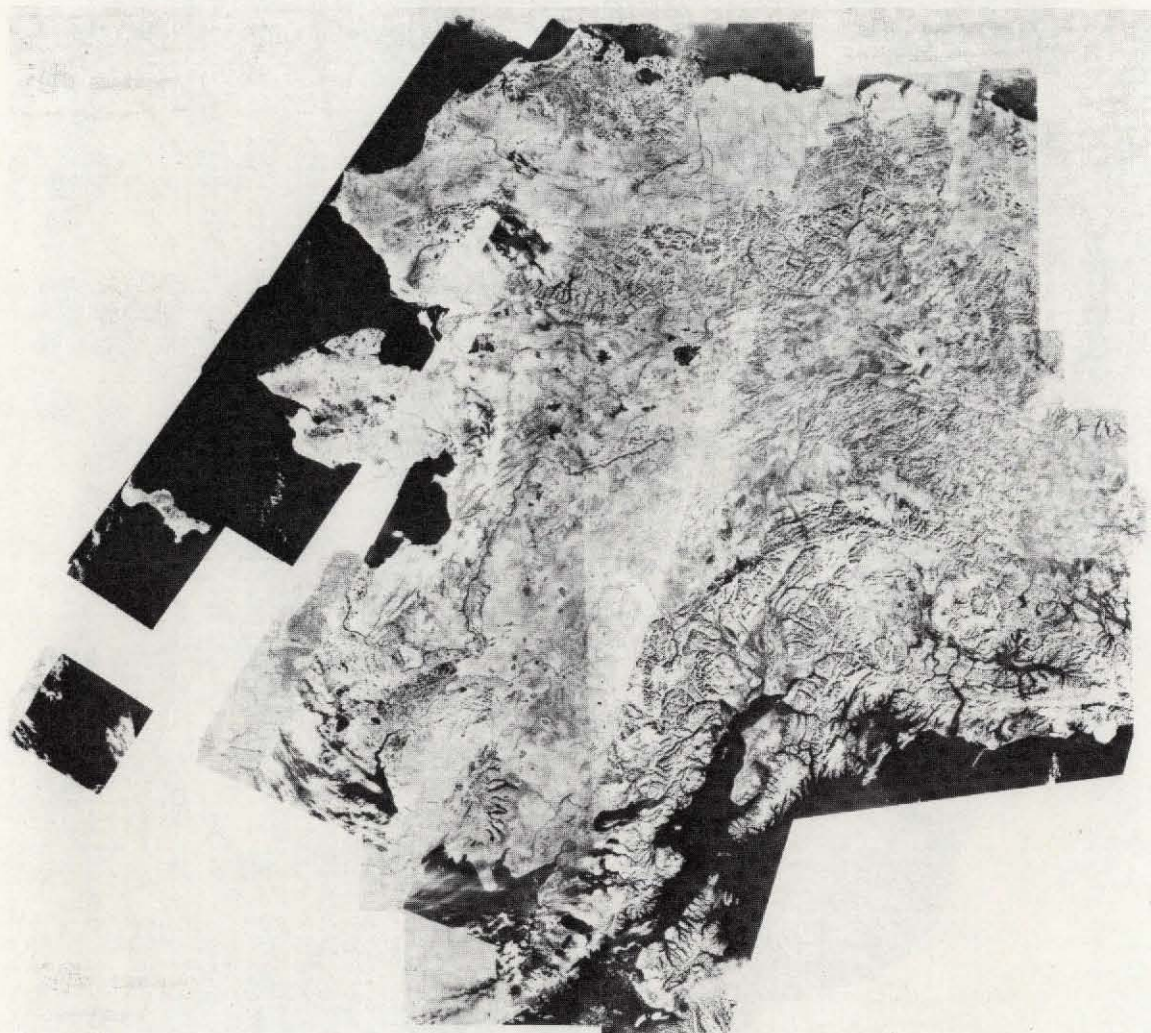


Figure 14. Preliminary version of the ERTS red band mosaic of the state of Alaska, made from data acquired in September and October of 1972. Scale of master product is 1:1,000,000.

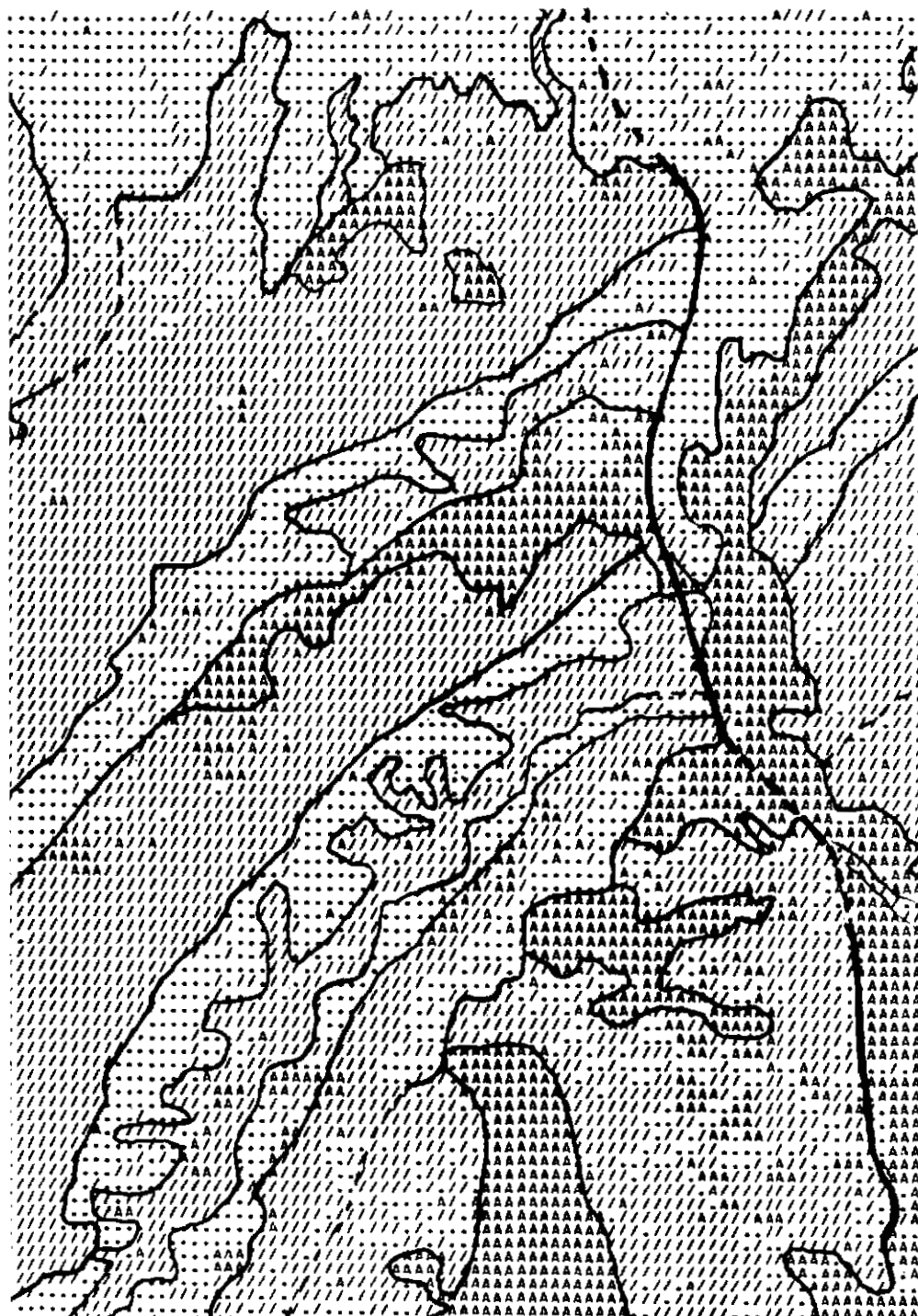


Figure 15. Computer-generated geologic units map of an area near Durango, Colorado. Alphanumeric symbols are: A = sandstone; / = shale, . = sandstone. Original scale 1:24,000. (From Melhorn and Sinnock; op. cit.)



Figure 16a. ERTS red band image of a region in Western Australia just south of the northwest coast near Port Hedland showing several large igneous plutons cutting into metamorphic rocks (mantling bands).  
Compare with 16b.

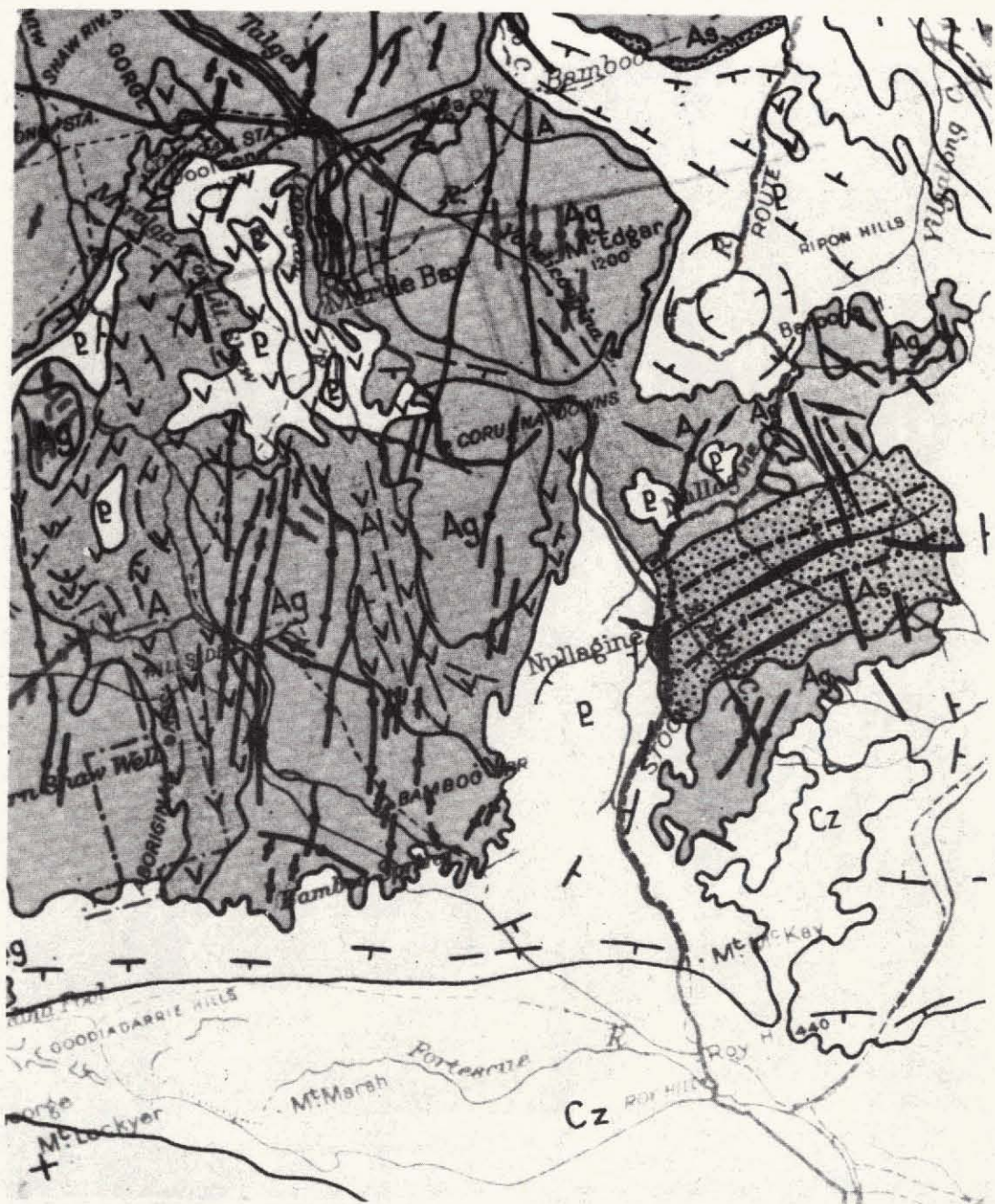


Figure 16b. A portion of the Tectonic Map of Australia (original in color) that includes almost all of the area imaged in 16a. Ag, As, and A refer to Archean granitic rocks and metamorphic units; P denotes Proterozoic metasediments; and Cz to Cenozoic unconsolidated sediments. Horizontal dimension of figure equivalent to approximately 120 miles. Close comparison between mapped unit boundaries and those evident in the ERTS image of Figure 16a reveals that improvements in the precise locations of these boundaries on the map can be made using the ERTS image. (Map courtesy of Bruce Moore, University of Kentucky.)

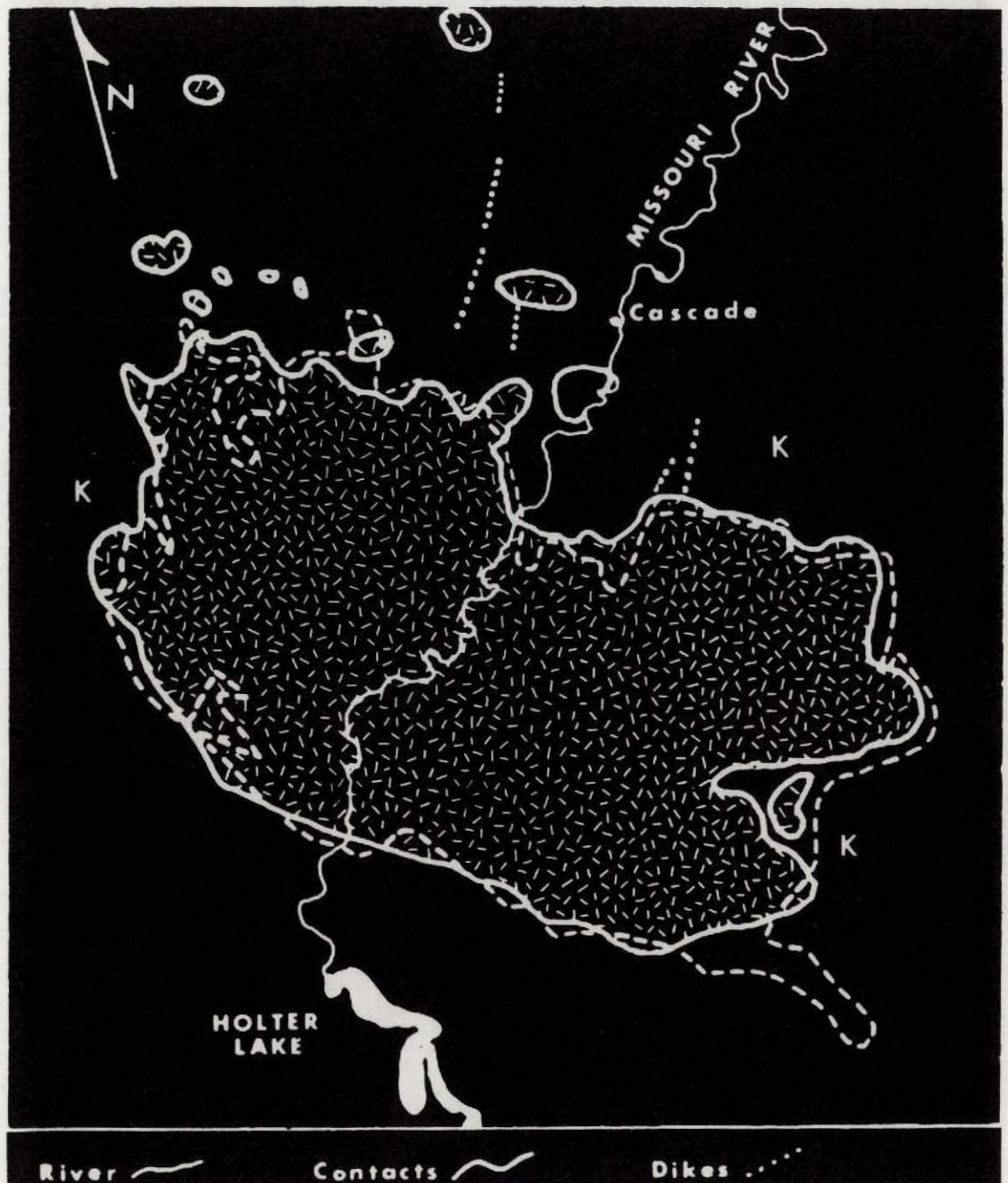


Figure 17a. A "goodness of fit" map of the Adel Mountain volcanic field in western Montana in which the contact determined from ERTS imagery (solid line) is compared with that shown on the state geologic map (dashed line). (From Weidman, et al., op. cit.)

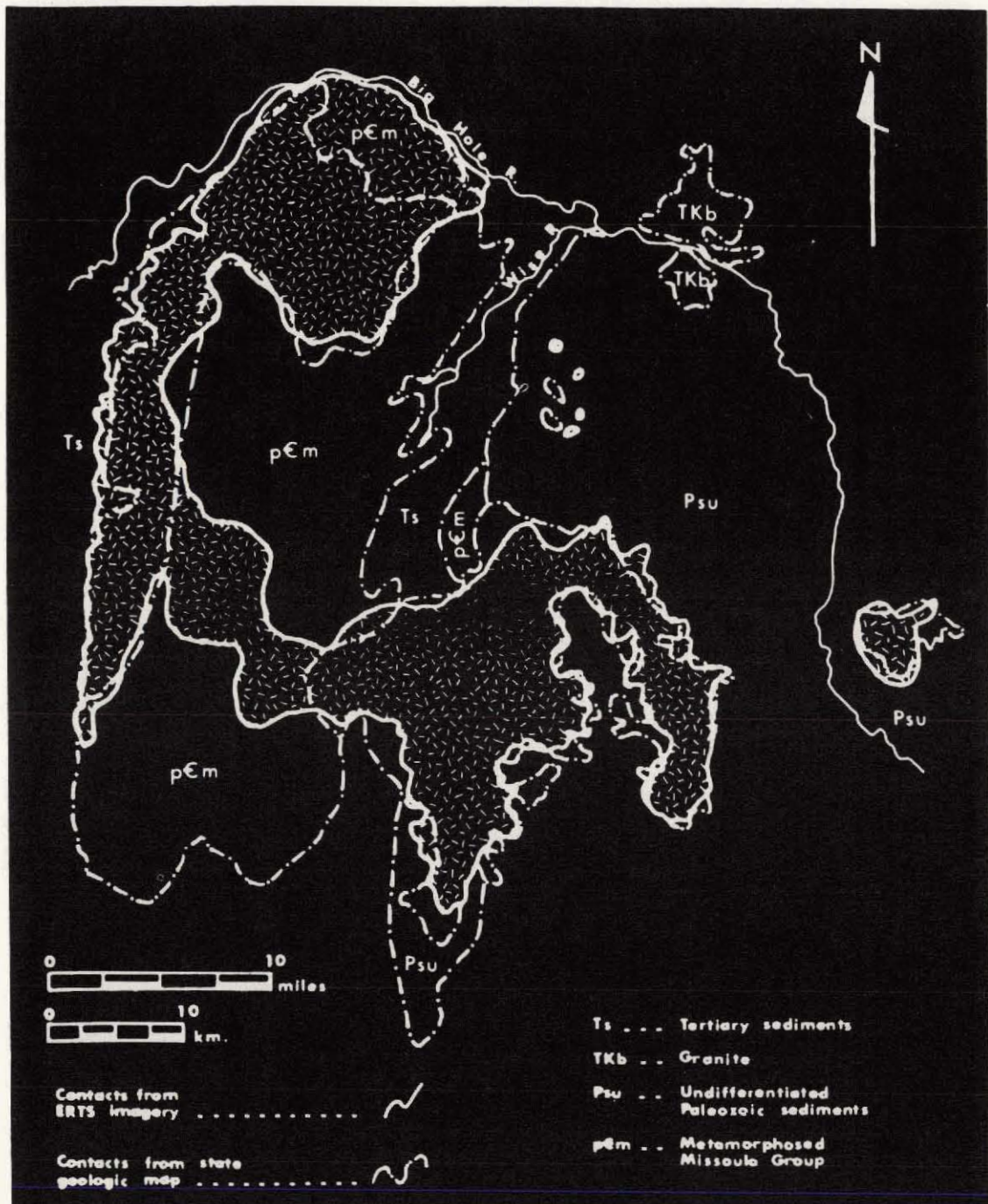


Figure 17b. Granitic and metamorphic unit contacts in the Pioneer Mountains of western Montana as picked out in an ERTS image (solid line). The boundaries do not coincide with those on the state geologic map (dashed line) in much of the area. (From Weidman, et al.; op. cit.)

| Symbol   | Symbol    |
|--|-----------|
| <b>Landforms Due to Endogenic Forces</b>   |           |
| <b>(A) Tectonic Forms</b>  |           |
| (1) Slopes of fault scarps   |           |
| (a) heavily modified   |           |
| (b) slightly changed with a gradient of 2–4°   |           |
| 9–19°  |           |
| 19–45°   |           |
| 45–64°   |           |
| more than 64°  |           |
| (2) Slopes of monoclinal scarps (see §A1)  |           |
| (3) Slopes of thrust scarps (see §A1)  |           |
| (4) Flanks (slopes) of tectonic folds  |           |
| (5) Open earthquake rifts  |           |
| (6) Small tectonic scarps  |           |
| (7) Local subsidence   |           |
| <b>(B) Forms due to Vulcanicity</b>  |           |
| (1) Slopes of volcanic cones with gradients of   |           |
| 2–4°   |           |
| 4–9°   |           |
| 9–19°  |           |
| 19–45°   |           |
| (2) Remnants of volcano slopes (see §B1)   |           |
| (3) Rim of crater  |           |
| (a) fresh  |           |
| (b) modified   |           |
| (4) Inner slope of crater (see §B1)  |           |
| (5) Rim of caldera   |           |
| (a) fresh  |           |
| (b) heavily modified   |           |
| (6) Inner slopes of calderas   |           |
| (7) Parasitic cones  |           |
| (8) Lava tongues (confined to valleys)   |           |
| (9) Lava flows   |           |
| (10) Lava fields   |           |
| (11) Lava bridges or tunnels, spatter cones, driblet cones, lava cascades and tumuli, spines |           |
| <b>Landforms due to Exogenic Forces</b>  |           |
| <b>(A) Forms Due to Denudation</b>   |           |
| <b>(i) Destructive Forms Due to Denudation</b>   |           |
| (1) Remnants of a structural surface   |           |
| (a) flat (with gradients up to 4°)   |           |
| (b) inclined (with gradients of 4–9°)  |           |
| consisting of sandstone  | -   -   - |
| quartzite  | -   -   - |
| limestone  |           |
| dolomite   | - - - - - |
| marl   | - - - - - |
| lava   | CCCCC -   |
| Remnants of a late mature relief not rejuvenated:  |           |
| (2) Remnants of an erosion surface   |           |
| (a) flat (with gradients up to 4°)   |           |
| (b) inclined (with gradients of 4–9°)  |           |
| initiated during the Paleogene   |           |
| Miocene  |           |
| Pliocene I   |           |
| Pliocene II  |           |
| Pliocene III   |           |
| (3) Remnants of pediments formed by erosion and denudation                                   |           |
| with gradients of ...  |           |
| (4) Remnants of pediments formed by slope wash   |           |
| with gradients of ...  |           |
| (5) Remnants of surfaces of planation  |           |
| (a) flat   |           |
| (b) inclined   |           |
| exhumed during the ...   |           |
| (6) Fragments of structural surfaces uncovered during the ...                                |           |
| (7) Remnants of the planed surfaces exhumed from beneath a sheet of insoluble residue        |           |
| (a) flat   |           |
| (b) inclined   |           |
| during the ...   |           |
| (8) Breaks of slope separating different surfaces of planation or different pediments        |           |
| (9) Ridges at the intersection of valley sides:  |           |
| (a) sharp and rocky (crest)  |           |
| (b) narrow and rocky   |           |
| (c) narrow and rounded   |           |
| (d) broad and rounded  |           |
| (10) Resistant ridges  |           |
| (a) sharp and rocky  |           |
| (b) narrow and rocky   |           |
| (c) narrow and rounded   |           |
| (d) broad and rounded  |           |
| consisting of sandstone  |           |
| quartzite  |           |
| limestone  |           |
| volcanic rocks   |           |
| other crystalline rocks  |           |

Figure 18a. Part of a classification of landforms, with symbols, proposed in 1963 to the International Commission for Landforms Symbols of the International Geographic Union.

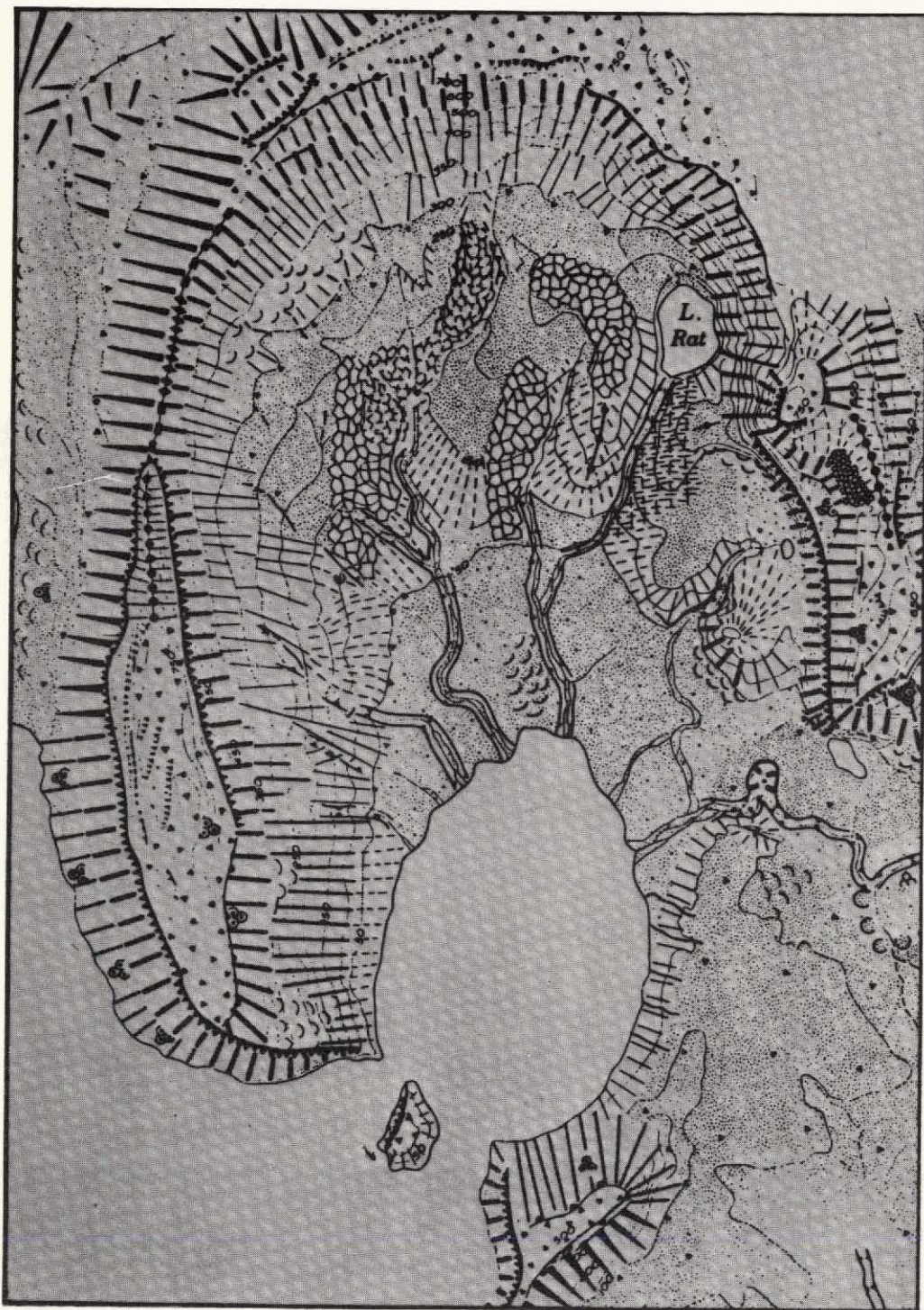
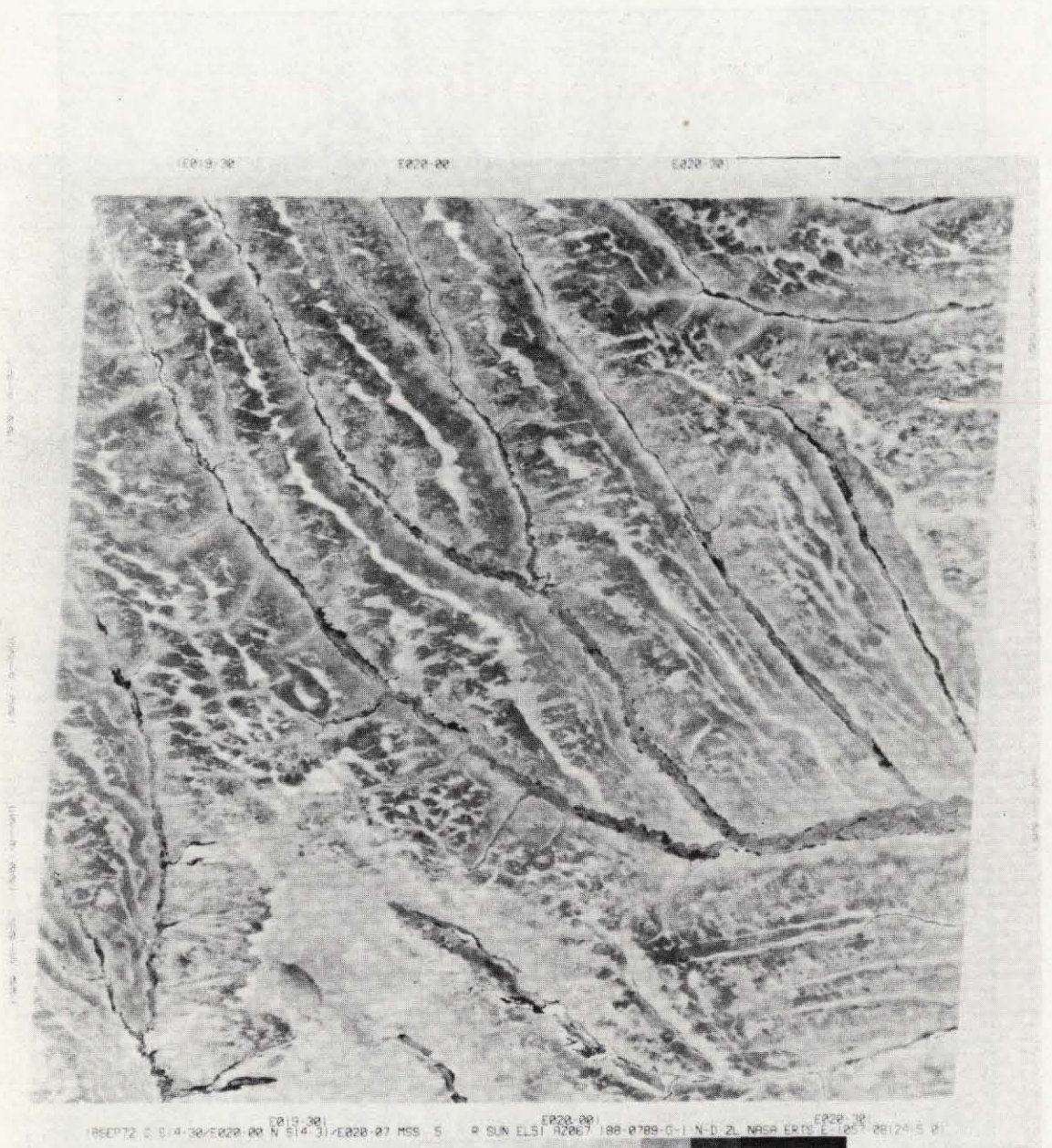
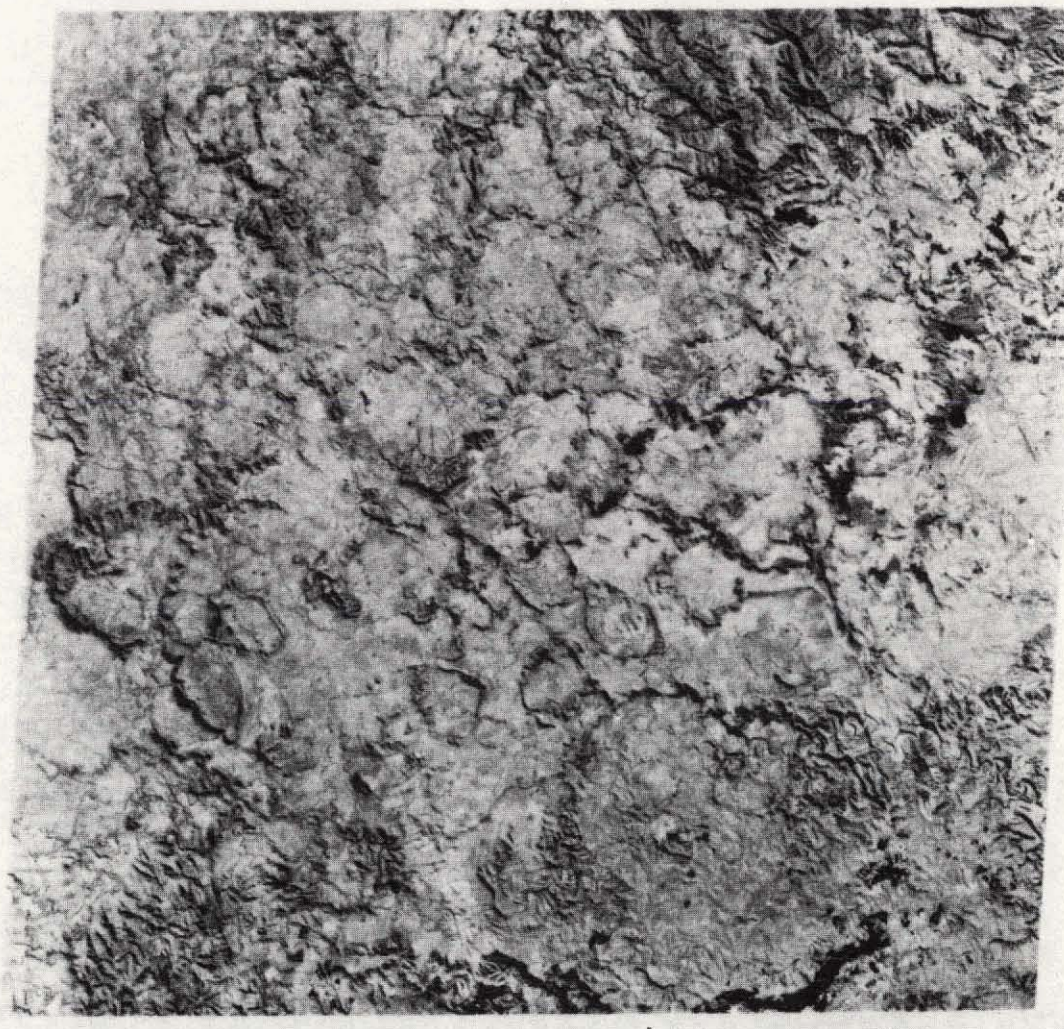


Figure 18b. Hypothetical example of a landforms map using symbol system described in 18a.



**Figure 19a. Drainage basin of the Cuando River in southeast Angola, in the northern Kalahari, a region of moderate rainfall characterized by savannah, sandy soils, and salt-encrusted flats.**



1E026-20 1E026-30 1E027-30 1E027-20  
1E027-20 1E026-57 N S31-43/E027-02 MSS 5 R SUN EL37 R2052 190 0677 R-1 N D-2L NASA ERTS-1 1969-07-31 S 02

**Figure 19b.** The enclave of Swaziland (surrounded by South Africa; east of Johannesburg), in which unusual ridges (many forming closed plateau-like landforms) are developed on a granitic-metamorphic terrain.

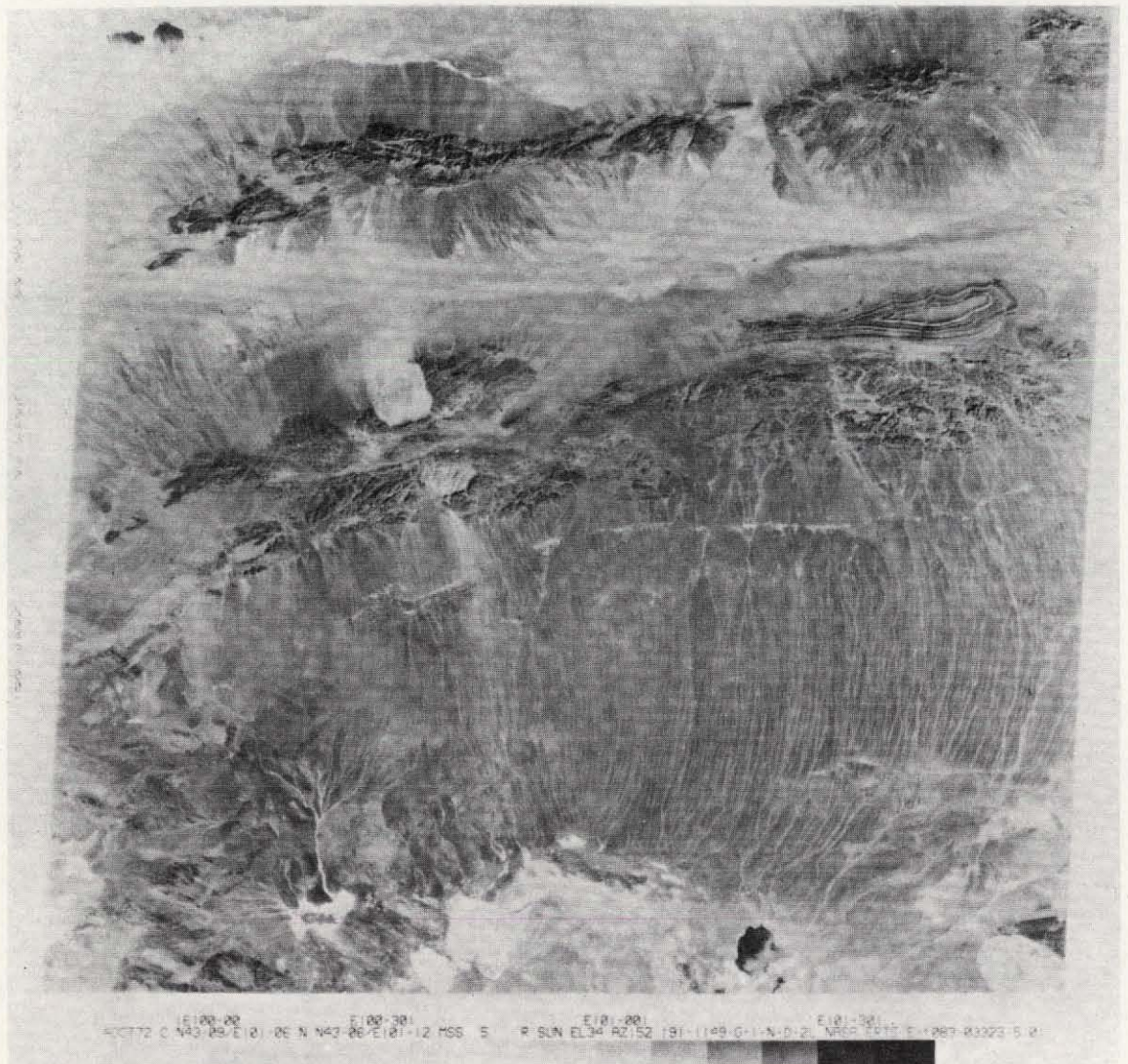


Figure 19c. A region in the southernmost part of the Mongolian Republic showing vast stretches of alluvial fan plains which have coalesced into continuous bolsans.

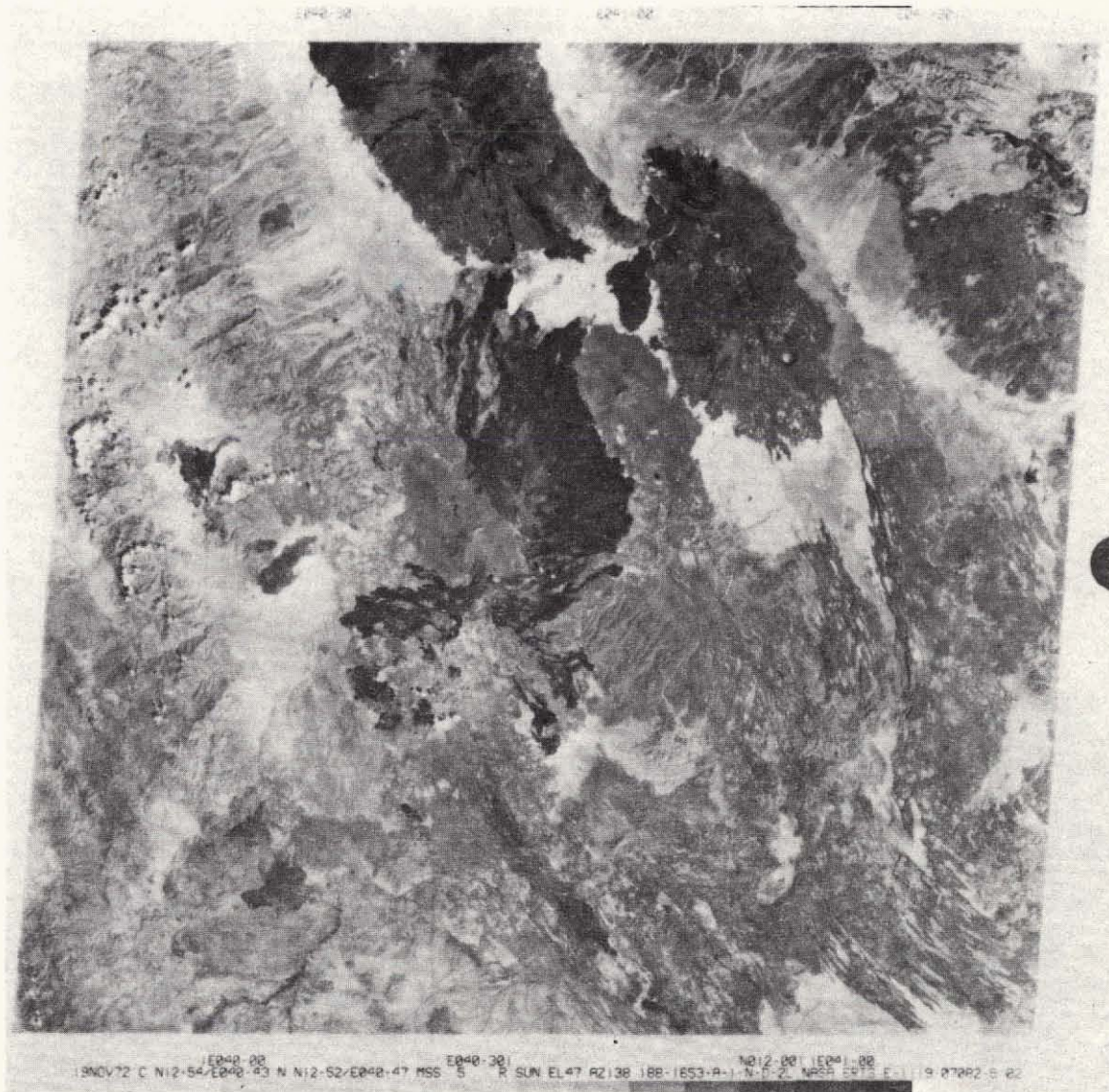
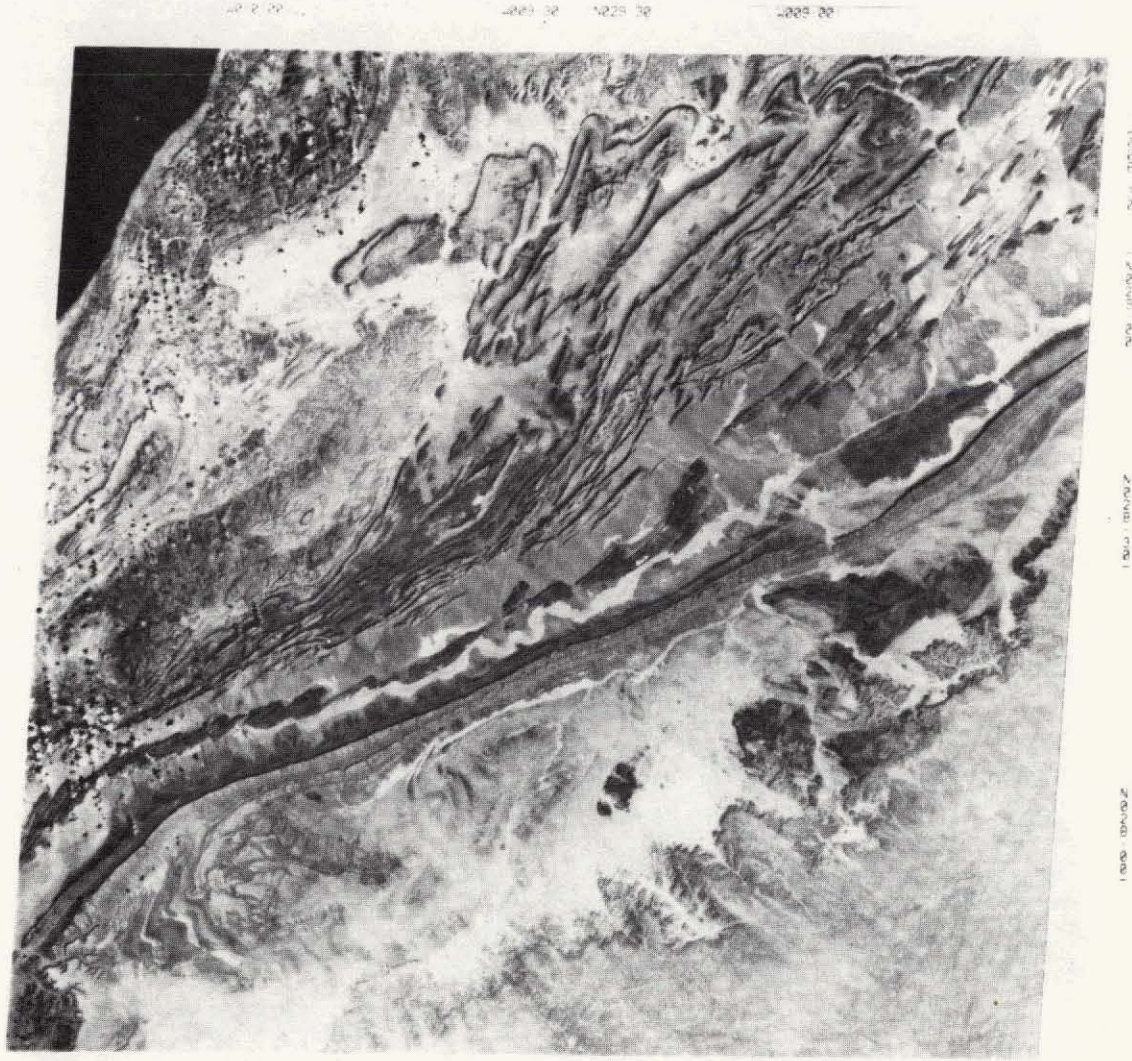


Figure 19d. Part of eastern Ethiopia, west of the Afar, a region dominated by volcanic rocks; much of the recent volcanism seen in this image is resulting from the emergence of this area as newly "created" land being produced by seafloor-spreading.



Figure 20a. The Piedmont, Blue Ridge, and folded Appalachians in southern Virginia south of Roanoke. Structural features are enhanced in this image by the light snow cover and lower sun angle ( $24^\circ$ ).



1W018-38  
03NOV72 C N28-41/W009-48 N N28-39/W009-38 MSS 6 R SUN EL39 R2147 190-1432-R-1-N-D-2L NASA ERTS E-1103-12413-6

**Figure 20b.** The Anti-Atlas Mountains and the northern rim of Tindouf Basin, a region of folded sedimentary and crystalline rocks, in southern Morocco.

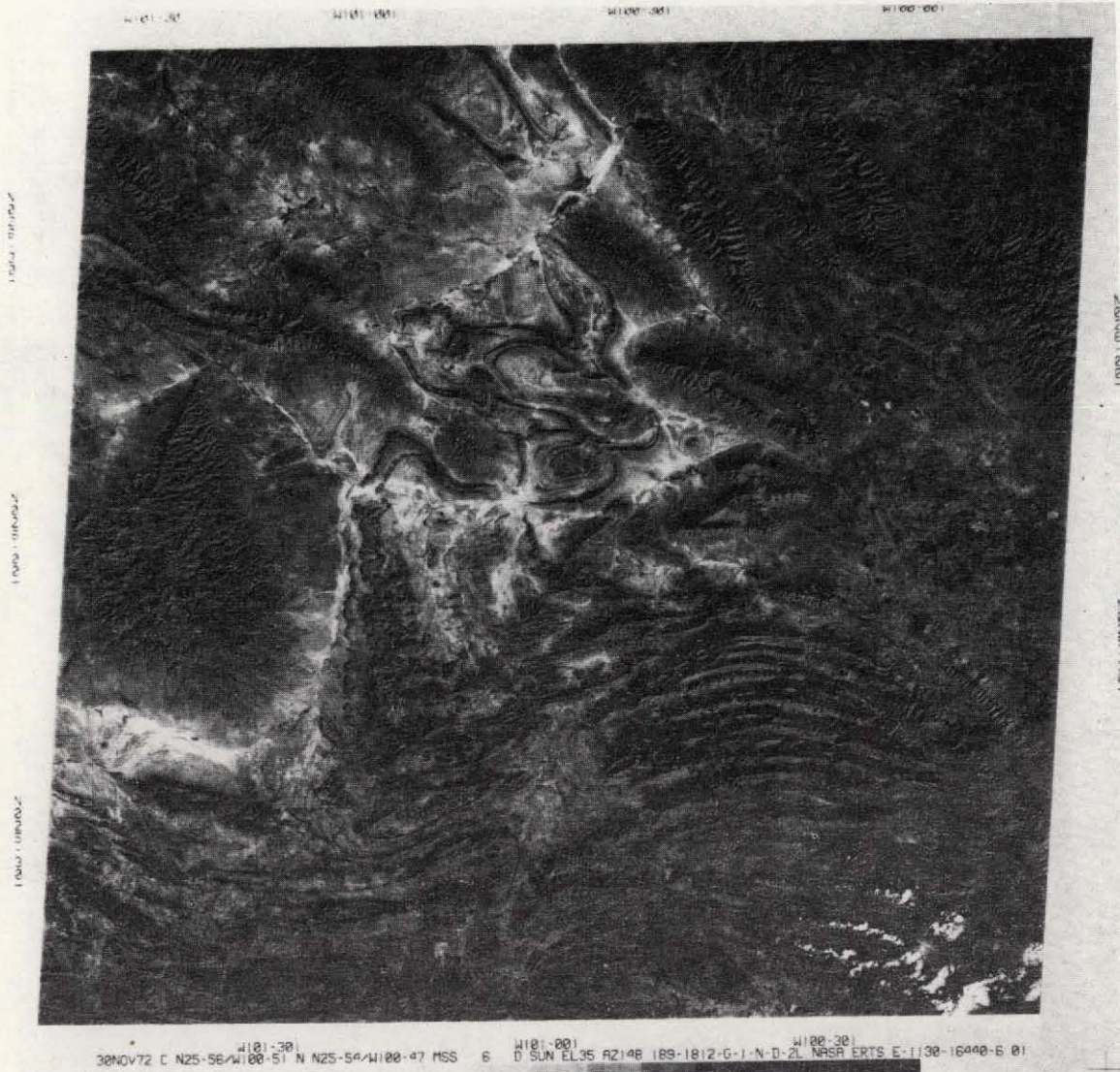
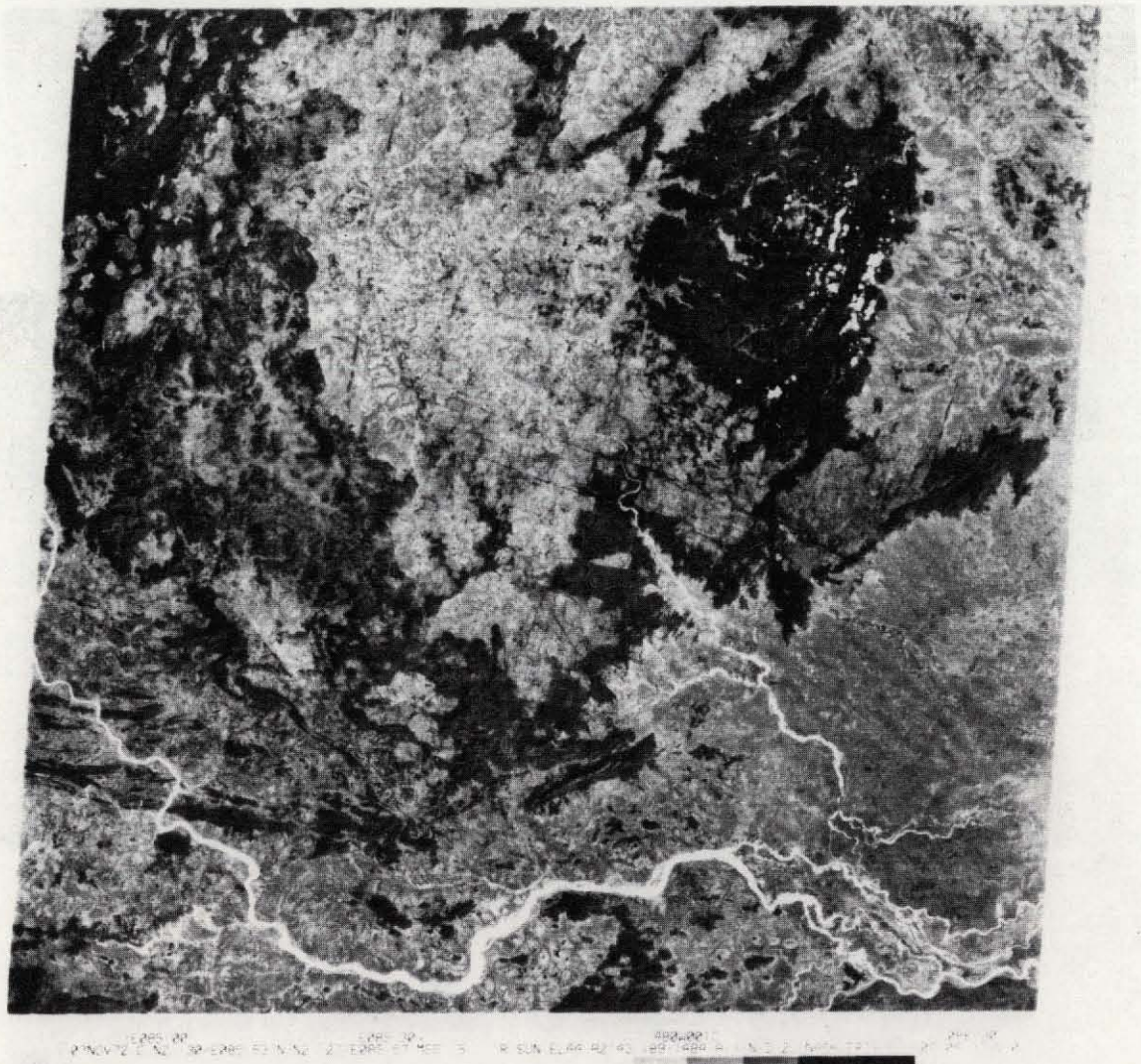


Figure 20c. Part of the Sierra Madre Orientale of Mexico. Monterrey and Saltillo are located near the bottom of the scene. The tightly folded Jurassic and Cretaceous sedimentary rocks west of Monterrey are part of a miogeosynclinal sequence; the dissected dome on the west (left center) is developed in platform sediments of Cenozoic age.



Figure 20d. The northeast edge of the Takla Makan desert in Sinkiang province of western China. A prominent strike-slip fault offsets the folded rock units southeast of the Possut'eng Hu lake. This fault can be traced for more than 300 miles on adjacent ERTS images.



**Figure 20e.** Regional jointing in the southern end of the Chota Nagpur Plateau of eastern India (State of Orissa). Basalts overlie sedimentary rocks. The Mahanadi River appears at the bottom of the image.

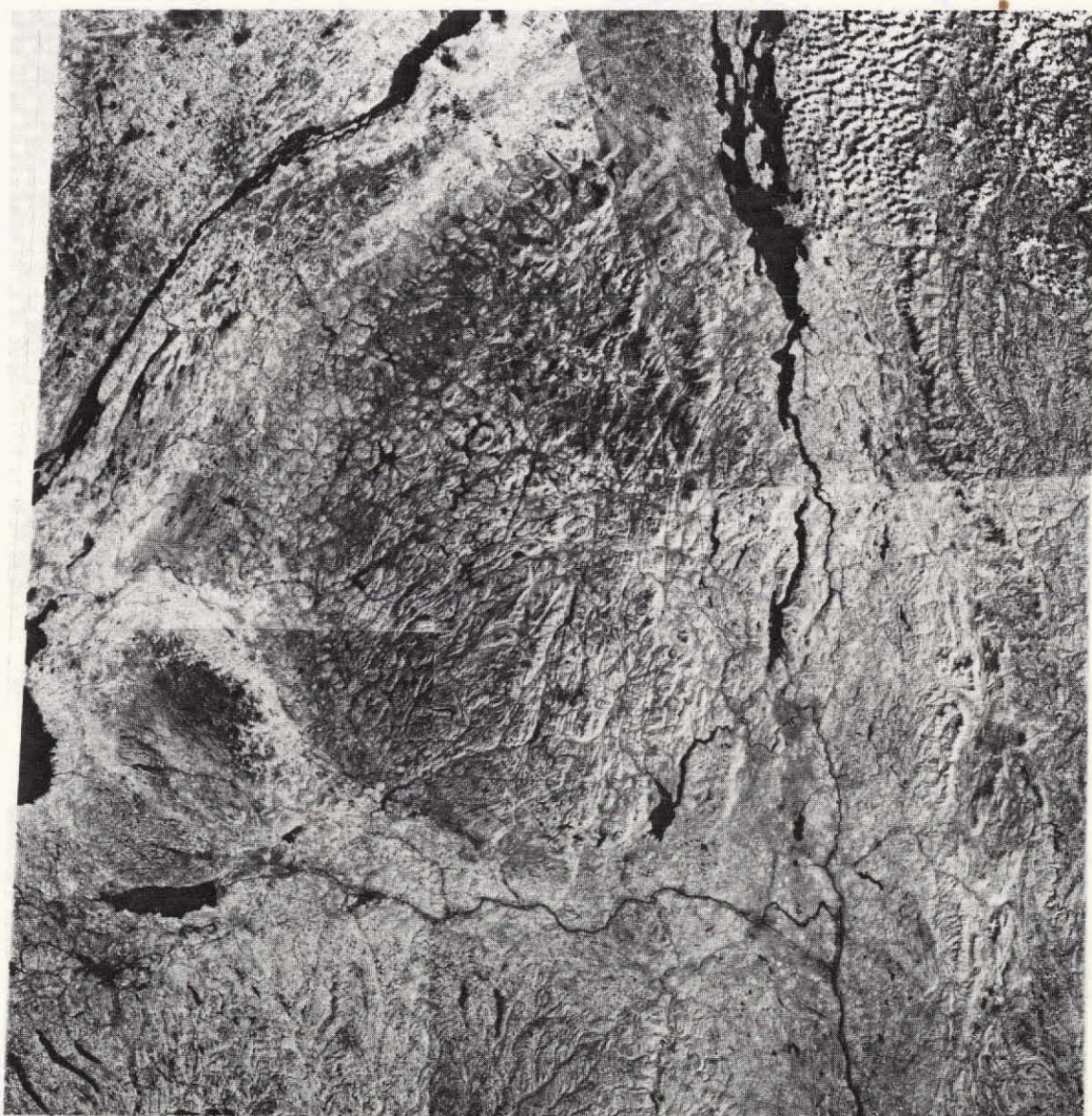


Figure 21a. ERTS mosaic showing the entire Adirondacks Mountains of eastern New York. The St. Lawrence River appears at the upper left; Lake Champlain at the upper right and the edge of the Catskills at the bottom. (Courtesy Y. W. Isachsen; op. cit.)

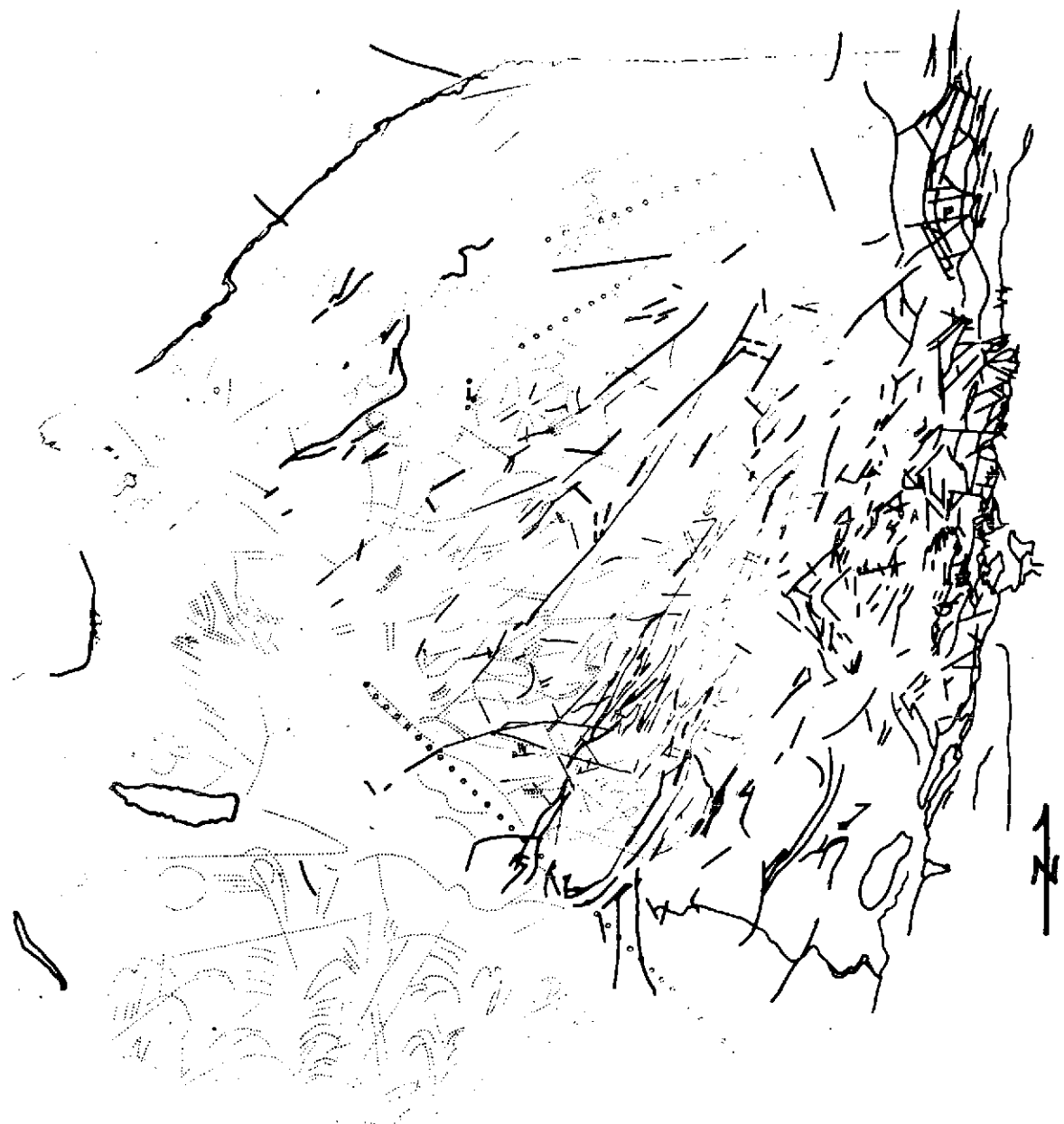


Figure 21b. Sketch map of previously mapped major lineaments (solid lines) and new "linears" (not all of which have proved to be rock fractures) observed in ERTS images of eastern New York. (From Isachsen et al., op. cit.)

81



Figure 22a. Partly controlled mosaic of Montana (MSS Band 5) and adjacent areas prepared from late summer and fall, 1972 ERTS imagery by the Forest Service, Division of Engineering Photoreproduction Section, U.S.D.A., Missoula, Montana (see Weidman, et al., op. cit.).

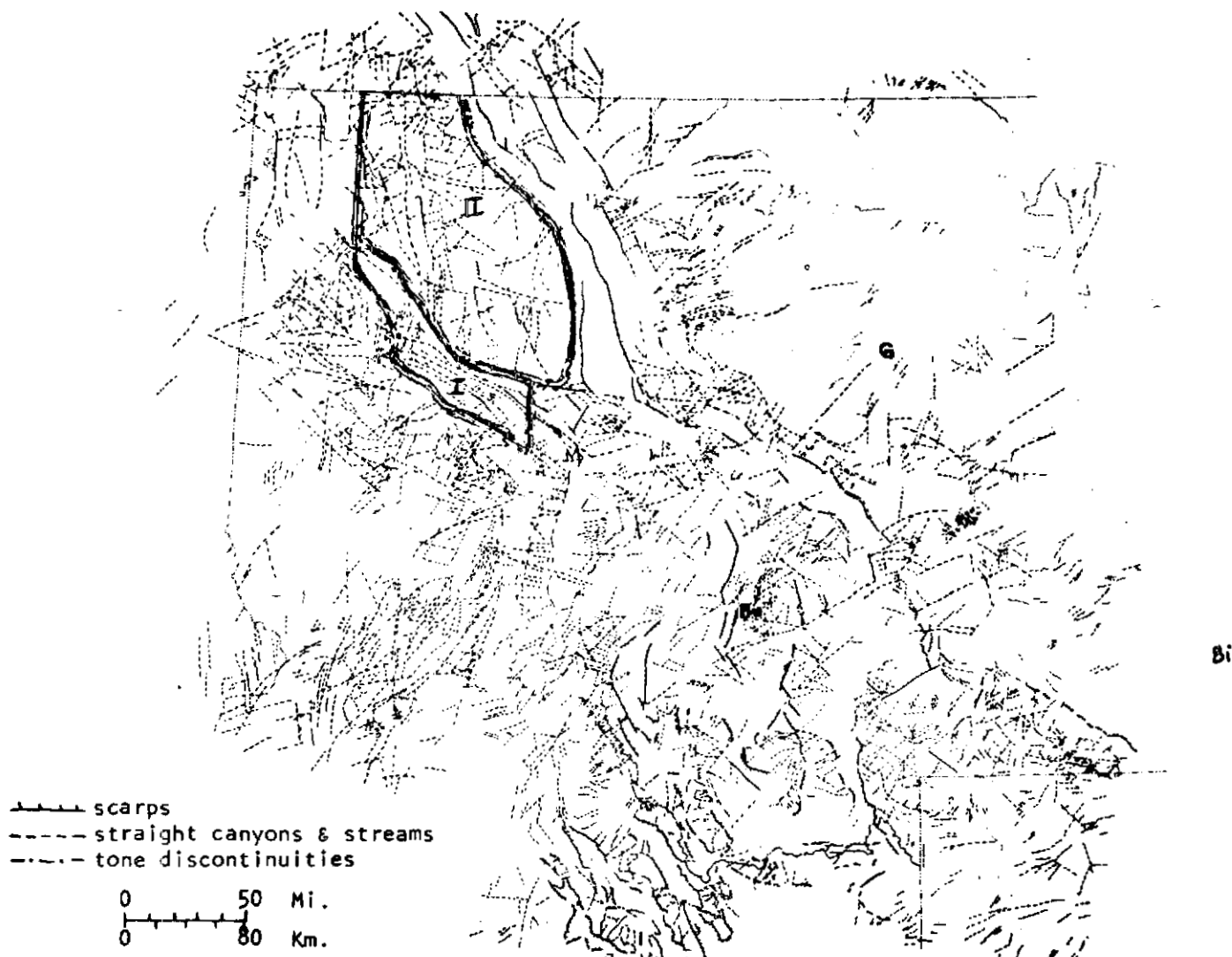
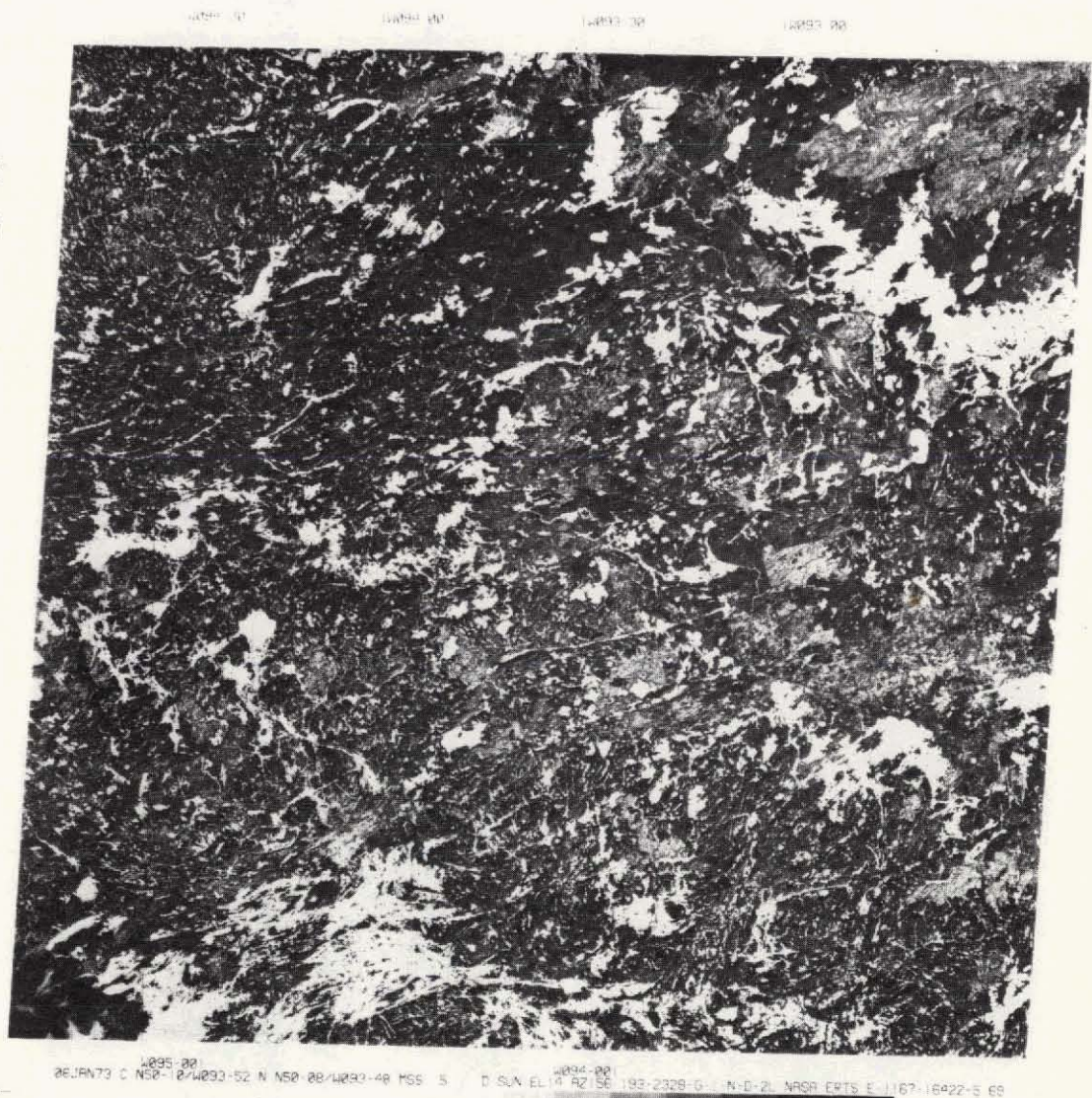
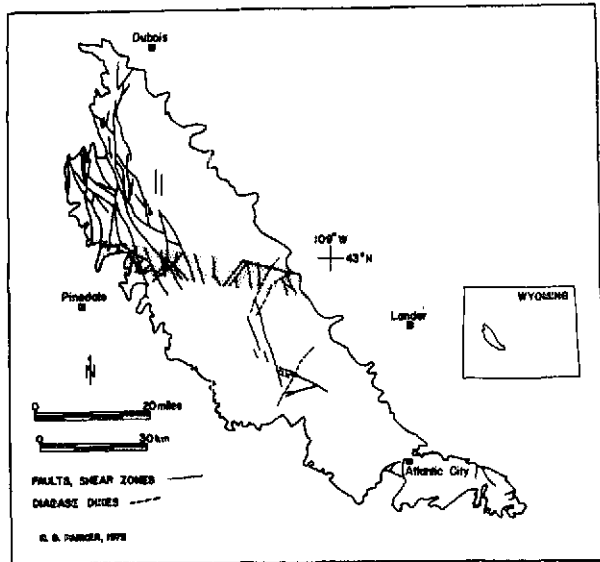


Figure 22b. Interpretation by Weidman, et al. (op. cit.) of linear features observed in ERTS images of western Montana.

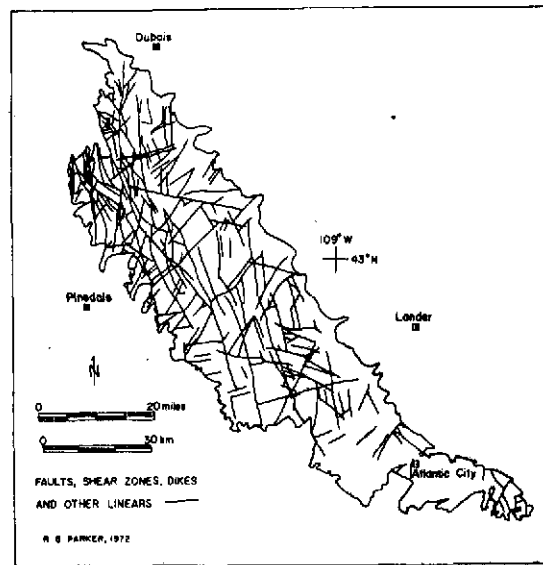


**Figure 23.** Part of the Canadian Shield in Western Ontario (near Kenora, north of Lake of the Woods) showing regional fractures (whose intersections in places produce "knobby" hills) and different lithologic units (tonal variations; however, lighter areas are snow-covered clearings).



## MAPPED PRIOR TO ERTS-1

Figure 24. Interpretation of major fracture systems in the Wind River Mountains of western Wyoming made by R. B. Parker (University of Wyoming) from field studies prior to 1972 and then updated by analysis of a single ERTS image (1013; August 5, 1972).



## OBSERVED BY ERTS-1



Figure 25. Fractures map developed from study of ERTS imagery in Chino Valley-Verde Valley region southwest of Flagstaff, Arizona (ERTS Frame 1014-17375); heavy lines denote previously mapped faults and lighter dashed lines are lineaments (mainly joints) first recognized in the ERTS image. (From Goetz, et al., op. cit.)

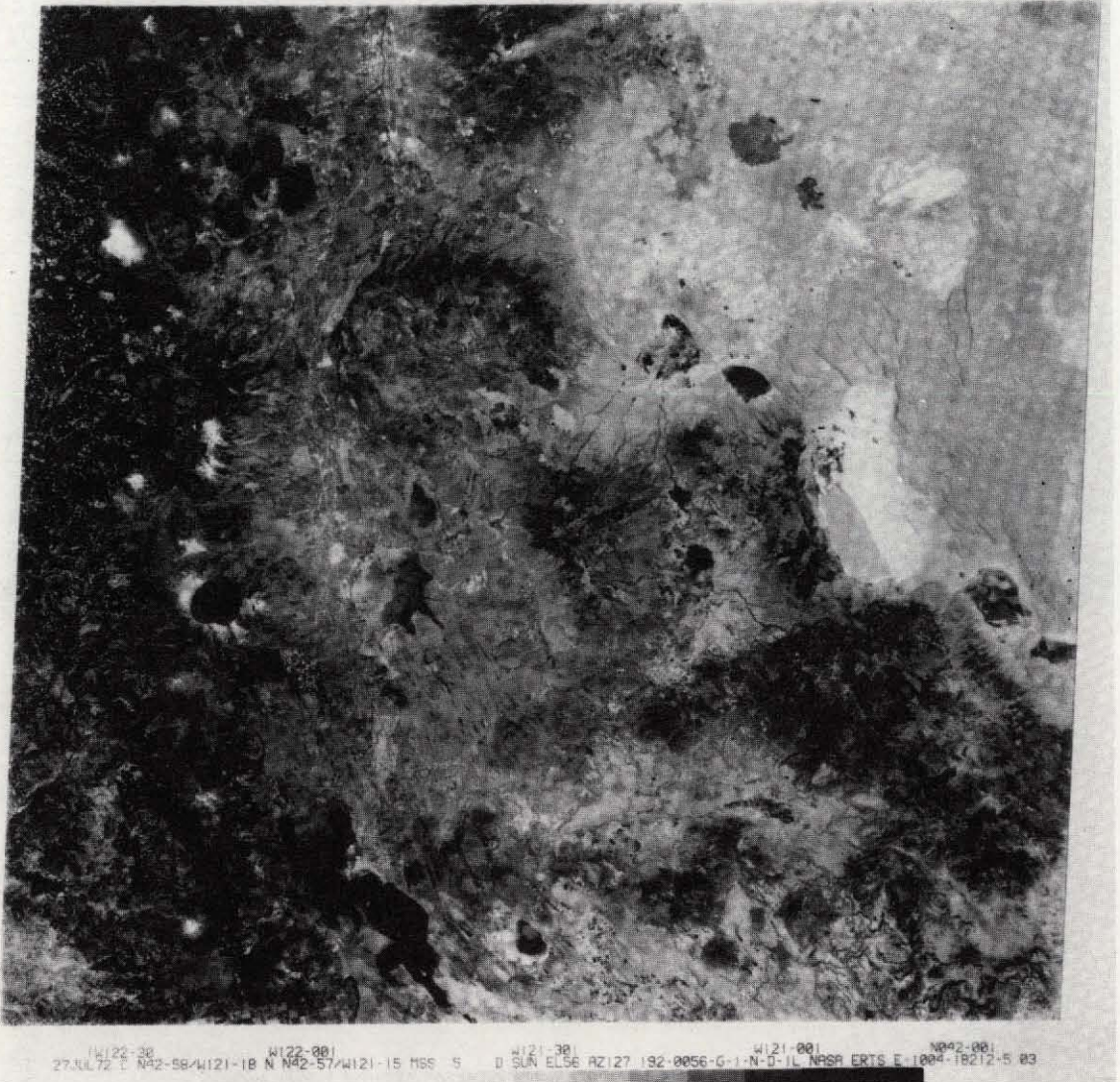


Figure 26. ERTS MSS-5 image of south-central Oregon showing Crater Lake (lower left), Newberry Volcano (center top), and volcanic deposits (John Day and others) (right). A prominent elliptical structure (left center) has been discovered in this image; it is outlined by evergreen forest cover.

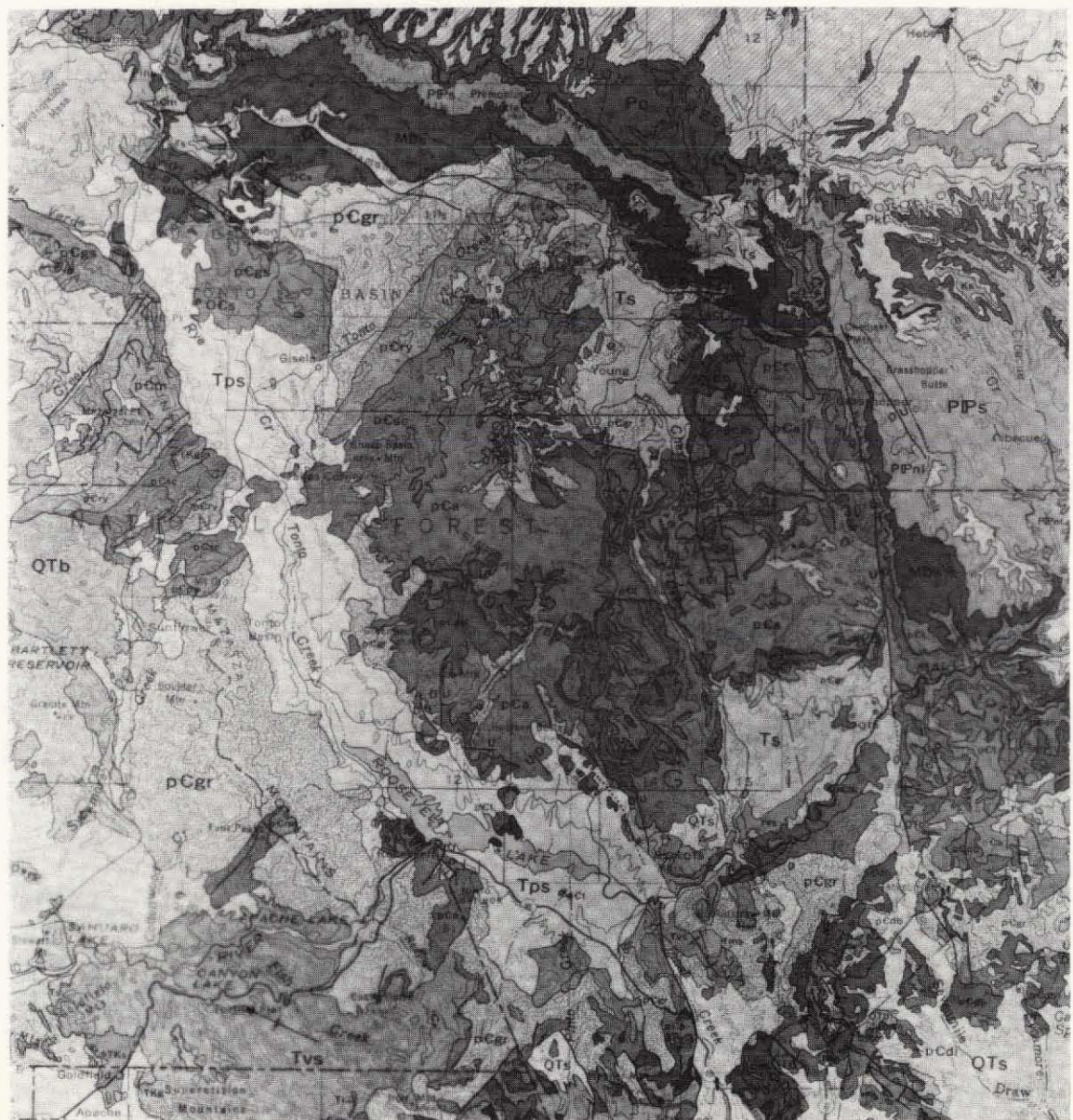


Figure 27a. A section of the geologic map of Arizona showing a region northeast of Phoenix. Close examination reveals an elliptical pattern bounded in part by the Mogollon Rim and Tonto Creek.

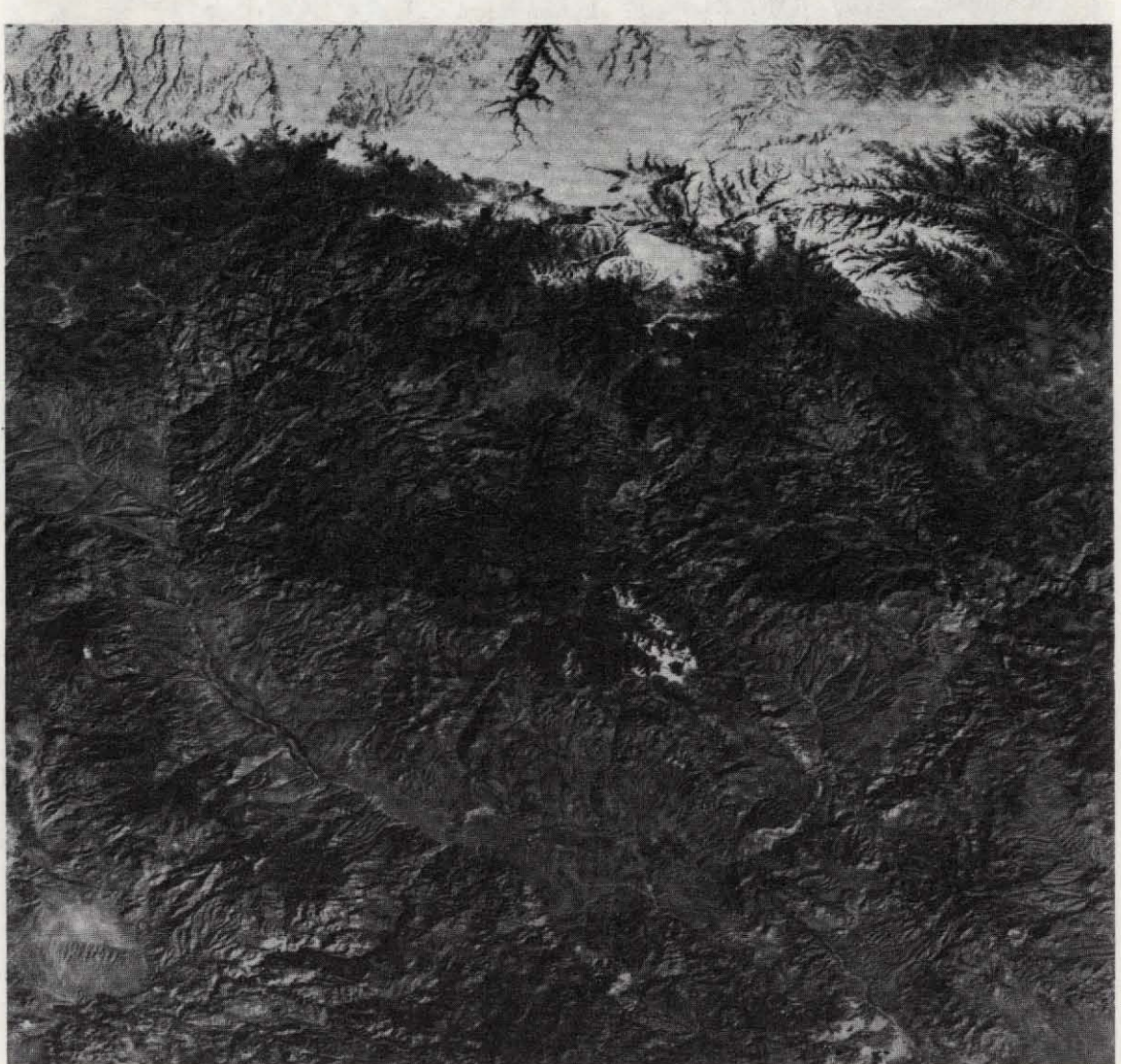


Figure 27b. Part of an ERTS image covering the same area shown in 27a in which the elliptical pattern is strongly expressed in the topography.



Figure 28. An enlarged portion of an ERTS frame of an area west of Brasilia in Brazil showing the double ring structure (darker tones are heavy vegetation) of the Araguainha Dome which has recently been identified as an astrobleme or ancient meteorite impact crater.

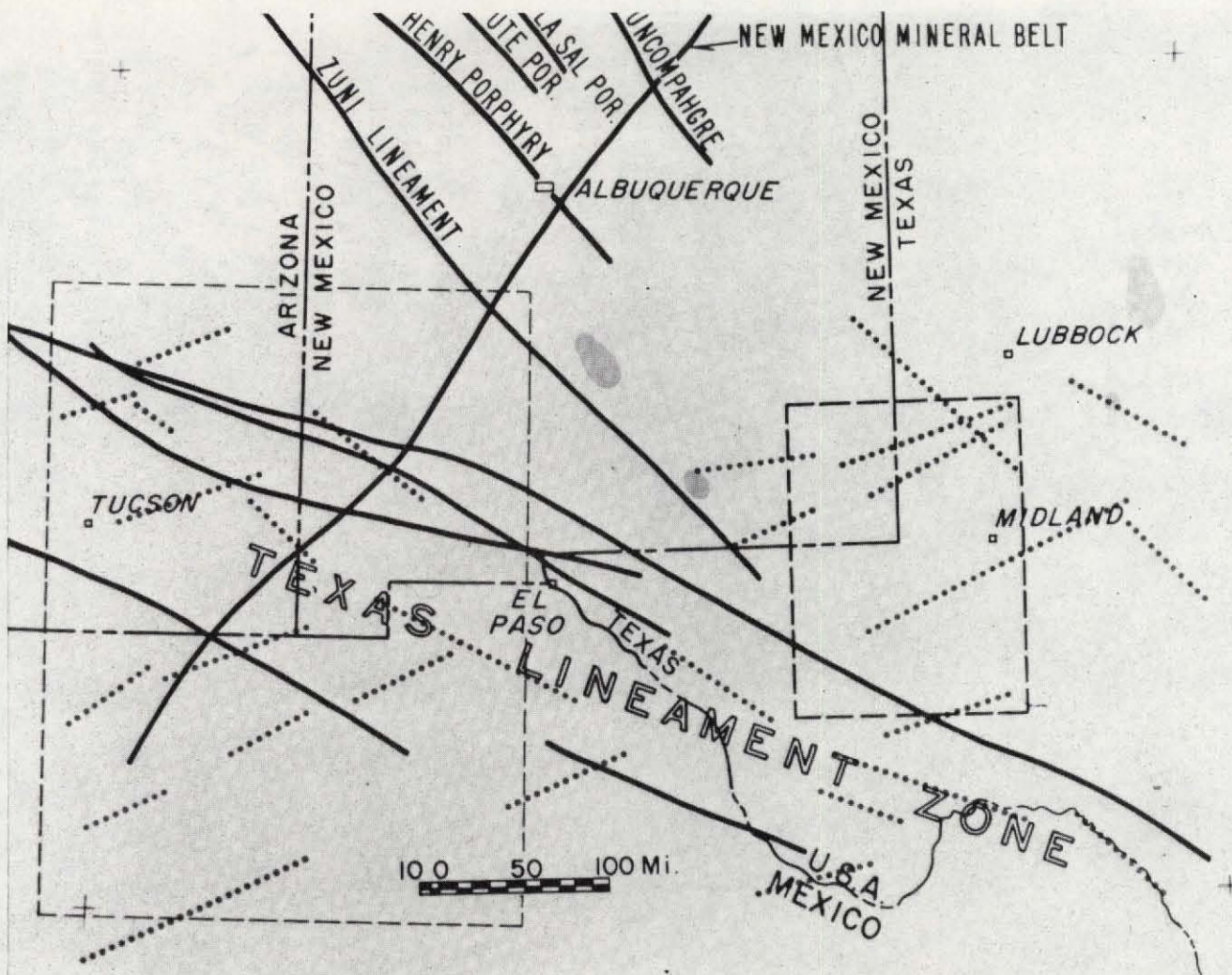


Figure 29. Lineaments in the southwestern United States which are recognizable in ERTS imagery; dotted lines refer to new linear features (from Saunders and Thomas, Paper G 30, pp. 523-530, March 1973 ERTS Symposium).

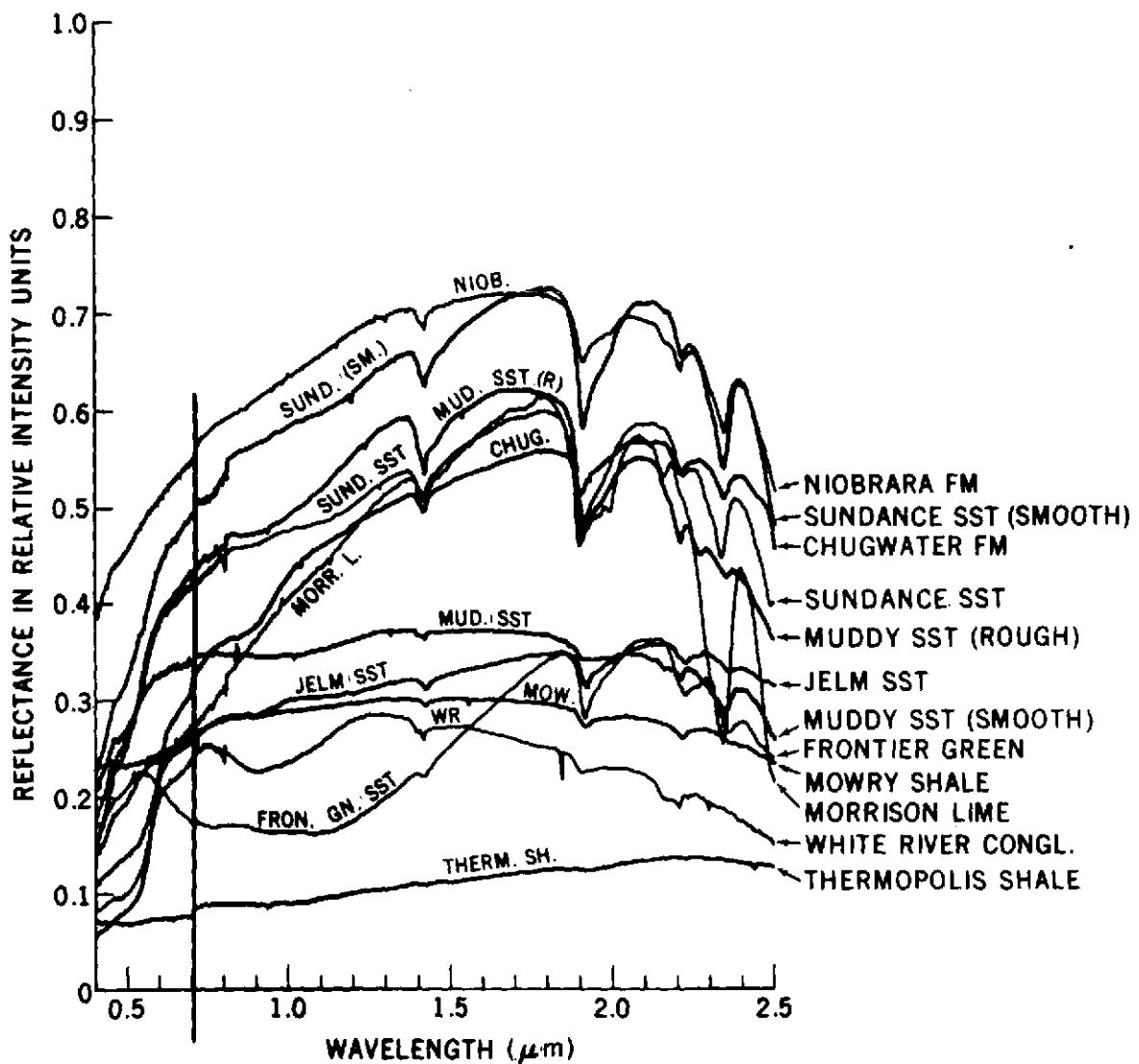


Figure 30. Spectral response curves of a group of rocks from Wyoming determined on a Cary 90 Reflectance Spectrometer. (N. M. Short, unpublished.)

## EXPECTED ERTS-1 $R_{75} = \frac{L_7}{L_5}$ RATIO RANGES

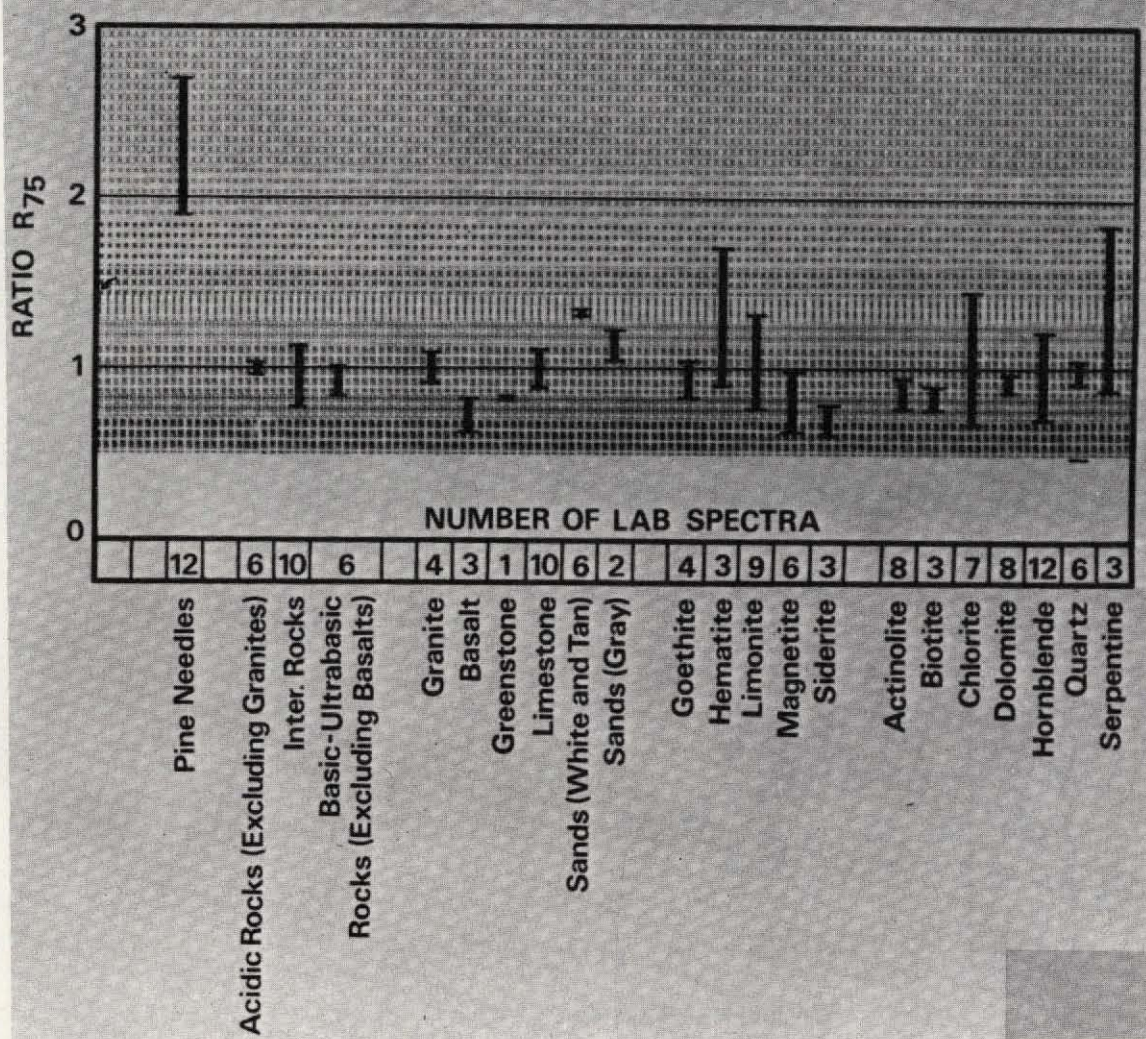
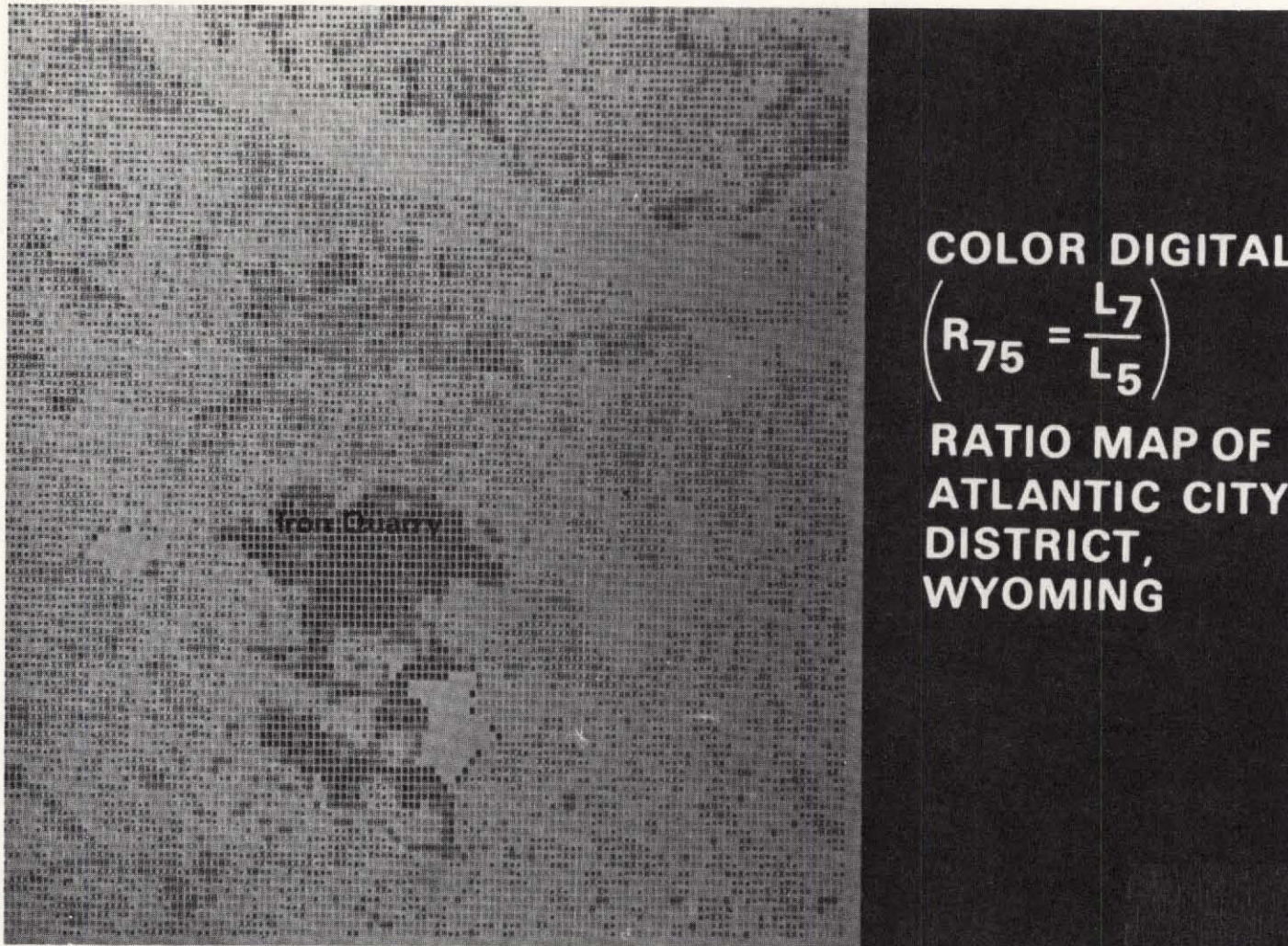


Figure 31. Plot of ratios of reflectances measured in the laboratory over the wave regions covered by ERTS MSS Bands 7 and 5 on the rocks and minerals listed (numbers of samples shown in parentheses) (from Vincent, op. cit.).



COLOR DIGITAL  
 $(R_{75} = \frac{L_7}{L_5})$   
RATIO MAP OF  
ATLANTIC CITY  
DISTRICT,  
WYOMING

Figure 32. ERTS digital gray map (original in color) of computer-calculated ratios of ERTS MSS Bands 7 to 5 for an area in the southern Wind River Mountains near Atlantic City, Wyoming (from Vincent, op cit.).



Figure 33. Part of an ERTS mosaic of Iran (original in color) showing the region around Tabas. Geologic structure and surface unit identifications have been made by photo-interpretation of the imagery supplemented by reconnaissance field work (Courtesy Earth Satellite Corp., Washington, D.C.).



Figure 34a. Sediments in the northern Caspian sea south of Astrakhan in the southern Soviet Union, imaged by ERTS.

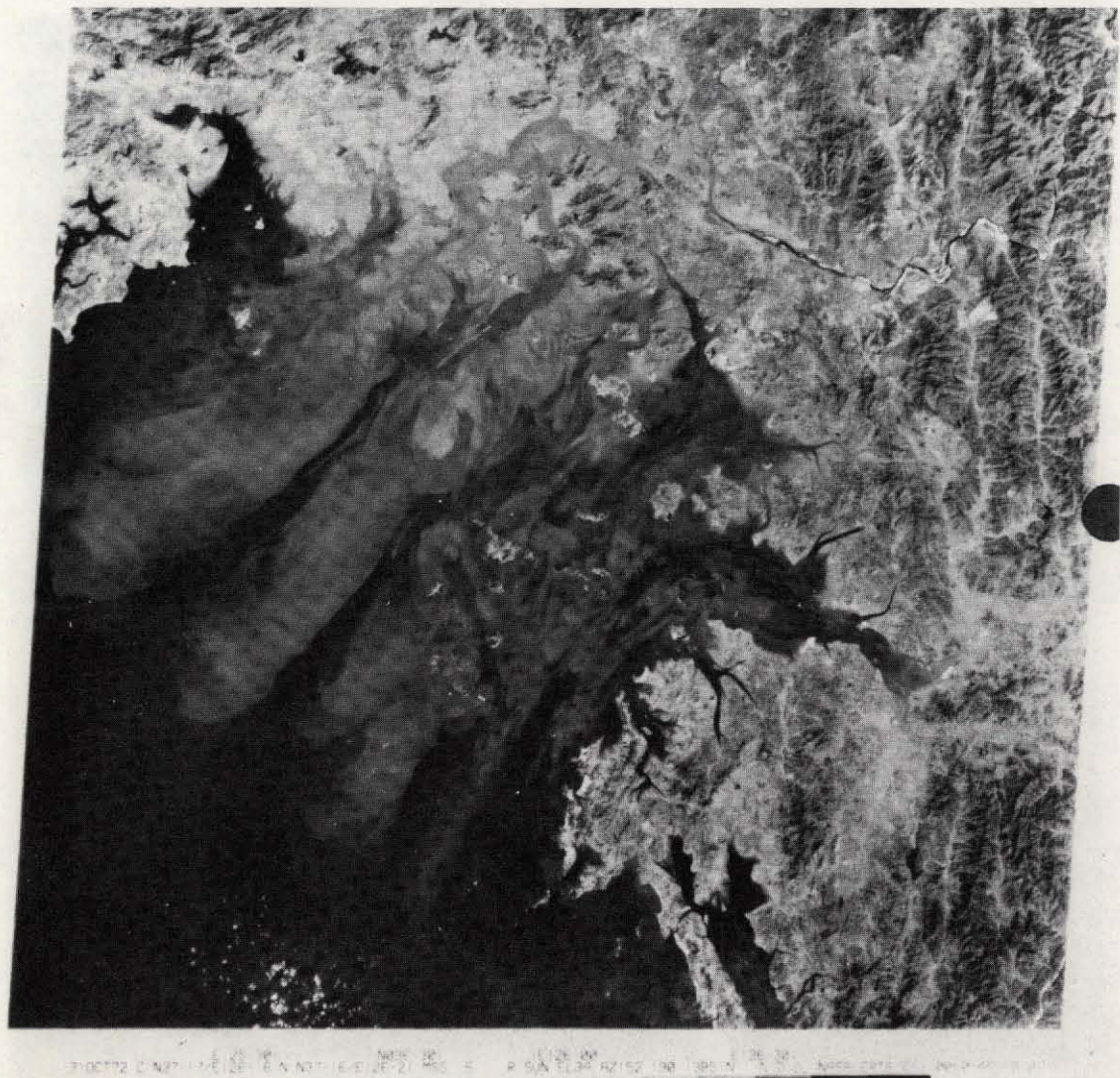


Figure 34b. Sediments from the Han River northwest of Seoul, Korea being carried into the Yellow Sea, as seen from ERTS.

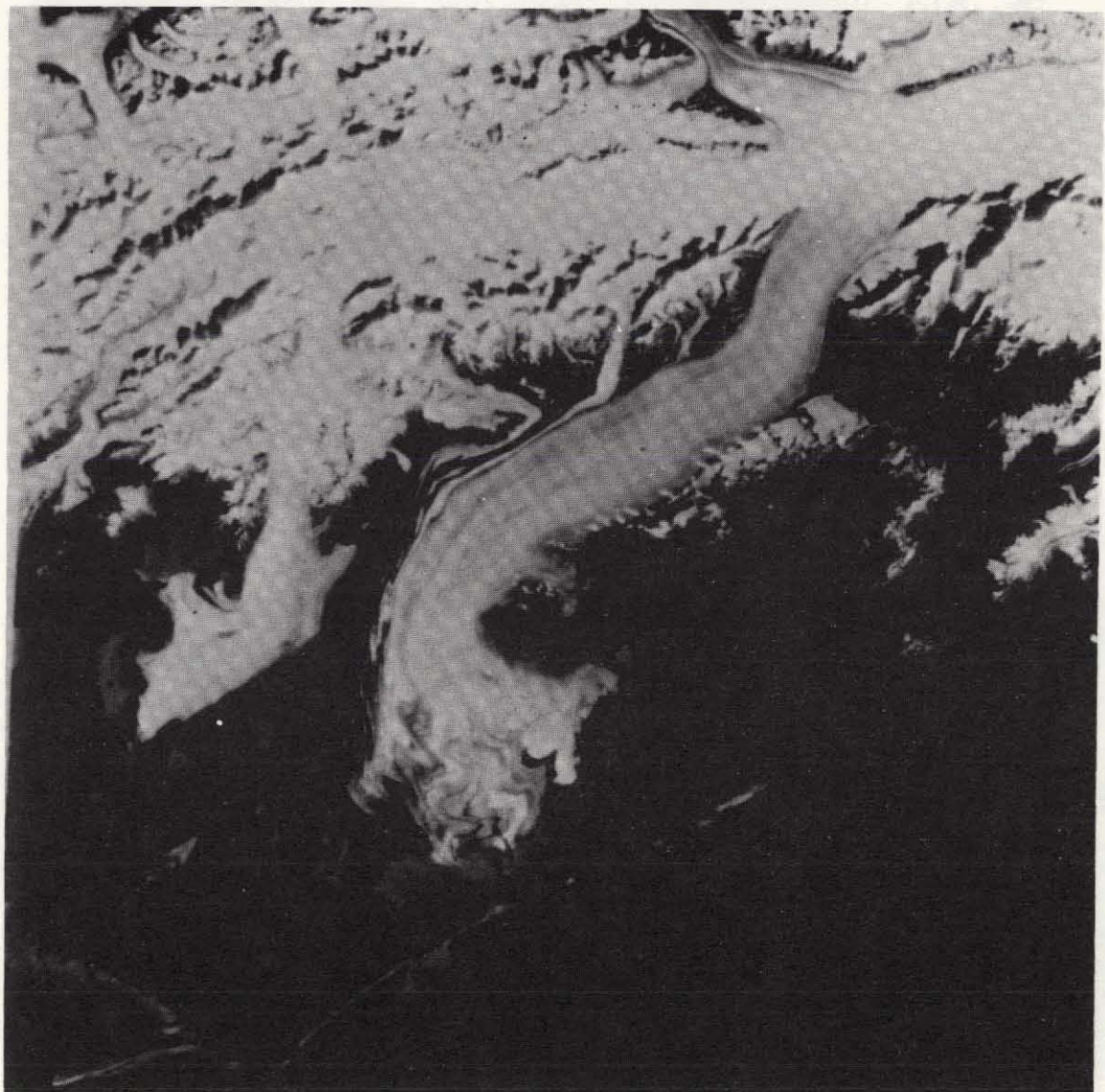


Figure 35. Blow-up of part of an ERTS image of the Chugach Mountains along the south coast of Alaska east of Anchorage showing the Bering glacier extending into an inlet before reaching the sea. The area now covered by the lower reaches of the glacier is considerably less than shown on geographic maps of the region.

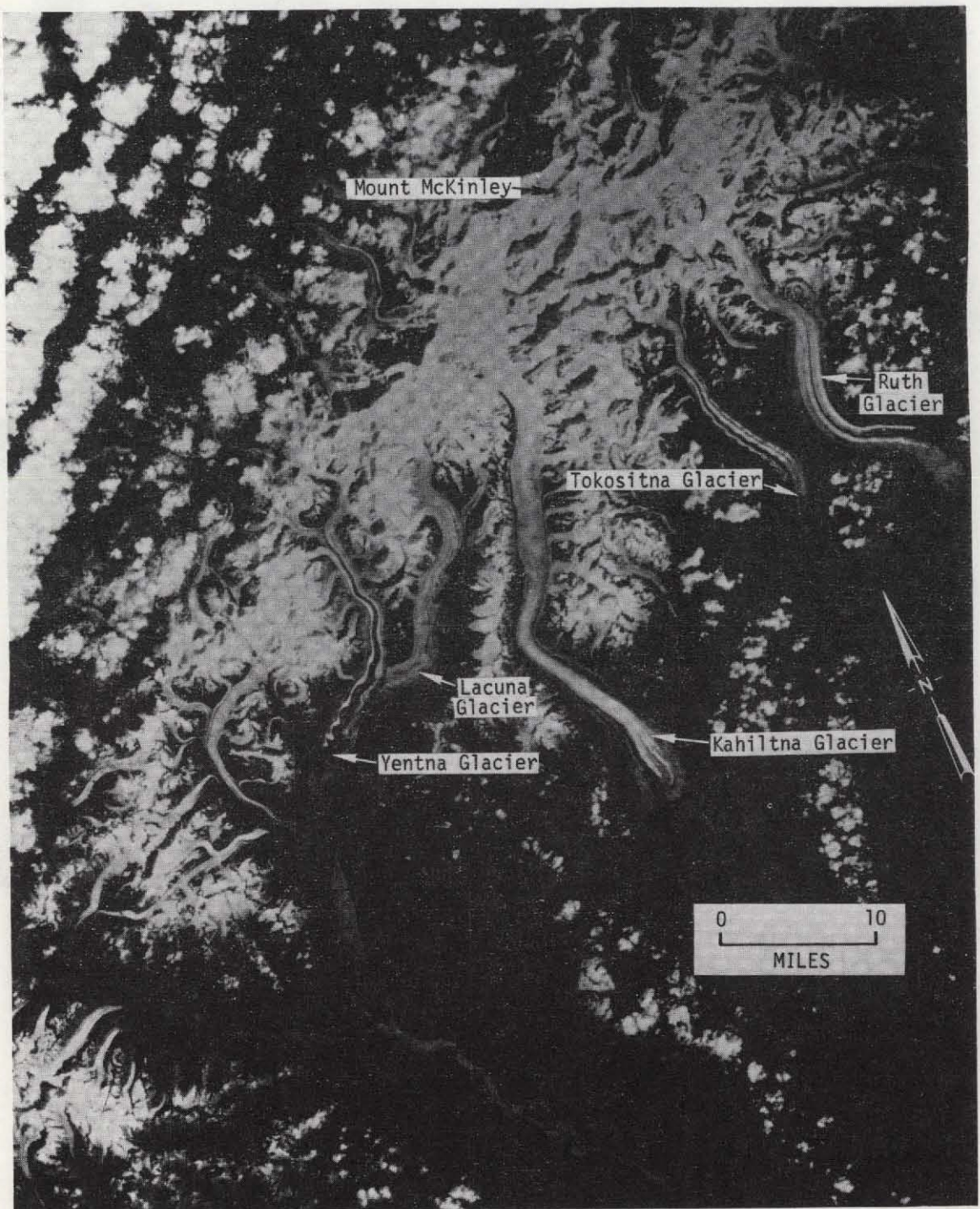


Figure 36. Surging glaciers (indicated by crenulation of moraines on the ice surface) in south-central Alaska, as seen in this enlarged view from ERTS. (Courtesy U.S. Geological Survey.)



Figure 37. Aligned glacial lakes south of Point Barrow in northern Alaska as imaged by ERTS. At least some of these lakes may be thermokarst depressions related to permafrost effects.

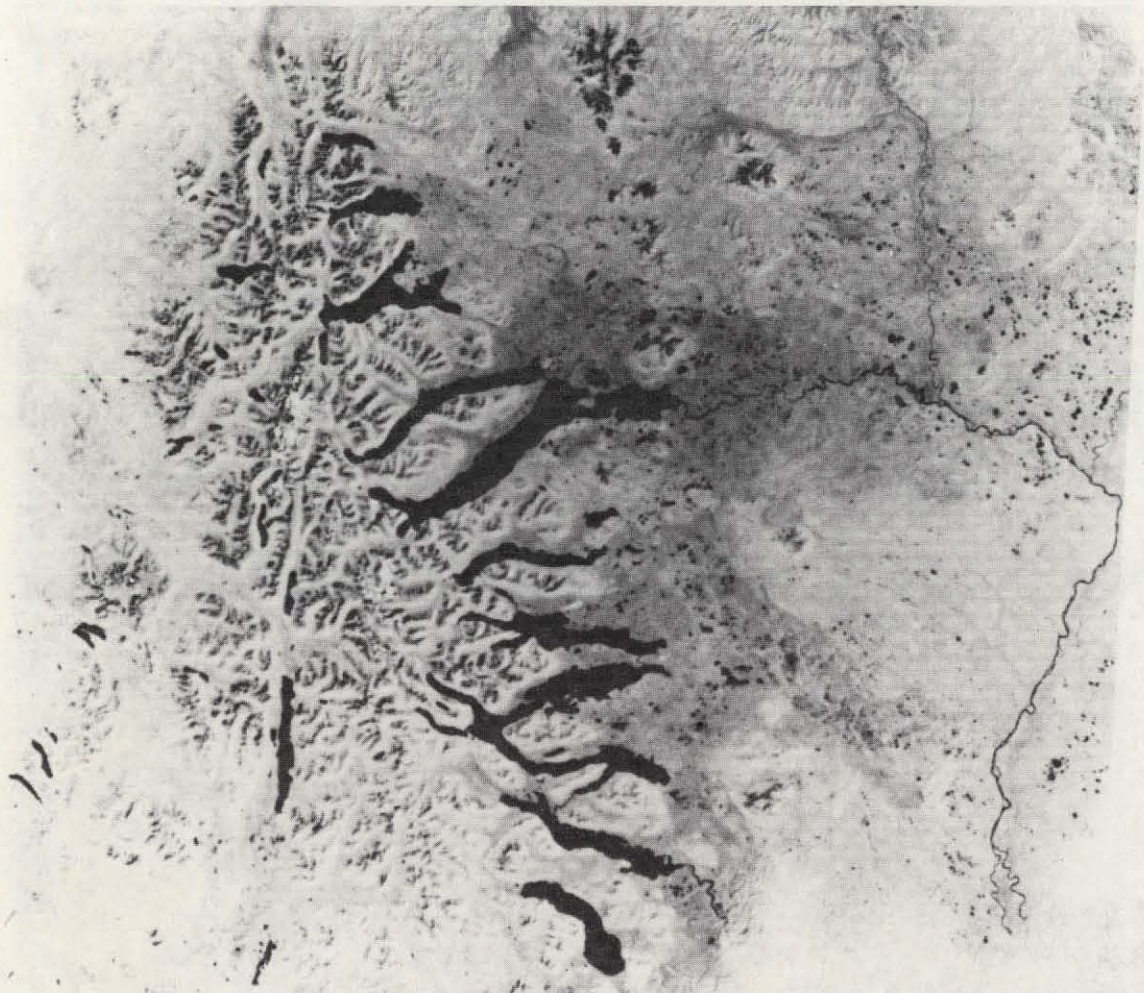


Figure 38. Glacial-scour-produced "finger lakes" in the Kilbuck Mountains of southwest Alaska. This ERTS MSS Band 7 image enhances differences in the glacial outwash plains being drained by the Nuyakuk River. The long linear valley west of the lakes is the westernmost extension of a great, accurate strike-slip fault that carries across Alaska into Canada.



**Figure 39.** Sea ice forming in the Greenland sea just off the coast of King Christian Land in eastern Greenland; image taken by ERTS in early October of 1972.

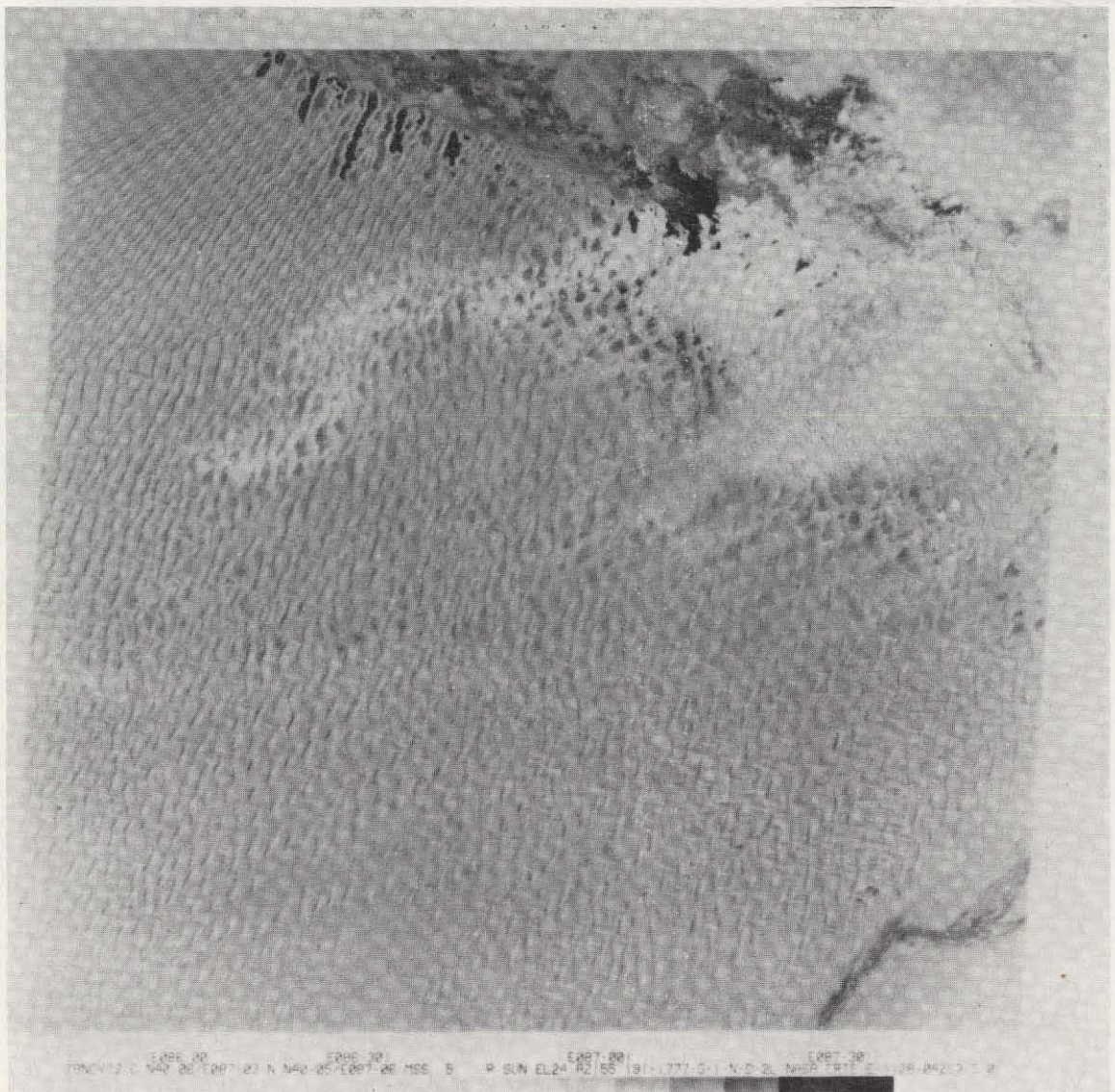


Figure 40. Distinctive dunes in a "sand sea" in the Takla Makan Desert of western China in an ERTS image taken in late November of 1972.

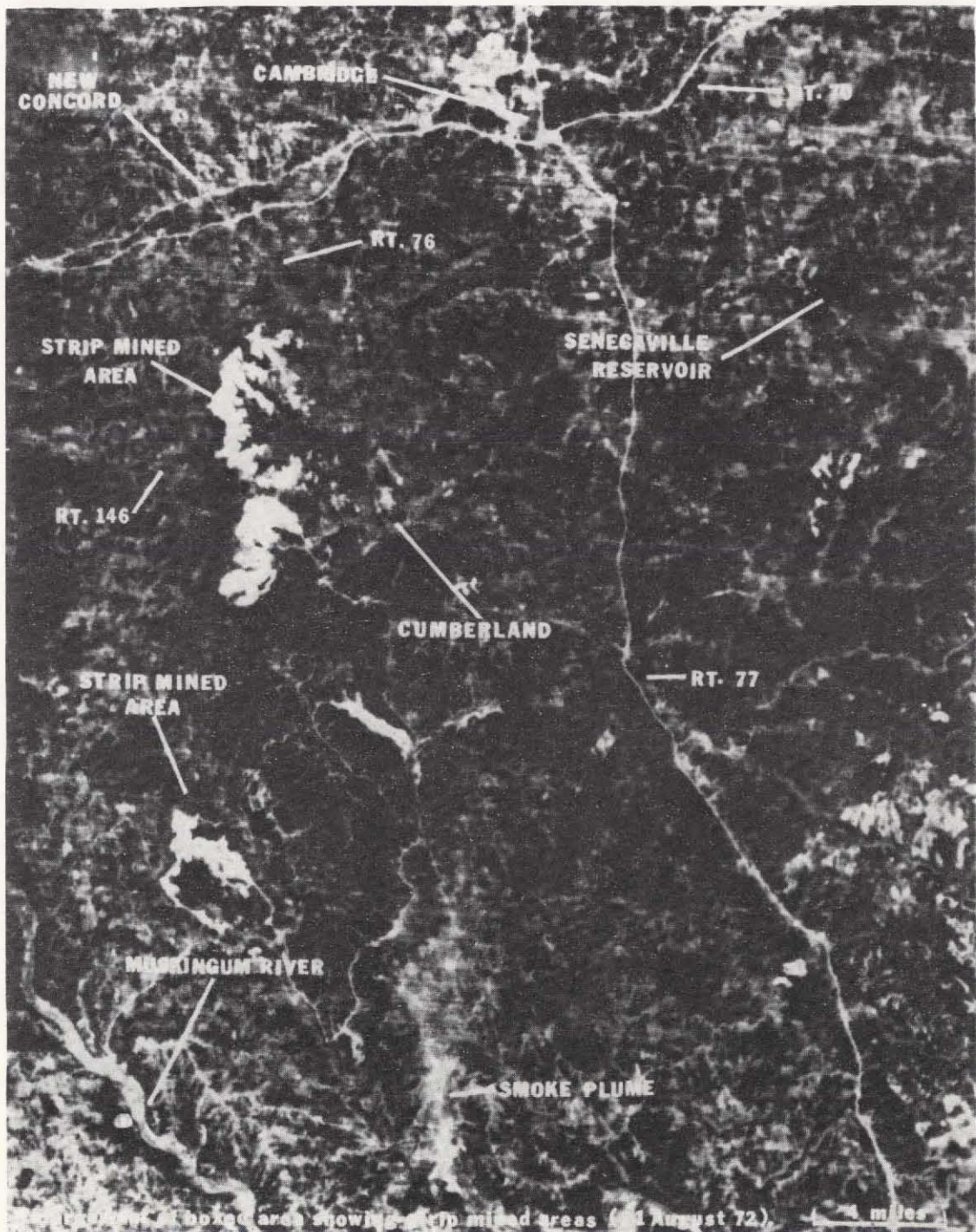


Figure 41. Part of an ERTS image (21 August 1972) taken over southeast Ohio (Zanesville lies to the northwest) showing strip-mined areas in the Pennsylvanian coal deposits of the western Cumberland Plateau. (Courtesy U.S. Geological Survey.)



Figure 42. Skylab 2 EREP photography: This photo of the San Rafael Swell (a breached anticlinal dome and nearby Desolation Canyon in east-central Utah was taken by the S 190A multispectral camera. Original of this photo recorded on SO-356 High Resolution Aerial color film.

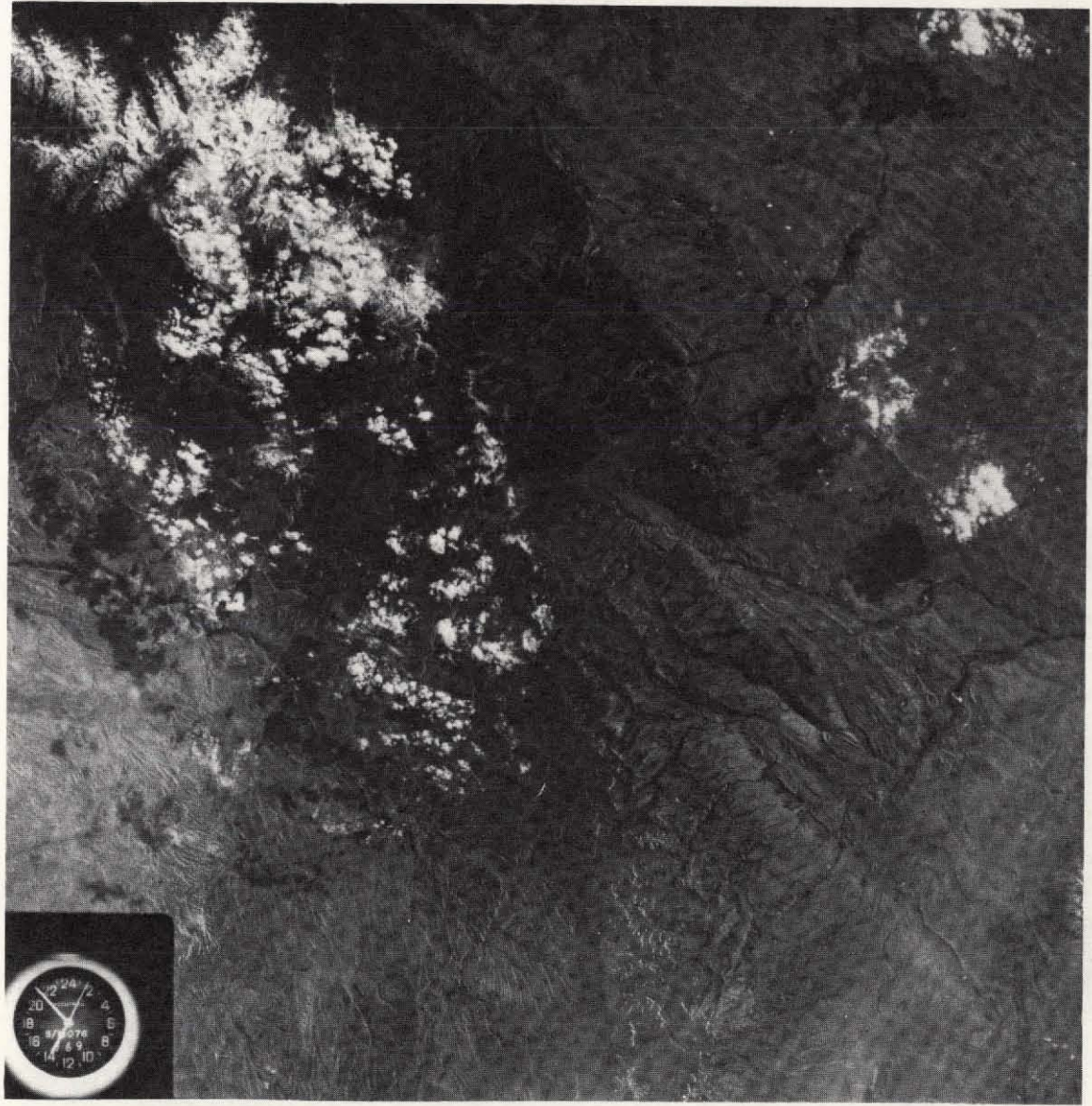


Figure 43. Skylab 2 S 190B metric camera black and white (EK 3414 film) photo of the southern Big Horn Mountains and adjacent Power River Basin, from Mayoworth (south) to Buffalo (north).

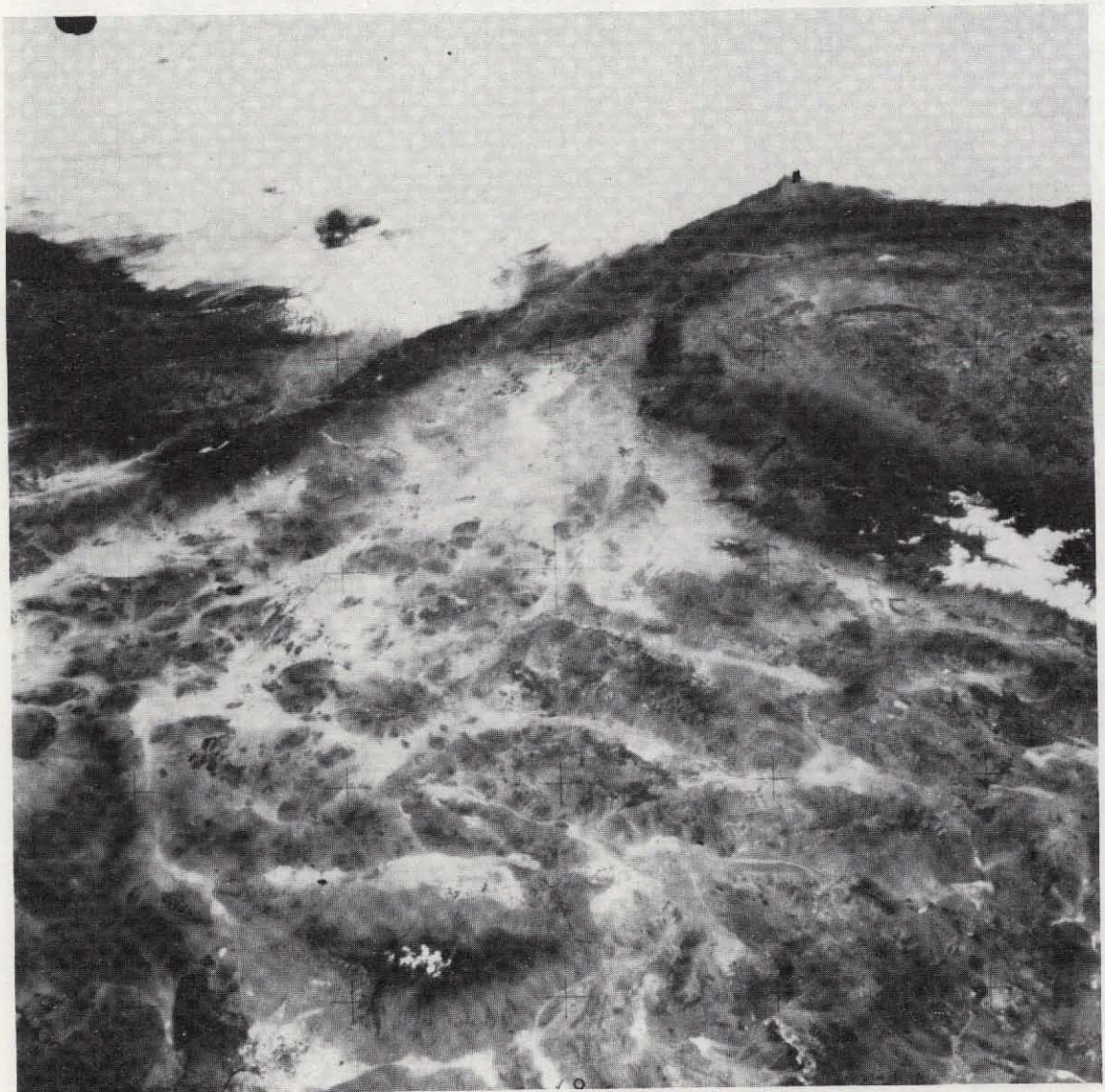
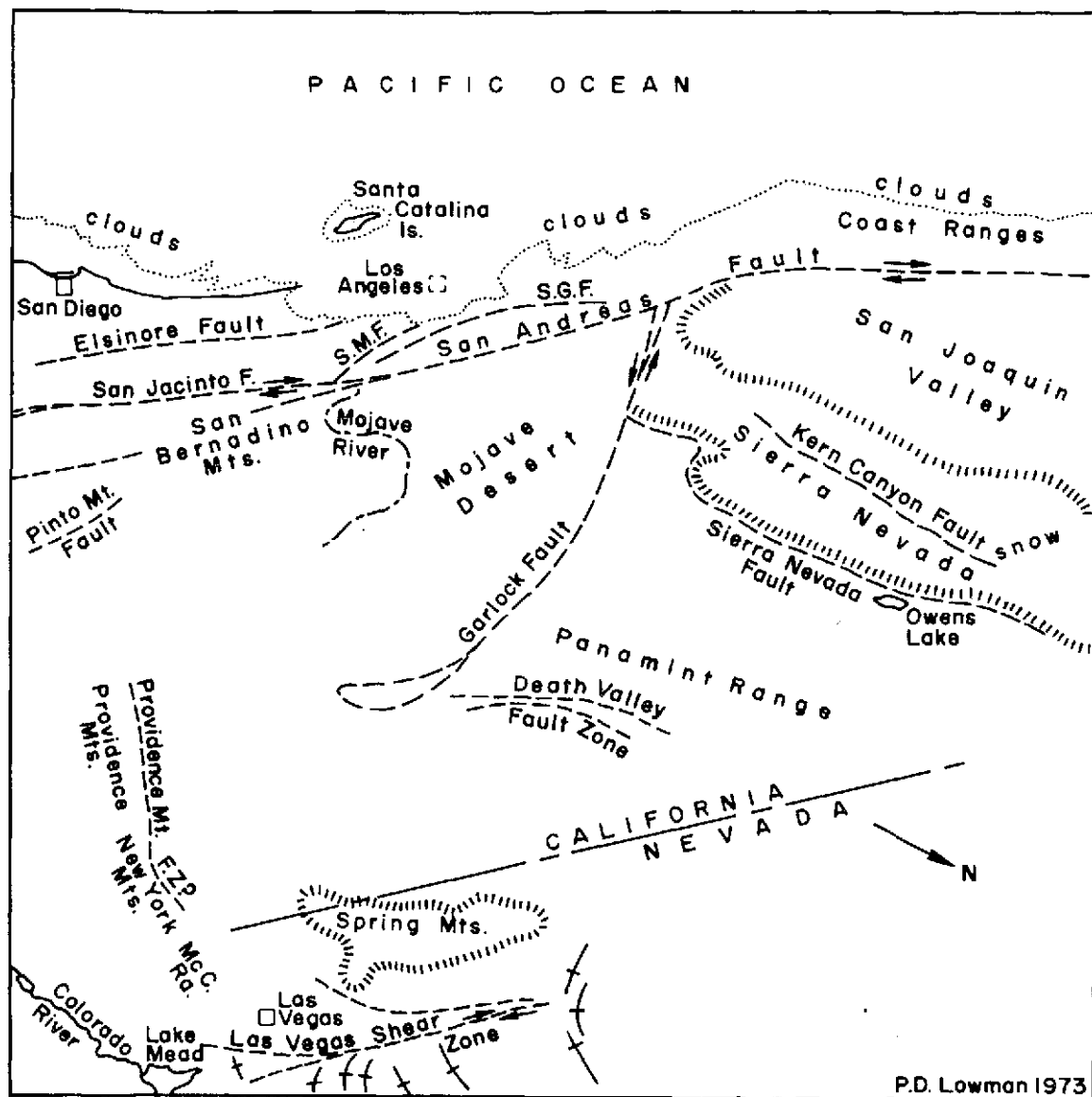


Figure 44. Hand-held (Hasselblad camera) 70 mm oblique photo of the Mojave Desert of southern California taken during the Skylab 2 mission.



### INDEX MAP

SKYLAB I PHOTOGRAPH SL2-5-469

Scale variable: Owens Lake - San Diego  
distance 400 km. (250 miles)

S.G.F. - San Gabriel Fault

S.M.F. - Sierra Madre Fault

Figure 45. Sketch map showing interpretation by P. D. Lowman, Jr. of features seen in the Figure 44 photo.

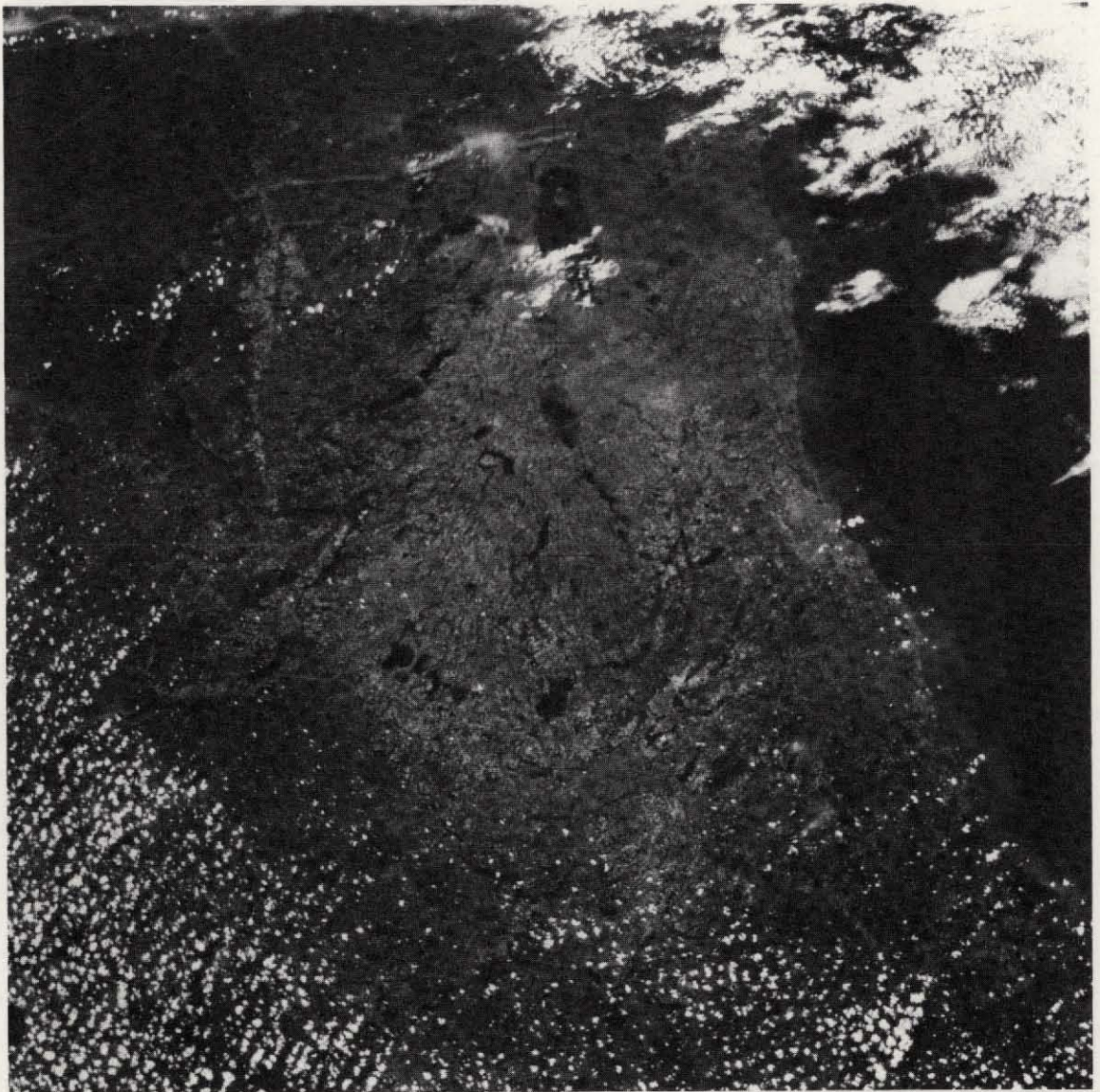
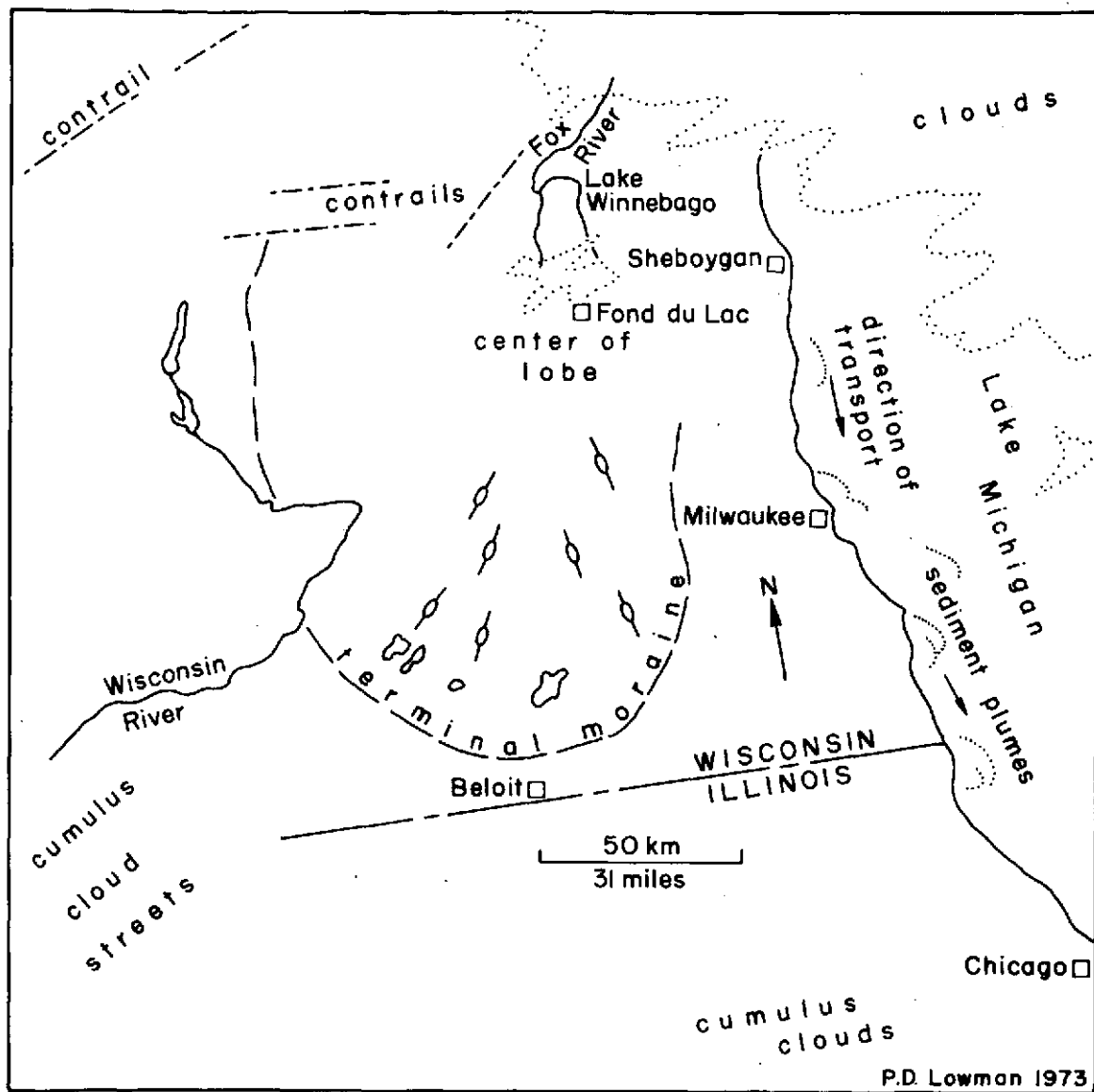


Figure 46. Near-vertical view of southern Wisconsin and northern Illinois obtained with a Hasselblad camera during Skylab 2.



**INDEX MAP**  
**SKYLAB I PHOTOGRAPH SL2-5-320**  
 —○— Drumlin orientation

Figure 47. Sketch map of region shown in Figure 46 indicating interpretation of glacial features made by P.D. Lowman, Jr.

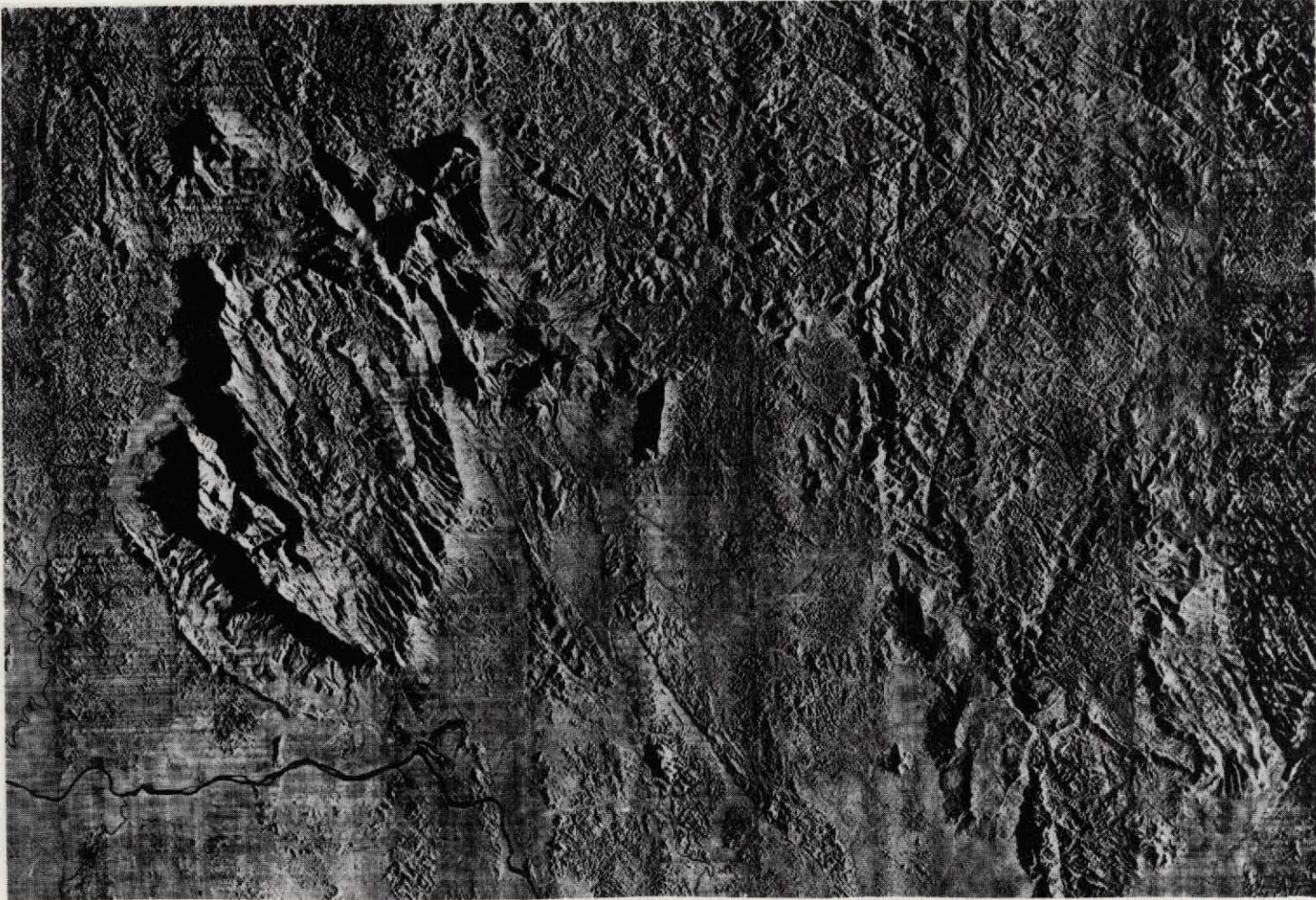


Figure 48. K-band Radar mosaic (SLAR) of the Esmeralda Quad in southern Venezuela (Amazonas Province) which includes the headwaters of the Orinoco River. The region is heavily vegetated (jungle). Horizontal dimension of the image covers approximately 100 miles. (Courtesy Goodyear Aerospace Corp.)

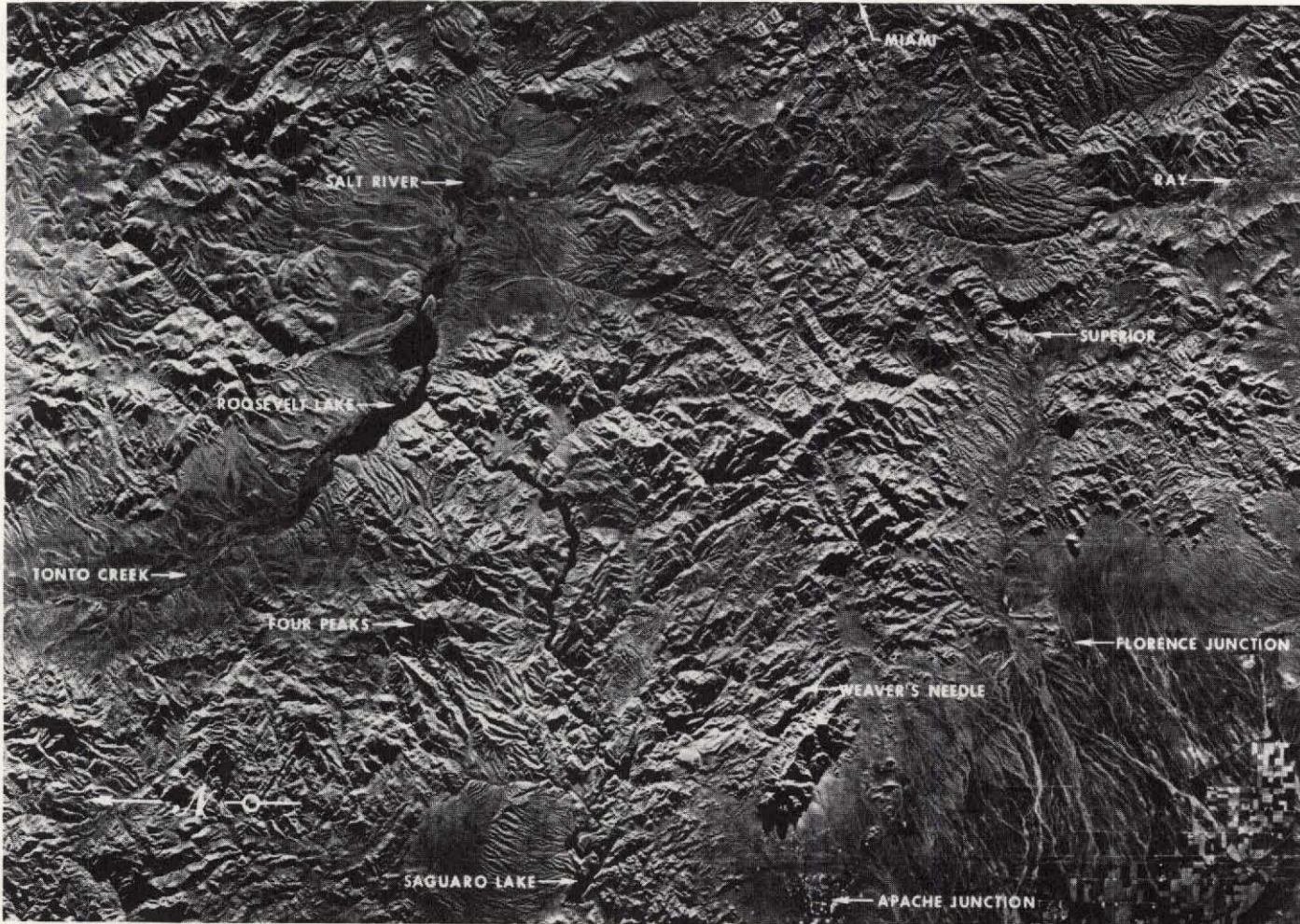


Figure 49. Radar mosaic of part of south-central Arizona east of Phoenix. North is to the left. Compare the radar rendition of the region around Roosevelt Lake-Tonto Creek with the ERTS version of the same scene in Figure 27b. (Courtesy Goodyear Aerospace Corp.)

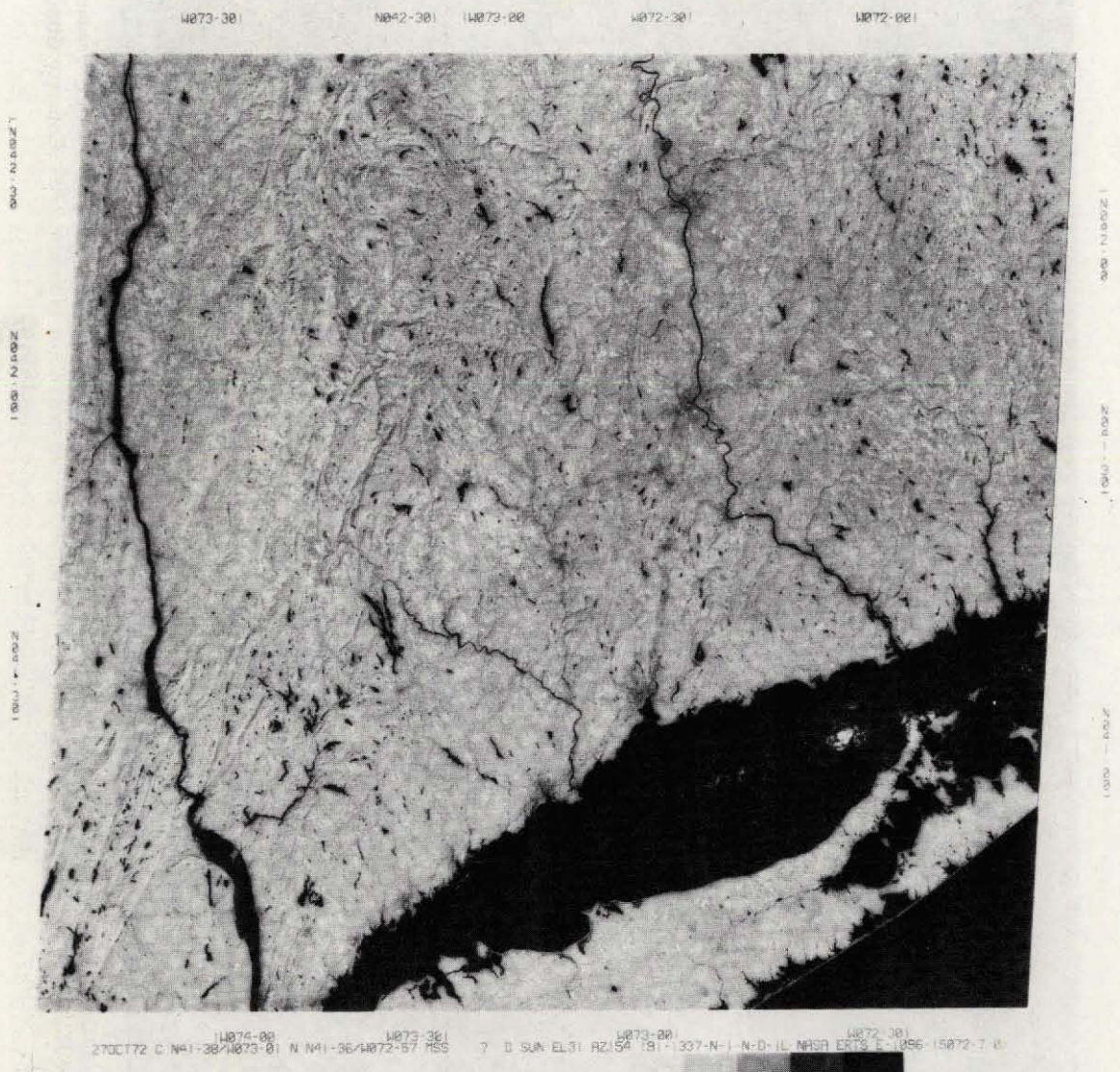


Figure 50. ERTS Band 7 (0.8-1.1  $\mu\text{m}$ ) image showing southern Connecticut and eastern New York (part of Long Island and the Hudson Valley) in late October.

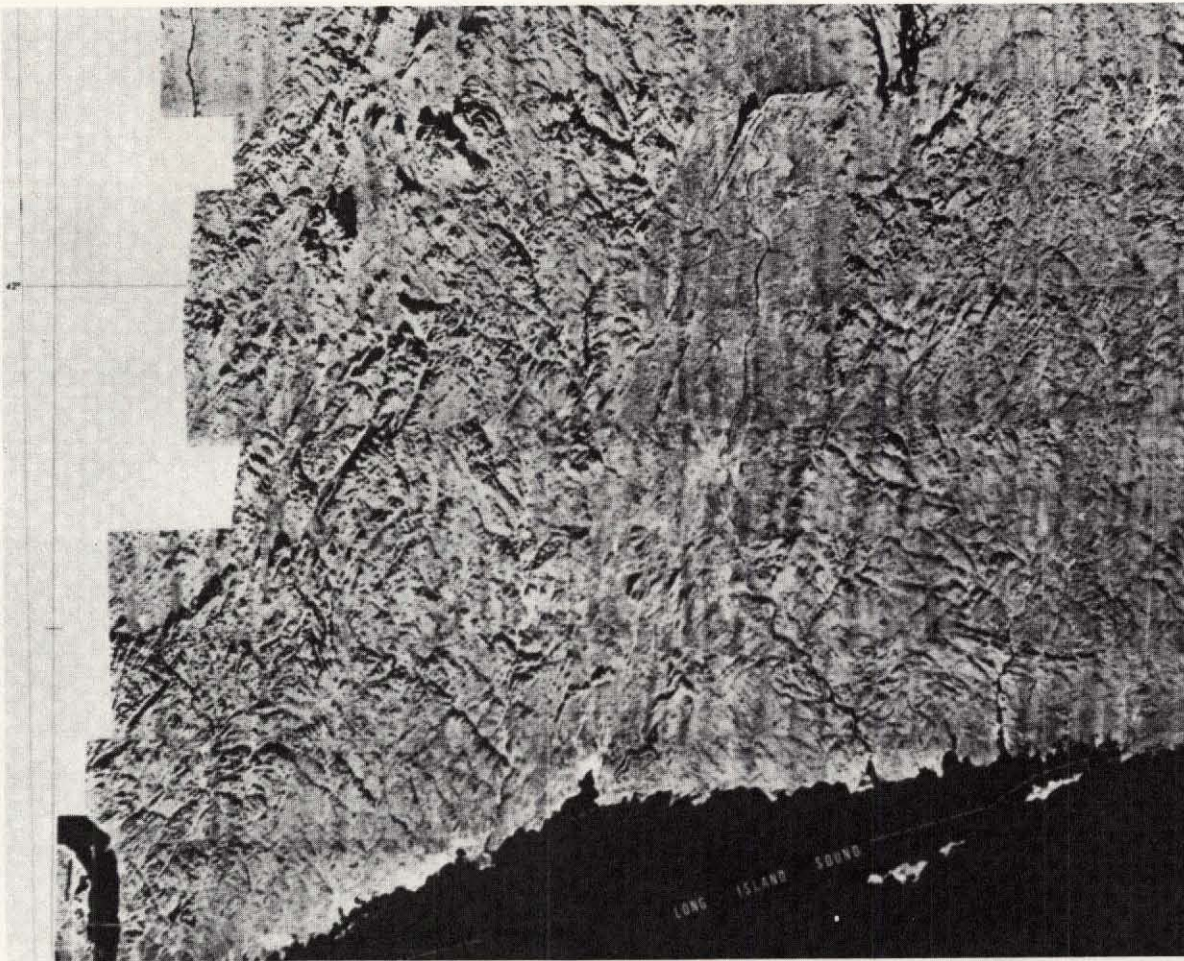


Figure 51. Photo-copy (considerably degraded from the enlarged original) of a portion of the K-band radar mosaic produced by Grumman Ecosystems Corp. for the U.S. Geological Survey that covers much of the same area of southern Connecticut shown in Figure 50 (Hudson River on bottom left; Connecticut River near center).

**a****b**

Figure 52. a) Aerial photo of the Mill Creek test site in the Arbuckle Mountains of Oklahoma showing the major rock units G = granite, S = sandstone, L = limestone, and D = dolomite; F = faults; b) Pre-dawn (0600) thermal-infrared image of the Mill Creek site obtained in December 1968 (units same as in a);



C



d

Figure 52. c) Mid-morning (1100) thermal-infrared image of same area; d) mid-afternoon (1400) thermal infrared image. North is at the top of all images. The pre-dawn thermal contrast between limestone and dolomite is not evident in the daytime images. The granite responds similarly to the limestone (from Watson, et al., 1971).